ISAS - INTERNATIONAL SCHOOL FOR ADVANCED STUDIES

Study of spontaneous and rhythmic activity expressed by a synaptic circuit *in vitro*: The organotypic spinal cord co-cultures

Thesis submitted for the degree of "Doctor Philosophiae"

Biophysics sector

Candidate:
Micaela Galante

Supervisor:
Dr. Laura Ballerini

SISSA - SCUOLA INTERNAZIONALE SUPERIORE DI STUDI AVANZATI
TRIESTE
Via Beirut 2-4

TRIESTE

Table of contents

Acknowledgments

I would like to express my gratitude to my supervisor, Dr. Laura Ballerini, whose expertise, understanding, and patience, added considerably to my graduate experience. I appreciate her vast knowledge and skills, which contributed the most to my education. Laura, you most of all have brought me to this point. Thank you for your encouragement, direction and insight. I would like to thank Micaela Grandolfo not only for the immunohistochemistry but also (and more importantly) her ever-lasting friendship. Micaela, I was very greatly fortunate to have your support and ease as a friend and a colleague whenever I needed throughout all these years. I would also like to thank Andrea Nistri. I appreciated his insightful discussions, and scientific wisdom. I also thank Silvia Di Angelantonio for the confocal microscopy. I am most greatly indebted to my family for the support, encouragement, and love, they provided me through my entire life.

NOTE

- Part of the data reported in the present thesis have been published in the articles listed below. In all cases the candidate personally performed the experimental work and data analysis, and contributed to paper writing.

Ballerini, L., and Galante M. 1998. Network bursting by organotypic spinal slice cultures in the presence of bicuculline and/or strychnine is developmentally regulated. *Eur. J. Neurosci.*, **10,** 2871-9.

Ballerini L, Galante M, Grandolfo M, Nistri A. 1999. Generation of rhythmic patterns of activity by ventral interneurones in rat organotypic spinal slice culture. *J Physiol.*, **517,** 459-75.

Galante M, Nistri A, Ballerini L. 2000. Opposite changes in synaptic activity of organotypic rat spinal cord cultures after chronic block of AMPA/kainate or glycine and GABAA receptors. *J Physiol.*, **523,** 639-51.

- In all the studies presented and cited in this thesis, the embryonic day 1 was established as the day when the vaginal plug was first detected.

ABSTRACT

In the central nervous system rhythmic oscillations are observed in several developing circuits and rely on a set of cellular and network characteristics often difficult to unreveal in complex neuronal structures. The mammalian spinal cord is a useful tool to study such oscillatory activity because it is able to produce locomotor-like rhythmic patterns even when isolated from higher brain centers or sensory feedback. It is widely accepted that spinal cord contains local neuronal networks termed central pattern generators (CPGs) which are ensembles of spinal cord interneurons that provide the timing of motoneuron discharge even in the absence of external feedback. However the operation of CPG interneurons in functional spinal circuits and their plastic changes during development aren't fully described. Fundamental questions are whether interneurons in a spinal segment can express rhythmic activity or whether intersegmental connections are required to support it and how do ventral interneuron rhythmogenic properties change during *in vitro* development. To study these issues, organotypic co-cultures of spinal cord and dorsal root ganglia from rat embryos have been performed. This *in vitro* preparation not only allows visualization of interneurons in a structure that maintains the basic synaptic organization of a spinal cord segment, but also provides information concerning spinal network activity during *in vitro* development.

Patch clamp recordings (voltage or current clamp mode) have been performed on visually identified ventral horn interneurons, under whole cell configuration. When Cl^- mediated transmission is pharmacologically blocked, ventral interneurons in the organotypic spinal cultures expressed spontaneous rhythmic bursts analogous to those found in the isolated neonatal rat spinal cord. This rhythmic activity was dependent on spike activity in the slice and was detected after 8 as well as after 14 days *in vitro* (DIV). The frequency, the duration of such a rhythm and its sensitivity to ionotropic glutamate receptor antagonists, however, differed between these two ages in culture. Rhythmic bursts could also be induced in ventral interneurons by increasing the extracellular K^+ concentration, a stratagem known to induce locomotor-like patterns in the isolated neonatal rat spinal cord. Such a rhythmic activity was generated at network level since tetrodotoxin or low Ca^{2+} high Mg^{2+} solution blocked it.

Bursting was fully suppressed by block of AMPA/Kainate receptors and reduced in amplitude and duration by NMDA receptor antagonism without any change in periodicity. Regular, rhythmic activity also appeared spontaneously in Mg^{2+} free solution. In summary, block of fast Cl^- mediated synaptic transmission, or raised extracellular K^+ concentration or removal of the extracellular Mg^{2+} induced rhythms with distinct frequencies and mediated by different neurotransmitter systems.

Another substantial issue investigated in the present thesis is related to the ability of developing spinal networks to compensate for long-lasting suppression of certain synaptic inputs. As a consequence of such a treatment, a novel form of synaptic plasticity (homeostatic plasticity) has been described in several preparations, in which neurons respond by changing their firing activity, the distribution of certain postsynaptic receptors or their network connectivity. To address this issue, three experimental protocols have been utilized on organotypic spinal cultures: (a) chronic block of AMPA/Kainate glutamate receptors with CNQX, (b) chronic block of voltage-dependent Na^+ channels with TTX and (c) chronic block of glycine and $GABA_A$ receptors with strychnine and bicuculline. After chronic CNQX treatment the frequency of spontaneous postsynaptic currents (PSCs) and miniature currents (mPSCs) was almost doubled with respect to control, untreated cultures while after chronic strychnine and bicuculline treatment the frequency of both PSCs and mPSCs was decreased in most cells. The amplitude of mPSCs was not affected by chronic treatment suggesting that in these developing spinal networks, homeostatic plasticity was manifested mainly at the presynaptic level, presumably affecting the number of functional synapses. After chronic TTX treatment neither the frequency nor the amplitude of spontaneous events was changed, suggesting that miniature activity during chronic treatment was sufficient to maintain the fundamental network operation.

Finally, the question of whether chronic block of excitatory transmission affect only spontaneous ongoing activity or also the rhythmogenic properties of ventral interneurons has been dressed. Chronic CNQX treated cultures consistently generated rhythmic activity following each one of the three paradigms (namely in the presence of high extracellular K^+, in Mg^{2+} free solution and following coapplication of glycine and $GABA_A$ receptors blockers) known to generate rhythmic patterns in untreated cultures. However high K^+ induced rhythmic

bursts, in a half of the chronically treated interneurons, had shorter cycle period and burst duration compared to control cultures and presented a burst profile characterized by a slow rise time: single bursts consisted in summation and overlap of spontaneous events apparently without a marked synchronization. The present thesis denotes that a spinal culture that contains few cell layers in a preserved cytoarchitecture of a spinal segment contained a neural circuitry sufficient to express rhythmic activity and homeostatic compensatory mechanisms.

INTRODUCTION

1. Spontaneous synchronous activity in developing neuronal circuits

The assembly of functional synaptic circuits in the brain during development is thought to rely on both activity-independent and activity-dependent mechanisms. In the early activity-independent phase, neurons first develop distinct phenotypes, later migrate to characteristic positions within a developing structure and established an initial set of connections (Goodman and Shatz, 1993). In the later, activity-dependent phase, neural activity is thought to promote refinement and remodeling of the initially coarse connectivity (Shatz, 1990, Goodman and Shatz, 1993). Experimental evidence indicates that it is not neural activity *per se* to determine the process of connection refinement but rather it is the correlated neural activity among sets of inputs to mediate such a process (Schmidt and Eisele, 1985). Patterned spontaneous activity consists of rhythmic bursts of action potentials temporally correlated between neighboring cells and it is observed in several developing circuits, including hippocampus (Ben-Ari et al., 1989, Gaiarsa et al., 1990, Garaschuk et al., 1998) retina (Galli and Maffei, 1988, Meister et al., 1991, Feller et al., 1996) and spinal cord (Landmesser and O'Donovan, 1984, Nishimaru et al., 1996). During the first postnatal week CA3 hippocampal pyramidal cells exhibit large depolarizing synaptic events lasting for hundreds of milliseconds, called giant depolarizing potentials (GDPs) (Ben-Ari et al. 1989). These giant potentials (fig. IA) are characterized by periodical network-driven bursts with a frequency variable from cell to cell (0.05-0.2 Hz) but very regular in each cell (Ben-Ari et al., 1989). They are detected also in interneurons of strata oriens in CA1 and CA3 (Khazipov et al., 1997) and are widely observed in both pyramidal cells and inteneurons in CA1 (Garaschuk et al., 1998). Paired recordings from pyramidal cells and interneurons localized in the stratum radiatum of the CA3 subfield, (Khazipov et al., 1997) reveal that during the generation of GDPs in pyramidal cells, interneurons simultaneously fire bursts of action potentials. The generation of network-driven GDPs therefore results in a complex interaction between the population of interneurons and pyramidal cells. They are mainly mediated by activation of $GABA_A$ receptors (Ben-Ari et al. 1989) and modulated by glutamate (Ben-Ari et

al. 1989, Cherubini et al. 1991, Gaiarsa et al. 1990) as well as acetylcholine (Avignone and Cherubini, 1999). After the first postnatal week GDPs become rare, and this developmental change corresponds to a shift in the Cl^- gradient that determines the passage from depolarizing to hyperpolarizing response of $GABA_A$ receptor activation. The physiological role of GDPs is presently unknown. In keeping with the trophic action of GABA and glutamate during early stages of development (Cherubini et al., 1991) it is proposed that these periodic events may regulate neuronal growth and establishment of synaptic connections in immature hippocampus. Moreover, consistent with the recent finding that GDPs trigger increases in intracellular Ca^{2+} concentration in both interneurons and pyramidal cells (Leinekugel et al., 1995, 1997, Garaschuk, 1998) they might mediate the strengthening of immature synapses (Khazipov et al., 1997).

Mechanisms underlying the occurrence and the maintenance of hippocampal GDPs are unknown. Recently it has been proposed that glial cells might play an important role in allowing the expression of the oscillatory neuronal activity observed in cultured hippocampal neurons (Verderio et al., 1999). A large portion of hippocampal neurons grown in primary cultures displayed intracellular Ca^{2+} oscillations corresponding to bursts of action potentials (Bacci et al., 1999, Verderio et al., 1999). These network-driven oscillations were synchronous among neighboring neurons and entirely mediated by glutamate (Bacci et al., 1999). Synchronous spontaneous activity was found in a large portion of neurons lying in close association of astrocytes, while in the absence of neighboring astrocytes, neurons displayed spontaneous post synaptic potentials or single action potentials but never bursting activity (Verderio et al., 1999). Furthermore it emerged that the role of glial cells in the occurrence of these oscillations, consisted mainly in glial-mediated removal of extracellular glutamate suggesting that a fine control on the extracellular glutamate concentration might play a crucial role in the generation of synchronous neuronal activity (Verderio et al., 1999).

A wealth of recent investigations revealed that retinal neurons spontaneously fire action potentials even before the photoreceptors become functional. *In vivo* single electrode recordings in embryonic rat retina revealed that the output neurons of the retina, the ganglion cells, fired spontaneous action potentials in a rhythmic burst-like fashion (Galli and Maffei, 1988).

Simultaneous *in vitro* recordings from large populations of cells later demonstrated a striking correlation in spontaneous bursting activity of neighboring cells in the neonatal ferret retina (Meister et al. 1991). These multielectrode recordings showed that periodic spontaneous bursts of action potentials propagate across the ganglion cell layer in a 'wave-like' manner. Optical recordings of intracellular Ca^{2+} levels (fig. IB) enable a more complete assessment of the properties of the waves (Wong et al., 1995, Feller et al. 1996, 1997). In fact the retinal waves are found to occur at any given retinal location approximately every 1-2 min, they have a limited domain size and do not propagate across the entire retina. Furthermore the domain boundaries alter with time, suggesting the absence of pacemaker regions and that any region has equal probability of participating in a wave (Feller et al. 1996). Waves spread in unpredictable and different directions (Meister et al., 1991, Feller et al., 1996, 1997) but they tend not to occur consecutively in the same retinal region (Feller et al., 1996, 1997). In the last ten years much effort has been focused on elucidating mechanisms underlying this pattern of activity. Calcium imaging and patch clamp recordings from neonatal ferret suggest that both ganglion cells and cholinergic amacrine cells participate in a functional synaptic network that generates retinal waves (Wong et al., 1995, Feller et al., 1996, Zhou, 1998). In the early postnatal development of ferret (<P10) cholinergic synaptic transmission is required for wave initiation and propagation (Feller et al., 1996). However cholinergic synaptic transmission during waves is not blocked by tetrodotoxin suggesting that action potentials are not required for the initiation and propagation of retinal waves (Stellwagen et al., 1999). In older ferrets (>P18) waves are insensitive to cholinergic antagonists and modulated by glutamate, glycine and GABA (Fischer et al., 1998, Wong, 1999).

Several efforts have been made to clarify the spatio-temporal pattern of initiation, propagation and termination of retinal waves. It has recently been shown that spatio-temporal properties of spontaneous waves are determined by a cAMP-PKA cascade, which is regulated by endogenous adenosine within the developing ferret retina. Increasing cAMP levels increases the size, speed and frequency of the waves while inhibition of cAMP prevents wave activity (Stellwagen et al., 1999). Recently a model has been proposed in which wave properties depend on the fraction of recruitable cells in a given area and not on their biophysical properties. Amacrine cells have

three discrete states: recruitable, active and refractory. Activity spreads when the number of active cells in a region exceeds a threshold, causing recruitable neighbors to become active (Butts et al. 1999). Previously active cells will not be able to participate to a new event until they are in the refractory state. Mechanisms responsible for refractory period are still unknown, some possibilities include changes kinetics of nicotinic acethylcholine receptor desensitization (Gurantz et al., 1994) or the presence of synaptic depression mechanisms which prevent amacrine cells from releasing transmitter for a finite period of time. A similar mechanism has been proposed to explain silent period of spontaneous activity in the developing chick spinal cord (Chub and O'Donovan, 1998). It has been suggested that cAMP could modulate the refractory period (Stellwagen et al., 1999).

Developmental cues encoded in the pattern of waves are actually a matter of study. Many lines of evidence suggest that the correlated firing of ganglion cells is required for the formation of precise sets of connections between retinal ganglion cells and their targets (Goodman and Shatz, 1993). Furthermore the recent finding that retinal waves are triggered by cAMP intracellular level raise the possibility that this phenomenon can control amacrine cell differentiation and cell survival (Stellwagen et al., 1999).

Theoretical considerations and experimental evidences indicate that the emergence of adult patterns of connectivity requires neural activity among sets of inputs correlated in time and in space (Katz and Shatz, 1996). Therefore synchronization can represent an amplifier of neuronal activity by increasing both the depolarization of individual neurons and the number of active neurons by summating their synaptic inputs. Increases in intracellular Ca^{2+} concentration have been recorded across a large number of neurons participating to GDPs in rat hippocampus (Leinekugel et al., 1995, 1997, Garaschuk, 1998) or neurons participating to retinal waves in neonatal ferret (Feller et al., 1996, 1997) as well as in spinal motoneurons during embryonic periodic synchronous activity (O'Donovan et al., 1994). Elevation of intracellular Ca^{2+} could control a variety of processes such as neuronal survival (Franklin and Johnson, 1992), outgrowth of dendrites and axons (Kater et al. 1988, McAllister et al. 1996), gene expression and establishment of cell phenotype (Berridge, 1998). In the developing mammalian visual system, eye-specific layer formation in the lateral geniculate thalamic nuclei results from

synchronous activity of ganglion cells (Katz and Shatz 1996, Crair 1999). According to the majority of models studying layer formation in an eye-specific manner, retinal waves establish correlation among neighbor ganglion cells within an eye and the long silent periods between rhythmic bursts support a light link between the two eyes. Spontaneous activity may further play a role in the maturation process of the retina as well as retinal differentiation (Taylor and Reh, 1990), modulation of survival of retinal ganglion cells (Stellwagen et al. 1999), and growth cone formation (Ming et al. 1997).

2. Spontaneous rhythmic activity in developing spinal networks.

The earliest direct recordings of spinal cord activity were obtained from chick embryos *in ovo* (Provine 1972, Oppenheim et al. 1975) using microelectrode recordings from lumbosacral spinal neurons. Spontaneous electromyogram activity has been shown to exist *in ovo* (fig. IIA, top) as soon as motoneurons make functional contacts with their target muscles (Bekoff et al. 1975, O'Donovan and Landmesser, 1987), resulting in spontaneous periodic episodes of limb movements. A similar pattern of activity has been observed in the absence of sensory and supraspinal inputs in an isolated *in vitro* spinal cord-hindlimb preparation from chick embryo (fig IIA, bottom) (Landmesser and O'Donovan, 1984) showing that neuronal networks within the spinal cord are able to generate spontaneous activity which retains the rhythmicity and the pattern of that responsible for the generation of movement. A recent work from Milner and Landmesser (1999) shows that spontaneous rhythmic activity is first recorded from chick lumbosacral motoneurons at the embryonic stage E4, when motor axons just begin to bundle together and do not contact their targets yet. At this stage motoneurons exhibit regular rhythmic episodes consisting of a single short burst (about 500 ms) every ~3 min. Shortly after, at E6 when motor axons contact first their targets, this frequency slows down to approximately one in every 3-5 min, (in some case flexors and extensors activated out of phase) and each episode usually consists of multiple activity bursts (Landmesser 1978). At later stages (E10-E11), spontaneous rhythmic activity is composed of recurring episodes during which motoneurons discharge rhythmically alternating extensor and flexor muscles (O'Donovan and Landmesser, 1987, O'Donovan, 1989). At this stage of embryonic development the periodicity of such an

activity is around 5 min and the duration of bursts is 30-40 s. The neurotransmitter driving spontaneous bursting activity varies throughout the development of the chick cord starting with acetylcholine at the embryonic age E4-5 and glutamate at E10-E11 (Sernagor et al. 1995, Chub and O'Donovan, 1998).

A remarkable property of developing spinal networks is the ability to recover the spontaneous rhythmic pattern during prolonged pharmacological block (Barry and O'Donovan, 1987, Chub and O'Donovan, 1998, Milner and Landmesser, 1999). For example, block of cholinergic transmission in the early embryonic stages suppresses rhythmic activity, but after about an hour in the continuous presence of the blocker, rhythmic activity recovers (Milner and Landmesser, 1999). This 'new' rhythmic activity is mediated by GABA acting through $GABA_A$ receptors. Similar phenomenon is present also during the later phases of development, e.g at E10-E11: after blocking glutamatergic transmission spontaneous episodes are abolished, however about an hour later, activity recovers (Barry and O'Donovan, 1987, Chub and O'Donovan, 1998). Recovery from neurotransmitter receptor blockage occurs even after simultaneous suppression of glutamergic and cholinergic neurotransmission. It has been shown that this restored rhythmic activity is mediated by $GABA_A$ and glycine receptor activity (Chub and O'Donovan, 1998). Collectively these observations raise the possibility that network output may be homeostatically regulated and this phenomenon can play an important role in developing spinal networks to achieve an adequate level of excitation of postsynaptic targets (O'Donovan, 1999). To date mechanisms responsible for spontaneous rhythmic activity in embryonic spinal cord are not clear and the role of such an activity during development is poorly understood. Imaging experiments reveal that, during episodes of motoneuron rhythmic activity, rhythmic changes in fluorescence are widespread in the spinal cord with the highest proportion in the ventrolateral part of the cord (O'Donovan et al., 1994). The significance of such a temporally and spatially coordinated variation in the intracellular calcium concentration has not been elucidated, however it may be have several roles during development such as strengthening of synaptic connections between neurons involved in rhythmic activity, gene expression (Berridge, 1998), establishment of muscle phenotypes and expression of muscle proteins (Jarvis et al., 1996, Calvo et al., 1996).

In rat fetuses the earliest spontaneous movements are observed at the embryonic day 15 (E15) both *in utero* (Narayanan et al. 1971) and *in vitro* (Suzue, 1992). Morphological and electrophysiological studies show that at this embryonic age dorsal root afferents project to the gray matter and start to establish polysynaptic contacts with motoneurons (Kudo and Yamada, 1987, Ziskind-Conhaim, 1990). It is not known however, whether the earliest movements in rat fetuses are evoked by reflex pathways or neuronal networks within the spinal cord. In the isolated rat spinal cord periodic, network-driven, spontaneous bursts are present in the cervical spinal cord as early as E14 (Nakayama et al., 1999), and, in the lumbar spinal cord, as E15 (Nishimaru et al., 1996, Greer et al., 1992) (see fig. IIB). This spontaneous rhythmic activity is synchronous in both left and right ventral roots and is detected until E18. At E19 rhythmic, spontaneous bursts are not present although sporadic discharges are occasionally observed (Nishimaru et al., 1996, Nakayama et al., 1999). Duration and frequency of spontaneous bursts are developmentally regulated. Starting from E15 when the duration of the burst is about 7 s and the cycle period is around 2.5 min, duration of a single burst becomes progressively shorter whereas the burst frequency higher (Nishimaru et al., 1996). Burst occurrence in the cervical and lumbar ventral roots is strictly correlated (Nakayama et al., 1999). At early stages (E15-16), spontaneous bursts in the cervical region precede those in the lumbar region, while at later stages (E17-18) this temporal relationship is inverted and bursts in the lumbar ventral roots precede the corresponding bursts in the cervical ones. These results suggest that the location of the neuronal circuit initiating the periodic spontaneous bursts shifts during development from the cervical to the lumbar region in the fetal rat spinal cord (Nakayama et al., 1999). An analogous phenomenon is observed, at the same stages of embryonic development, during neurogenesis (Nornes and Das, 1974). In fact neurogenesis starts in the cervical region and systematically progressed caudally to the thoracic and lumbar regions of the rat embryo spinal cord. In both cervical and lumbar spinal cord, at E15-E16, block of $GABA_A$ receptors reduces the amplitude of spontaneous bursts nonetheless suppression of glycine-mediated activity completely abolishes them, suggesting that glycine and GABA play a major role in mediating the earliest spontaneous motoneuronal activity (Nishimaru et al. 1996, Nakayama et al., 1999). Glutamatergic transmission is involved to a lesser extend at these ages but it becomes the

predominant transmitter responsible for generating spontaneous bursts by E16 in the cervical ventral roots and by E17 in lumbar ones (Nishimaru et al., 1996, Nakayama et al., 1999). The role and possible mechanisms responsible for spontaneous patterned activity in the embryonic rat spinal cord have not been investigated as deeply as in the chick embryo, however it has been hypothesized that the spontaneous synchronous firing of motoneurons might play a role in the development of neuromuscular connection and network formation (Nishimaru et al., 1996).
In the developing spinal cord the frequency and the pattern of motoneuron firing is important for the development of muscle fiber types, for the regulation of the expression of muscle proteins and other aspects of muscle phenotype (Jarvis et al., 1996, Calvo et al., 1996). Furthermore, recent results reveal that transient elevations of intracellular Ca^{2+} in growth-cones regulates both the rate of axon extension and the guidance of axons in the *in vivo* spinal cord of *Xenopus* embryos (Gomez and Spitzer, 1999). In particular it seems that the rate of axon outgrowth is inversely related to the frequency of Ca^{2+} transients in growth-cone.

3. **Mechanisms underlying spontaneous rhythmic activity in developing spinal cord**

Spontaneous patterned activity in developing spinal cord is a network-driven phenomenon that depends upon the state of network maturation rather than its detailed or specific connectivity (O'Donovan et al., 1998b). In fact spontaneous rhythmic activity can recover in the presence of the major neurotransmitter receptor antagonists (Chub and O' Donovan, 1998) and it can be generated by isolated portions of the *in vitro* embryonic spinal cord (Ho and O'Donovan, 1987 for the chick and Nakayama et al., 1999 for the rat). These findings rise the question about how spontaneous rhythmic activity is generated in the developing spinal cord. In the chick embryo two features have been proposed being responsible for the expression of spontaneous motoneuronal activity (Chub and O'Donovan 1998, O'Donovan et al., 1998b): the excitatory nature of developing spinal neural ensembles and the presence of activity-dependent depression of network excitability. The interaction between these two properties (excitability and depression) results in the expression of periodic bursts by the network. The extensive excitability of embryonic spinal networks may result from several conditions. One could be the presence of positive feedback excitation in networks that are recurrently connected. Another

possible source of excitation can be represented by the depolarizing action of the classical inhibitory neurotransmitters (GABA and glycine) in early spinal development (Sernagor et al., 1995, Nishimaru et al., 1996). The presence of some mechanism of synaptic depression in embryonic chick spinal cord is suggested by several experimental clues: a) the membrane potential of many spinal interneurons is hyperpolarized after an episode of rhythmic burst and recovers progressively ("depolarizing ramp", O'Donovan, 1999) b) electrical stimulation of several synaptic pathways (whose neurons are rhythmically active during an episode) produces smaller synaptic potentials after an episode of rhythmic activity (Fedirchuk et al., 1999) c) the amplitude of spontaneous synaptic currents recorded from ventral interneurons shows a post-episode reduction (O'Donovan, 1999). Chub and O'Donovan (1998) proposed a model to account for these observations. Shortly, "after an episode of spontaneous rhythmic activity, network excitability is depressed and the network is refractory to further stimulation. During recovery, the functional connectivity and excitability of the network increase and some neurons begin to fire. As network excitability increases further the discharging neurons may recruit other neurons and, once a critical fraction is active, another episode of activity takes place."

There is no experimental support for pacemaker neurons in the chick embryo spinal cord to play a role in rhythmogenesis (O'Donovan et al., 1998a). Although NMDA can induce membrane potential oscillations in spinal neurons in the presence of TTX (Chub et al., 1998), these are not essential for rhythmogenesis because spontaneous rhythmic activity can occur even in the presence of NMDA receptor antagonists (Barry and O'Donovan, 1987, Chub et al. 1998, Chub and O'Donovan 1998).

Mechanisms similar to those described above have been proposed to account for the generation of spontaneous bursts of activity in organotypic cultures of the embryonic rat spinal cord (Streit, 1993). Motoneurons in these cultures express rhythmic, network-driven periodic bursts following the suppression of chloride-mediated transmission. A strong correlation between burst duration and the interburst interval is observed, namely the duration of a burst is significantly correlated with the interval preceding the burst itself, and it is not correlated with the following interburst interval. These findings led Streit to propose a model in which rhythmic motoneuronal activity induced by block of glycine and/or $GABA_A$ receptors is controlled by the

reverberation of activity within the whole network. Bursts are terminated by a gradual decrease in synaptic efficacy and/or in the excitability of the neurons (Streit, 1993, 1996). The episode occurrence, then, is related to the time of recovery from synaptic depression (Streit, 1993).

4. Homeostatic regulation of network excitability

As previously mentioned, a remarkable property of chick embryo spinal networks is their ability to recover their output during pharmacological blockade: block of glutamatergic and cholinergic transmissions engages compensatory mechanisms causing the recovery of rhythmic activity after a period of hours (Chub and O'Donovan, 1998). This phenomenon suggested that spinal network output might be homeostatically regulated.

Recent works on a wealth of developing neuronal systems, revealed the presence of homeostatic mechanisms involved in the maintenance of an adequate level of excitation of the postsynaptic target (i.e., neuromuscular junction, Davis and Goodman, 1998), in the modulation of the strength of excitatory and inhibitory connections or in the regulation of intrinsic excitability of individual neurons (i.e., neocortical cultures, Desai et al., 1999) in response to external perturbations. The effects of long-lasting changes in the level of neuronal excitability have been recently described in cultured mammalian neurons from various brain regions. Chronic block of synaptic transmission, over a period of days, in cortical dissociated cultures increases the amplitude of AMPA-mediated miniature currents at synapses between pyramidal cells without affecting miniature frequency (Turrigiano et al., 1998). This is a synapse-specific effect and it is not observed in bipolar interneurons subjected to the same chronic treatment. Chronic block of $GABA_A$ receptors induces the opposite phenomenon, namely the AMPA-mediated miniature currents appear significantly reduced in amplitude (Turrigiano et al., 1998). Similar results are obtained in hippocampal primary cultures chronically exposed to $GABA_A$ receptor blocker picrotoxin (Lissin et al., 1998). These changes in miniature event amplitude are due to changes in the number and/or properties of AMPA receptors at the postsynaptic site (Turriggiano et al., 1998, Lissin et al., 1998). However these findings are in contrast with previous reports of no changes in AMPA receptor clusters following chronic exposure to TTX or CNQX in spinal (O'Brien et al., 1997) and hippocampal primary cultures (Rao and Craig, 1997). A different

effect is observed in organotypic hippocampal cultures when the NMDA receptor-mediated transmission is chronically suppressed (McKinney et al., 1999). The frequency but not the amplitude of AMPA-mediated miniature currents in pyramidal cells is strongly increased suggesting a change in synapse number or an upregulation in the probability of release rather than postsynaptic modifications (McKinney et al., 1999). In summary, these recent results suggest that the level of neuronal excitability can be regulated in a homeostatic manner by long-lasting changes in synaptic activity (Craig, 1998, Turrigiano, 1999) and that this phenomenon may be functionally important during network development.

5. Spinal cord development

The nervous system begins to develop at a relatively late stage in embryogenesis. Prior to its formation, three main cell layers have been generated (Kandel et al., 2000). The endoderm -the innermost layer-, the mesoderm –the middle layer-, and the ectoderm –the outermost layer-, the latter gives rise to the major tissues of the central and the peripheral nervous system (fig. IIIA, IVA). During embryonic development of the central and peripheral nervous system several developmental processes can be distinguished. a) Neural ectoderm is induced by interactions with the mesoderm to define the neural plate (Garcia-Castro and Bronner-Fraser, 1999) b) The neural plate is generated as a columnar epithelium and is flanked by axial mesoderm cells of the notochord and paraxial mesoderm and is flanked by epidermal ectoderm (fig. IIIB, IVB). The induced neural plate then folds inwards and rounds up to form the neural tube (fig. IIIC, IVC) (Tanabe and Jessell, 1996). c) The neural tube generates roof plate cells at its dorsal midline and neural crest cells (NC in fig. IVC), which emigrate from the dorsal neural tube. The different neuron populations within the neural tube differentiate into specialized neurons and begin to establish functional neuronal circuits. d) Neuroepithelial cells proliferate and differentiate into neurons located at different dorsoventral positions: subclasses of commissural (C) and association (A) neurons differentiate dorsally, close to the roof plate, whereas motoneurons (M) and ventral interneurons (V) differentiate ventrally near to the floor plate (fig. IVD) (Tanabe and Jessell, 1996). Dorsal root ganglion neurons are generated from post-migratory neural crest cells (fig. IVD).

6. Temporal pattern of neurogenesis in rat spinal cord

The neurogenesis in the embryonic rat spinal cord has been studied with [^{3}H]thymidine autoradiography by Nornes and Das (1974). On the basis of the diameter of labeled neurons, these authors distinguished three categories of spinal neurons: large-sized neurons (diameter >30 μm, presumed motoneurons), medium-sized neurons (20-30 μm diameter), and small-sized neurons (diameter< 20 μm). They showed that neurons of the rat spinal cord are originated between E11 and E16. From a topographic point of view along the rostrocaudal axis, neurogenesis starts in the cervical region and systematically progresses caudally to the thoracic and lumbar regions of the spinal cord. Similarly, along the ventrodorsal axis neurogenesis starts in the ventral area and then progresses dorsally. At a cytological level, the large-sized motoneurons which are located primarily in the ventral horn, originate first (E11-13). With some time overlap, they are followed by the medium- and the small-sized neurons of the intermediate gray region (E12-15) and finally (E14-16) by the small-sized neurons in the dorsal region of dorsal horns, the substantia gelatinosa. Moreover the technique of [^{3}H]thymidine autoradiography provided information about migration pathways of neurons from the ventricular zone (where cells proliferate) and their subsequent settling in the intermediate zone (differentiating cells). The site of origin of the earliest forming neuron (E11) is the most ventral region of the ventricular zone (fig. VA). Later in development (E12-15) the ventricular zone exhibits a progressive regression in the dorsal direction (compare fig. VB, C, D). Motoneurons are organized in a continuous longitudinal column along the rostrocaudal axis on embryonic day E12, but by day E15 they appeared segregated in two clusters, one located ventrally and the other one intermediolaterally. Neurons of the intermediate gray region display limited migratory behavior. They originated initially from the ventral part of the ventricular zone, and as development continues, they gradually start to originate from more dorsal areas. The created neurons settle medially and dorsally upon their predecessors. Finally, the neurons of the intermediate gray region provide a substratum through and upon which substantia gelatinosa neurons migrate and settle.

At early postnatal stages the inner region of the spinal cord is formed by the gray matter mainly

consisting the nerve cells. The outer part of the spinal cord is formed by the white matter that mainly contains ascending and descending axons. The gray matter is divided in nine (I-X) laminae plus the gray matter surrounding the central canal. Such laminae were originally described by Rexed (1952) and are characterized by different morphological features.

7. Establishment of connectivity between dorsal root axons and their target motoneurons

The dorsoventral termination pattern of dorsal root ganglion (DRG) primary afferents in the adult spinal cord is well studied (Brown, 1981). In the adult rat spinal cord, primary afferents have been classified according to both their fibre diameter and their electrophysiological response properties. Small sized myelinated and unmyelinated afferents, many of which mediate noxious cutaneous sensory information, terminate predominantly on the most superficial regions of the dorsal horn, in laminae I and II. However, large sized cutaneous afferents terminate in deeper laminae III-V and primary (Ia) afferents, that mediate muscle monosynaptic reflexes, terminate deeper in ventral horns.

The lipid-soluble tracers DiI and Dia have been used to study interactions between dorsal root afferent axons and their target motoneurons in developing rat cervical spinal cord (Snider et al., 1992). In fig. VI (A, B, C) the development of dendritic arborization of motoneurons is shown in the cervical segment C5. Primary afferent (Ia) axons first penetrate gray matter at E15 in cervical segments of the spinal cord (fig. VID) (Snider et al., 1992). Axons enter gray matter in fascicles of 4-10 axons each. Between E15 and E17 these fascicles converge in the intermediate zone and extend to motor pools (fig. VIE). Projection of these afferent fascicles toward the ventral horn is not a random process. A rough topography is present between fascicles moving towards medially located axial motor pools and laterally located pools. Bundles predestined for medially located axial pools separate from other fascicles high in the intermediate zone and grow along the midline toward the axial motor pools (fig. VIE). Most Ia axons remain fasciculated until they are within the vicinity of the motoneuron cell bodies, then they defasciculate and elaborate boutons beginning on E17 (Snider et al., 1992). At postnatal day 5 (fig. VIF), the overall arrangement is similar to that at E17.

At E15 in lumbar spinal cord only few primary afferents enter the dorsal gray matter (Kudo and

Yamada, 1987). At E16, axons appear to consist of two main groups. One group of axons is distributed mostly in the dorsal horn and run (at stages E18-20) predominantly ventrolaterally or laterally. The other group of axons runs ventrally from the medial part of the dorsal horn towards the ventral horn forming a bundle and starts to penetrate into the motor nuclei at E17. In the later embryonic stages (E18-20), these axons establish an increasing number of synaptic contacts with motoneurons. These results have been obtained tracing dorsal root fibers with horseradish peroxidase in the fourth lumbar (L4) segment of embryonic spinal cord at different stages of development (Kudo and Yamada, 1987). Electrophysiological experiments support these morphological results (Kudo and Yamada, 1987, Ziskind-Conhaim 1990). When L4 dorsal root is electrically stimulated, responses to the stimulation can be recorded from motoneuronal pool in the L4 ventral root (fig. VII). At E15 no evoked ventral root potentials are recorded, while evoked responses from L4 ventral roots are reliably recorded starting from E17. In particular at E19 (fig VII), the evoked potential shows a shorter latency than the one recorded at E17 and E18. This suggests that monosynaptic contact from primary afferent fibers to motoneurons starts to be present at E18 (Kudo and Yamada, 1987, Ziskind-Conhaim 1990).

8. Rhythmic patterns elicited by drug application in the rat spinal cord

Early progress in defining the locomotor circuits of the spinal cord originates from studies of locomotor behavior in decerebrated cats *in vivo* (Grillner and Zangger, 1979, Barbeau and Rossignol, 1991) that have shown that locomotor patterns can be evoked in the absence of inputs from higher brain centers and feedback from sensory afferents (Grillner, 1981). A wealth of studies on several different species of vertebrates and invertebrates, support the idea that locomotor rhythms are generated by the spinal cord through local neuronal networks termed central pattern generators (CPGs). These spinal networks consist of an ensemble of spinal interneurons that provide the timing of motoneuron discharge even in the absence of external feedback.

In the last years, the necessity to study cellular properties, network mechanisms and development of CPG in details led to the expansion of *in vitro* preparations from several vertebrate species. These *in vitro* preparations provide a better use of pharmacological tools to

trigger and modulate rhythmic patterns and allow the study of underlying cellular and synaptic mechanisms as well. Spinal pattern generation has been deeply investigated in spinal preparation from lower vertebrates such as the lamprey (reviewed by Grillner et al., 1991) and the Xenopus embryo (Dale and Roberts, 1984). These two preparations represent the better understood models for the generation of locomotor patterns in vertebrates and a comparable knowledge of pattern generation mechanisms in mammals has not been yet obtained.

Recent advances in understanding central pattern generation has been achieved using the *in vitro* spinal cord preparation of the neonatal rat, this preparation survives for several hours *in vitro*. Furthermore the actions of various drugs can be directly studied because they have direct access to neurons in a structure without blood brain barrier. The isolated spinal cord from neonatal rat with the hindlimbs attached has been used by Kudo and Yamada (1987) to study the pattern of activity generated by application of N-methyl-D,L-aspartate (NMA). Electromyographic recordings from extensor and flexor muscles on both sides of the spinal cord, during the application of NMA revealed a locomotor-like activity consisting in alternation of flexor and extensor muscles on both sides of the spinal cord. Rhythmic left and right episodes are alternating as well. This pattern of activity which is independent from the inputs coming from periphery afferents and higher brain centers is termed "fictive locomotion" (Rossignol, 1996). The frequency of this pattern increases in each muscle when the concentration of NMA is increased while the alternating feature of this pattern remains the same. Cazalets and colleagues (1992) studied the CPG for locomotion using the *in vitro* isolated brainstem-spinal cord preparation from neonatal rats. In this study N-methyl-D-aspartate (NMDA) or serotonin (5-HT) induced alternating bursts of action potentials recorded either from the hindlimb muscles (when legs were left attached) or at the level of the lumbar ventral roots. These alternating patterns showed a strong frequency dependence on the concentration of the agents, in fact burst frequency strongly increased with increasing doses of NMDA or 5-HT. Moreover this study shows that the lumbar ventral root L5 contains mainly axons of flexor motoneurons while L2 contains mainly extensor ones, thus they can be used to observe and record fictive locomotion activity. A more detailed electromyographic study of locomotor activity induced by application of 5-HT has been performed by Kiehn and Kjaerulff in 1996. In this work the

authors recorded motor activity from many extensor and flexor muscles of hip, knee, ankle in hindlimb-attached spinal cord preparation. In the presence of 5-HT the neonatal rat preparation display muscle phasing very similar to that observed in the adult. While in a percentage of cases the application of NMDA or 5-HT induces irregular or transient rhythmic patterns, the combination of NMDA and 5-HT evokes a very stable locomotor-like rhythmic activity with a frequency intermediate between that of NMDA or 5-HT alone (Sqalli-Houssaini et al., 1993). Another way to induce alternating well-coordinated rhythmic activity in the spinal cord consists in increasing the extracellular K^+ concentration in order to induce membrane depolarization in the spinal circuitry (Bracci et al., 1998). Following relatively small increases of extracellular K^+ (8 mM is the threshold for generating this pattern of activity) rhythmic bursts appear in left and right L2 or L5 ventral roots (fig. VIII, left) and simultaneous recordings from L2 and L5 displayed alternated rhythmic bursts characteristic of locomotor activity. The periodicity of rhythmic activity elicited by high K^+ depended on K^+ concentrations and it ranged from 1 and 2 sec, an interval comparable to that observed during fictive locomotion induced by NMDA and 5-HT (fig. VIII, right).

9. Development of CPG

Little is known about the functional development of the CPG in the prenatal period, however Kudo and coworkers studied the spatial and temporal changes of rhythmic motor activity chemically induced by NMDA and serotonin in the developing embryonic rat spinal cord (Ozaki et al., 1996, Kudo et al., 1991, Iizuka et al. 1998). Bath application of NMDA receptor agonists, such as NMA or NMDA, induces rhythmic activity in both left and right sides from E16 to birth. This rhythmic pattern is a network driven phenomenon evoked by chemical synapses from interneuronal circuits activated through the NMDA receptors. The frequency of this pattern of activity increases with embryonic age and at any age, the frequency depends upon drug concentration (Ozaki et al., 1996). At E16-E17 bath application of NMDA induces synchronous rhythmic bursts in ventral roots on the two sides of the spinal cord. The phase relationship of rhythmic discharges is variable at E18-E20 and three types of patterns are observed: alternating, synchronous and inconsistent. Stable alternated rhythmic activity in the

left and right ventral roots is evoked in E21 preparations by application of NMDA. The same stable pattern of rhythmic episodes with left-right alternation is recorded in newborn rats, even though the frequency is higher. It seems that glycinergic transmission is crucial in generating alternating rhythmic activity in prenatal rats. In fact at early stages of embryonic development, when NMDA induces synchronous episodes, addition of strychnine (that blocks glycine receptors) does not affect neither frequency nor the duration of rhythm. At E18-E20, when phase relationship of NMDA-induced rhythm is variable, addition of strychnine always induces synchronization. At E20 addition of strychnine causes the alternating rhythmic episodes in left and right ventral roots to synchronize, an effect similar to that observed in neonatal rats (Cowley and Schmidt, 1995).

10. Localization of neural networks responsible for locomotor activity

A critical stage in understanding the organization and developmental operation of premotoneuronal networks responsible for locomotor activity requires their localization. One way of mapping these networks is to label or monitor ensembles of neurons during patterned activity. Using the activity-dependent label sulforhodamine during locomotor-like activity in the *in vitro* rat spinal cord Kjaerulff et al. (1994) found consistent labeling in the medial intermediate gray matter and close to the central canal. This method however does not allow a dissection between labeled areas containing CPG networks and areas containing neurons driven by the CPG activation. A more direct method to investigate the localization of CPG networks consists in selective lesioning the spinal cord. With this technique in 1993 Ho and O'Donovan had shown that the ability to generate rhythmic activity is distributed along the lumbosacral spinal cord of the chick embryo and may be functional within a single segment. Rhythmic activity with alternation between left and right ventral roots is preserved in the isolated ventrolateral quadrant of the cord suggesting that networks in this region were sufficient to generate locomotor-like patterns. They found also that certain lesions result in abolition of the alternation without altering motoneuronal rhythmic activity. These results led to the remarkable finding that different mechanisms control rhythm generation (the production of periodic activity in motoneurons) and pattern generation (the timing and phasing of flexor and extensor

motoneuronal pools). Calcium imaging experiments confirmed these results supporting a ventromedial localization of rhythmogenic areas in the chick embryo spinal cord (O'Donovan et al., 1994). The conjecture about distributed CPG networks in the spinal cord of rat has been challenged by Cazalets in 1995. Exploiting the *in vitro* conditions of the neonatal rat, lumbar spinal cords are partitioned by building vaseline walls at various rostrocaudal levels. When segments L1 and L2 are exposed to a mixture of NMDA and 5HT, rhythmic locomotor-like activity is recorded in all lumbar segments. In contrast, when the same combination and concentration of drugs are bath applied to the lower lumbar segments (L3 to L6), only tonic discharges are observed in these segments and no activity in L1 and L2. These and other observations led the authors to conclude that in the rat spinal cord the network responsible for rhythmic activity is located between the thoracic segment T13 and L2, while the lower lumbar segments, containing most of motoneurons innervating hindlimbs, do not participate at all in spinal rhythmogenesis (Cazalets et al., 1995). This view contrasted with previous results on neonatal rats showing that the isolated L4 and L5 segments could produce an alternating activity in ankle flexors and extensors when the cord was exposed to NMA (Kudo and Yamada, 1987). A series of subsequent experiments supported these last findings producing results incompatible with the hindlimb locomotor CPG being restricted to L1 and L2 in the rat. Thus Kjaeruff and Kiehn (1996), with lesion experiments, showed that rhythm and pattern generation is not restricted to one or two rostral-lumbar segments but extend to more caudal lumbar segments and to thoracic segments as well (fig IX). However the amplitude and frequency of motor output are lower in the caudal lumbar segments compared with the rostral ones. Moreover the most important areas for rhythmogenesis are localized in ventral horns and are concentrated in the medial part (Kjaeruff et al. 96, fig. IX) rather than in the lateral one as in the chick embryo. Kremer and Lev-Tov (1997) obtained essentially similar findings. Different sets of experiments on spontaneous rhythmic activity in the neonatal spinal cord evoked by coapplication of strychnine and bicuculline (fig. X), reveal that the neuronal circuitry necessary to generate this rhythmic activity is located at the level of the ventral quadrant as well (Bracci et al., 1996b).

Taken together these results indicate that the rhythmogenic network controlling locomotor activity in the neonatal rat is distributed along the spinal cord and show a rostrocaudal gradient in the ability to generate rhythmicity.

11. Mechanisms for rhythm and pattern generation in the spinal cord

Although there is a wealth of information on localization and pharmacology of the spinal CPG, the cellular properties and network mechanisms underlying rhythmogenesis and the development are still elusive. Many mechanisms have been proposed for the generation of rhythmic activity in spinal neurons. One of the models proposed is based on the half-center hypothesis postulated by Brown in 1911 to explain the reciprocal activation of flexor and extensor muscles in the cat. All the neurons related to the flexors of one limb are lumped into a flexor module; all the neurons related to extensors of the same limb are lumped into the extensor module. Reciprocal inhibition between modules is hypothesized to be the main mechanism for rhythmogenesis and alternation ensuring that when one module is active the other is silent. In this way each 'half-center' by itself is not a rhythm generator. A strict bipartite organization of the motor output is implied: co-activation of all limb flexors alternates with co-activation of all extensors. The half-center model fails to account for behaviors in which there is co-activation of the flexors at one joint with the extensors at another joint. Several modifications of the classical half-center model have been proposed to account for more complex motor outputs. Grillner's 'unit burst generator' model is an important refinement and expansion of the half-center model (Grillner, 1981) and it is efficient for the description of CPGs underlying swimming in the Xenopus embryo and lamprey. In these animals spinal CPG is thought to be distributed along the cord in "unit-burst" and each spinal segment contains a pair of half-centers that generate alternating activation of the two sides of the cord (Grillner and Matsushima, 1991). This model could account for the swimming program of tadpole and lamprey consisting of left and right alternation of motoneurons at each segmental level. In mammals, on each side, also flexor-extensor alternation is present, thus models including reciprocal inhibition should consider that more than two pools should be linked by this kind of

relation or that left-right alternation and extensor-flexor alternation may be produced by different mechanisms (Sernagor et al., 1995).

In the neonatal rat spinal cord the alternating rhythmic motor activity evoked by NMA became synchronized following block of glycine receptors (Kudo et al., 1991). An analogous phenomenon is observed in rat embryos from stage E17 in similar pharmacological conditions (Nishimaru et al., 1996). These observations taken together suggest that spinal inhibition is important for alternation between limbs but not for rhythm generation itself, which probably rely on different mechanisms. This notion is supported by a recent study showing that in the neonatal rat spinal cord block of Cl^--mediated transmission elicits a consistent pattern of slow rhythmic bursts (Bracci et al. 1996a). The role of GABA in reciprocal inhibition is less clear. Cazalets and others (1994) found that the block of $GABA_A$ receptors does not prevent the reciprocal inhibition but rather increases the frequency of fictive locomotion activity. These results, however, are in contrast with observations by Cowley and Schmidt (1995), who showed that $GABA_A$ receptors are involved in reciprocal inhibition.

Another proposed mechanism for the generation of rhythmic activity in the rat spinal cord is based on pacemaker neurons. In a thin slice preparation of the neonatal rat spinal cord Hochman et al. (1994) demonstrated that high concentrations of NMDA induce TTX-resistant, membrane potential oscillations in a small percentage of neurons, located around the central canal. However since this slice preparation lacks rhythmic activity, it was not possible to establish the role of such intrinsic oscillators in the patterned locomotor activity. Membrane potential oscillations, induced by application of NMDA, have been detected also in the isolated neonatal rat spinal cord preparation (Kiehn et al., 1996) during rhythmic locomotor-like activity. Only a minority of interneurons (12%) possesses TTX-resistant oscillations induced by NMDA and the role of such cells in the generation of locomotion is still unknown. In fact it seems that they are not rhythm generators by themselves because in the absence of extracellular Mg^{2+} these NMDA-induced oscillations are abolished while locomotor activity is still present (Kiehn et al., 1996). Recently TTX-resistant oscillations are recorded in ventral roots of the neonatal rat spinal cord, in the presence of NMDA and serotonin (Tresch and Kiehn, 2000). These 'action potential-independent' oscillations are synchronous across a population of motoneurons and are

mediated by gap junctions. Even though such a rhythmic activity is detected in all lumbar ventral roots, there are no temporal correlation between the oscillations of different ventral roots either ipsilateral or contralateral to one another (Tresch and Kiehn, 2000). The latter feature suggests that this gap junction-coupled motoneuronal network is unable to support, *per se,* the production of locomotor-like activity in the spinal cord. Nevertheless a possibility is that during locomotion either intrinsic interneuronal oscillations (Kiehn et al., 1996) and gap-junction mediated motoneuronal rhythms (Tresch and Kiehn, 2000) can contribute to rhythmogenesis in the neonatal rat spinal cord.

The precise mechanisms for termination of spontaneous rhythmic activity in the spinal cord and the factors that control the duration of quiescent periods are not fully understood. One of the proposed mechanisms is synaptic depression (Streit, 1993, Fedirchuk et al., 1999, O' Donovan, 1999). Motoneurons in the organotypic cultures of embryonic rat spinal cord, exhibit regular bursts of synaptic potentials after block of Cl^- mediated inhibition (Streit, 1993). After each burst there is a correlation between the burst length and the preceding interburst interval, although no correlation has been observed between burst length and the following interval. The same phenomenon has been studied also in the chick embryo spinal cord (Tabak and O'Donovan, 1998) where it has been concluded that the interval between bursts acted as a recovery period. In other words, if the network triggers a burst before synaptic depression has fully recovered, then the episode will be short, while if episode generation is delayed, there will be recovery from the depression and the episode will be long. On the basis of these experimental observations, modeling studies have shown that a purely excitatory network with no well-structured synaptic connectivity underlying synaptic depression was able to generate rhythmic oscillations (Senn et al., 1996). Recently, a more general model has been described that can account for the occurrence of spontaneous rhythmic episode, rhythmic oscillations within a single episode and the developmental changes in episode duration and frequency in the chick embryo spinal cord (Tabak et al., 2000).

12. Perspectives

The previously mentioned results, highlight several features of spinal circuitry activity. Rhythmic and patterned activity in the isolated *in vitro* spinal cord have mainly been investigated at the level of motoneurons that represent the output element of CPG activation. The CPG is composed by networks of interneurons but, despite the importance of these cells, very little is known about their development, role and operation in functional spinal circuits. The present study aims at investigating the operation of spinal interneuronal networks in organotypic slice cocultures from embryonic rat spinal cord. This *in vitro* system provides an easy access to single neurons in a structure that maintains the basic cytoarchitecture of a spinal segment. Furthermore such an approach could also provide information concerning spinal network activity during development. In particular the present results should contribute to answer the following questions:

a. Are ventral horn interneurons able to generate rhythmic activity in *in vitro* conditions?
b. Is it possible to identify the minimal neuronal circuitry involved in the generation of such a rhythmic activity?
c. What are the properties governing these rhythmic oscillations and are these oscillations similar to those observed in the rat isolated spinal cord?
d. How do ventral interneuron rhythmogenic properties change during *in vitro* development?
e. Are ventral interneurons able to generate synchronous activity in response to different agents known to induce spinal rhythms?
f. What is the role of ionotropic glutamate receptors in the occurrence of spontaneous and rhythmic activity?
g. Finally, is homeostatic plasticity present at the level of ventral interneurons? How do homeostatic compensatory mechanisms affect spontaneous and rhythmic activity in ventral interneurons?

METHODS

1. Preparation of organotypic co-cultures

Organotypic cultures are an *in vitro* preparation that provides a good experimental access to individual neurons that can be visually and morphologically identified in a structure that maintains the basic synaptic organization of the explanted tissue. The Maximov culture (Crain, 1976) and interface culture (Stoppini et al., 1991) techniques, in which organotypic slices are incubated stationary, yield organized tissue cultures which remain many cell layers thick, even after prolonged time of incubation (Crain, 1976, Gähwiler, 1984). The roller-tube technique (Gähwiler, 1981) is a suitable method to obtain remarkable spreading and flattening cultures after few weeks *in vitro*, in fact individual nerve cells are often arranged in a monolayer.

In the present work co-culture of spinal cord and dorsal root ganglia are obtained with the roller-tube technique using a method similar to that described by Braschler (Braschler et al., 1989). The following points describe in details the main steps of the culturing procedure (see fig. XI).

Explantation

Pregnant rats (Wistar) are anaesthetized by intraperitoneal injection of chloral hydrate (10.5%, 0.4 ml/100g). Foetuses are delivered by caesarean section at embryonic day 13-14 (E13-E14). The day on which the vaginal plug is first detected is designated embryonic day E1. The embryos with their intact amniotic sacs are freed from the wall of the uterus and put in a Petri dish containing cold (+4°C) Hanks solution. The following dissection is then carried out under a laminar flow hood in sterile conditions and under microscope (Olympus SZ40) control. Through a small cut in the amniotic sac embryos are freed and placed into a Petri dish with fresh Hanks, here they are decapitated and their tails and legs cut away (fig. XIA). The inner organs are carefully removed and then backs are cut into 275 µm-thick slices with a tissue chopper (McIlwain) (fig. XIB). These transverse sections of the backs are put into a Petri dish with Hanks. Spinal cords with their dorsal root ganglia attached are separated from the rest of the slice (fig. XIC) with a blade and transferred in a new Petri dish with Hanks (fig. XID) and then maintained at + 4°C for an hour.

Hanks solution contains (g/l): $CaCl_2 \cdot 2H_2O$ 0.185, KCl 0.4, KH_2PO_4 0.06, $MgCl_2 \cdot 6H_2O$ 0.1, $MgSO_4 \cdot 7H_2O$ 0.1, NaCl 8.7, $NaH_2HPO_4 \cdot 2H_2O$ 0.06, Glucose 1. The pH is 7.4 and the osmolarity 296 mOsm.

Embedding

After an hour (in Hanks at + 4°C) single slices are placed in a drop (20 µl) of reconstituted chicken plasma (Cocalico) on a glass coverslip (fig. XIE). To keep the slices in place, the plasma is coagulated by addition of a drop (30 µl) of thrombin (Sigma-Aldrich). The plasma clot is coagulated for 30-45 min then coverslips are placed into tubes (Nunc) (fig. XIF).
Lyophilized chicken plasma is diluted in distilled water and then is centrifuged (Biofuge 15R, Heraeus) for 20 min at + 4°C at 3500 rotation per min. Lyophilized thrombin (Merck) is diluted in distilled water (200 u/ml).
Prior to use glass coverslips (12x24 m, thickness 1mm, Vitromed) are treated as follows: they are inserted in a teflon holder, submerged in hydrochloric acid 0.5 N for 24 h, repetitively washed with distilled water and soaked for 30 min in absolute alcohol; coverslips are then dried and sterilized at +150°C in a oven over night.

Medium and medium change

The coverslips bearing the slices are inserted in plastic tubes which contain 1 ml of nutrient medium (fig. XIF-G). The standard medium consists of 82 % Dulbecco modified Eagle medium (DMEM, Gibco), 8% sterile water (Gibco), 10% fetal bovine serum (Gibco), 5 ng/ml nerve growth factor (Alomone) diluted in Hanks and BSA (1mg/ml); the pH is 7.35 and osmolarity 300 mOsm. The first five days in culture at this standard medium is added 1% antibiotics-antimicotics (Gibco) and 15 ng/ml nerve growth factor. After this period the old medium is replaced with fresh, standard one with the addition of 0.1% antimitotics (Cytosine arabinoside, Fluoro-deoxyuridine, uridine, Sigma). After 24 h the medium is replaced with standard one which is replaced weekly.

Incubation

Following the addition of the medium, tubes are immediately placed in a roller drum (fig. XIH) which rotates approximately at 120 revolutions/h. Rotation is essential for feeding,

aeration and flattening of the cultures, so cultures are submerged in medium during half a turn and covered with a film of medium for the other half.

Cultures are incubated at +36.5 °C in dry atmosphere.

Slices are kept in culture for more than one month, however most of the electrophysiological and immunohistochemical experiments have been carried out within the first three weeks.

Flattening of the tissue

Flattening and spreading of the tissue during cultivation is important for visualization of single neurons. The degree of spreading depends on several factors such as rotation, tissue of origin and thickness of the original slice. Rapid rotation moreover caused the plasma clot to be washed away from the slice more rapidly allowing a better access to individual neurons for electrophysiological recordings. The speed of 120 revolutions per hour produces an adequate flattening of these spinal co-cultures. In fact it has been possible to estimate the degree of multilayer organization after two weeks in culture by confocal laser scanning microscope. For this purpose, slices are treated with propidium iodide (1 mM in phosphate buffered PBS supplemented with 0.4 mg/ml RNAse A) which marks cell nuclei. Their fluorescence is elicited by excitation with an Ar-Kr laser at 568 nm, using a rhodamine filter set, and detected with a photomultiplier tube of a Multi Probe 2001 confocal laser scanning microscope (Molecular Dynamics, Sunnyvale, CA, USA). A vertical scan of the slice culture reveals 3-4 cell layers through the spinal culture while dorsal root ganglia always flattened into a single layer of neurons.

2. Morphology

The spinal cord preserves its organotypic configuration *in vitro*. After two weeks in culture the slice appears as in fig. XIIA; the orientation of the spinal cord is clearly marked by the dorsal root fibres and by the central fissure (fig. XIIA, open arrow) which allows distinguishing ventral horns.

Dorsal root ganglion cells

At the day of explantation (E13-E14), DRG are located very closely to the spinal cord to which they are connected by very short dorsal roots. During the *in vitro* development the

DRG migrate and move away from the spinal cord elongating the dorsal roots and flattening into monolayers. The DRG cells are easily identified on the basis of their morphology: cell bodies display a large polygonal profile. Patch clamp recordings (current clamp mode) show that DRG cells had no spontaneous synaptic activity and they fire action potentials occasionally.

To test functional connections between DRG and spinal neurons, DRG cells are extracellularly stimulated using a bipolar focal electrode and evoked synaptic currents are recorded from ventral interneurons (fig. XIV). The extracellular low-resistance electrode is placed on a group of DRG cells and short voltage pulses are applied every 20s by mean of a Digitimer stimulator. Evoked synaptic currents are recorded from ventral interneurons patch-clamped in whole cell configuration and held at different membrane holding potentials. The transmission from DRG cells to interneurons involved mainly polysynaptic pathways as suggested by the latency (35 ± 4 ms) and by the shape of the evoked currents (fig. XIVA). Note that, for membrane potential held at -56 mV, evoked currents are inward, at -30 mV they have an early inward component followed by an outward one and at 0 mV they are completely outward, suggesting that they are made up by glutamate mediated multications currents as well as GABA and glycine mediated Cl^- currents.

Identification and morphology of interneurons and motoneurons

The aim of this work is to study spontaneous synaptic activity from ventral interneurons in the organotypic spinal cultures, their ability to generate synchronous activity and their plasticity properties. Ventral interneurons are visually identified on the basis of the following morphological criteria. First they are located in ventral horns which are identified by the central fissure (see arrow in fig. XIIA), second they have a diameter shorter than 20 μm and finally they are monopolar or bipolar cells. In fig XIIB an example of ventral interneuron filled with Lucifer Yellow (1.5 mg/ml, Sigma) is shown. Note the small diameter of its oval cell body. Another example of ventral interneuron (stained with biocytin 0.2%) is shown in fig. XIIIE. The stained cell displays a characteristic morphology with small cell body and widespread dendritic arborization.

In order to localize motoneurons, organotypic spinal co-cultures are stained using the choline acetyltransferase (ChAT) immunocytochemical technique (fig. XIII). Positive neurons are often localized on both sides of the central fissure and their large, multipolar

cell body suggests that these cells are motoneurons (fig. XIIIA-B). Fig. XIIIC shows an example of double staining in a culture at 14DIV: a ventral interneuron (arrowhead) is filled with byocitin during electrophysiology, then the slice has been processed for the ChAT and a presumed motoneuron is stained (arrow). Note that the ventral interneuron (fig. XIIIE) is ChAT-negative and display a small, round cell body while the positive cell (fig. XIIID) shows a large, triangle-shaped soma with multipolar dendritic prolongation.

3. Immunohistochemical staining

Acetylcholinetransferase staining

Cultures grown two weeks *in vitro* were fixed for 1 h with 4% paraformaldehyde in PBS, washed in PBS and treated with 2.3% Na metaperiodate in H_2O for 5 min at room temperature. After a rapid wash in H_2O, cultures were maintained in 1% Na borohydride in 100 mM Tris/HCl (pH 7.5) for 10 min followed by a wash in PBS + 0.1% Tween 20 (PBST) and incubation overnight at +4°C with goat antiChAT polyclonal antibodies (Chemicon Int., Temecula, CA) diluted 1:200 in 10% FCS in PBST. After several washes in PBST cultures were incubated in biotinylated anti-goat IgG antibody (Vector, Burlingame, CA) diluted 1:100 in 10% FCS in PBST. Two hours later the reaction was revealed with the ABC kit (Vector).

Interneuron staining

Putative interneurons were patch clamped and filled intracellularly with biocytin (0.2 %) for about 60 min; the stain was developed using the ABC kit.

4. Electrophysiological recordings

For electrophysiological experiments, a coverslip with a culture is placed in a Perspex chamber mounted on the table of an inverted microscope (Nikon TE200).

The organotypic culture is constantly superfused with standard Krebs and the flow is 5 ml/min. All experiments are carried out at room temperature (22 ± 2 °C).

Patch clamp whole cell recordings: voltage clamp

Individual neurons are patch clamped with micropipettes pulled from thin-wall borosilicate glass capillaries (Clark) by mean of a two steps puller (List-Medical); tip resistances are 5-7

MΩ when filled with the intracellular solution. To record currents an EPC-7 amplifier (List) or Axopatch 1D (Axon Instrument) are used allowing clamp of the membrane potential at constant values. Usually the membrane potential of interneurons is held at –56 mV, a value close to their resting membrane potential (-58 ± 7 mV) measured in current clamp conditions with zero current injection. Membrane potential values are systematically corrected for the liquid junction potential. After the formation of a Gigaohm (1-2 GΩ) seal the capacitance of the pipette is cancelled and after breaking through the membrane no series resistance compensation is adopted cause its value is usually below 15 MΩ (12 ± 4 MΩ) and no distortion in synaptic events is observed. Cell input resistance is assessed after the establishment of whole cell configuration and during the experiment by the pCLAMP software and varies from 300 to 400 MΩ depending on the cell. An example of spontaneous synaptic currents is shown in fig. XIIB where synaptic events are recorded in standard solution from the same ventral interneurons labeled above.

During experiments data are stored on videotape for further analysis, digitized at 20 kHz with pClamp software (Axon Instruments, version 6.2) and displayed on a chart recorder.

Patch clamp whole cell recordings: current clamp

Current clamp experiments are carried out using the same type of glass capillaries used in voltage clamp. Current is injected in the cell by means of an Axoclamp-2B (Axon Instruments) amplifier. When the electrode was placed in the bath its resistance is balanced in the bridge mode (fig. XIVB) and capacitive transients are minimized by negative capacitance compensation. In current clamp conditions, spiking cell activity is monitored. In fig. XIVB a ventral interneuron is injected with either a hyperpolarizing current pulse (-0.05 nA, 500 ms duration) or a depolarizing one (+0.04 nA, 500 ms).

When a positive current pulse is injected in the cell, the membrane potential reaches the threshold and fires an action potential as shown in fig. XIVB. Note the spike overshoot, which represents an evidence of cell viability, and the presence of a fast (≤50 ms) after-hyperpolarizing potential, which was not routinely observed and investigated in the present thesis. Fig. XIVC shows an example of train of spikes, evoked in a ventral interneuron (resting membrane potential around -56 mV) by injection of a depolarizing current pulse

(+0.04 nA, 500 ms), note the absence of spike accommodation and the presence of superimposed spontaneous activity.

Extracellular recordings

Extracellular field potential recordings are performed with a micropipette of 2-4 MΩ filled with NaCl 2 M. The pipette is placed on the culture and field potentials are amplified with an Axoclamp-2B (Axon Instruments), stored on a video tape and displayed on a chart recorder.

Extracellular electrical stimulation

Extracellular focal stimulation of DRG cells is performed with low resistance pipettes (1 MΩ) containing the standard extracellular solution. The pipette is placed on DRG cells and positive voltage pulses 100 μs long are delivered by a Digitimer stimulator at 0.05 Hz. Usually the stimulation intensity was increased until it reached the threshold for evoked currents and then fixed to a value slightly higher. Evoked currents are acquired and analyzed with pCLAMP software.

5. Solutions

Extracellular solutions

The standard Krebs extracellular solution contains (mM): NaCl 152, KCl 4, $CaCl_2$ 2, $MgCl_2$ 1, HEPES 10, Glucose 10. The pH is adjusted to the value 7.4 with NaOH and the osmolarity is 305 mOsm.

In the experiments with high $[Mg^{2+}]_O$ and low $[Ca^{2+}]_O$, the concentration of $MgCl_2$ is increased to 2.5 mM while that of $CaCl_2$ is lowered to 0.5 mM.

In nominally Mg^{2+} free solution, $MgCl_2$ is omitted and the concentration of NaCl is increased to 154 mM or $CaCl_2$ increased to 3 mM.

Intracellular solutions

a) The intracellular solution most frequently used contains (mM): potassium gluconate 120, KCl 20, $MgCl_2$ 2, Na_2ATP 2, HEPES 10, EGTA 10. The pH is adjusted to 7.35 with KOH and the osmolarity is 295 mOsm.

The liquid junction potential between the extracellular and intracellular solutions has been measured by mean of an Agar bridge and its value is 11 mV.

According to the Nernst equation, assuming that the Cl^- concentration inside the cell is the same than in the patch pipette solution, the ionic equilibrium potential for Cl^- is -49 mV. To test the precision of this theoretical value, we experimentally measured the reversal potential for current induced by exogenous application of GABA (fig. XV). Recordings are made in the presence of 1 μM TTX to block synaptic transmission and 0.1 mM GABA is added to the bath at different membrane potentials. The current evoked by GABA application was inward at -56 mV (fig. XVA, top), slightly outward at -30 mV (fig. XVA, middle) and outward with a large amplitude (fig. XVA, bottom) at -20 mV. Plot in fig. XVB shows the amplitude of the GABA-induced current at different membrane holding potentials, in the same cell as in fig. XVA and reveals a reversal potential around -40 mV. The outward rectification present at –20 mV Vh (fig XVB), was not routinely observed and it might be due to an increase in the probability of $GABA_A$ receptor channel opening at depolarized potentials (Bormann et al., 1987, Kaila, 1994). The permeation of K^+ through $GABA_A$ receptors could also contribute to that rectification, however in the spinal cord it has been shown that K^+ permeability through $GABA_A$ receptors is very low (Bormann et al, 1987). On a sample of $n = 6$ cells, the averaged reversal potential for GABA is -38.8 ± 1.9 mV. After correction for liquid junction potential, such a value for Cl^- reversal potential results close to the theoretical one.

b) In a group of experimental settings, low Cl^- intracellular solution is used containing (mM): potassium gluconate 140, $MgCl_2$ 2, Na_2ATP 2, HEPES 10, EGTA 10, QX-314 0.5. The pH of the solution is adjusted to 7.35 by addition of KOH.

The liquid junction potential, measured with the Agar bridge, is 17 mV.

The reversal potential for Cl^- calculated with Nernst equation now is -95 mV, a value not corresponding to the experimental one. In fact, following the same procedure described below, the reversal potential of GABA is -63 ± 3 mV ($n = 3$). Taking into account the junction potential value, the experimental Cl^- reverse is around -80 mV, which is more positive than predicted. A similar discrepancy has been found by Sernagor (Sernagor et al., 1995) recording from chick embryo motoneurons. A possible explanation for this

divergence consists in the improper assumption that intracellular chloride concentration is equal to the Cl^- concentration inside the pipette. Another possibility is that other ions with equilibrium potentials more positive than that for Cl^- contribute to GABA-induced responses. This issue is not addressed in the present work.

6. Drugs

Drugs were bath applied through the perfusion solution. Stock solutions of the agents were made usually at concentration 10^3 higher than the final ones and stored at –20C. The final concentration was obtained adding an amount of the stock solution to standard Krebs. The effects of drugs started to be detectable after about 30 s from the application, however they were measured at steady state (10 min). High extracellular K^+ solution was obtained by adding the required amount of KCl 1mM to standard Krebs solution.

The following drugs were used:

Strychnine nitrate (Sigma-Aldrich),

Bicuculline methiodide (Sigma-Aldrich),

3-((RS)-2-carboxy-piperazine-4-yl)-propyl-1-phosphonate (CPP) (Tocris),

6-Cyano-7-nitroquiloxaline-2,3-dione disodium salt (CNQX) (Tocris),

6,7-Dinitroquinoxaline-2,3-dione (DNQX) (Tocris),

N-Metyl-D-aspartate (NMDA) (Tocris),

5-Hydroxytryptamine (5-HT) (Sigma)

(S)-α-amino-3-hydroxy-5-methyl-4-isoxazolepropionic acid (AMPA) (Tocris)

Tetrodotoxin (TTX) (Affinity)

γ-aminobutyric acid (GABA) (Sigma-Aldrich)

Glycine (Sigma-Aldrich)

QX-314 (Alomone)

7. Chronic treatments

For experiments involving chronic treatments, organotypic cultures were incubated at 6 DIV in medium containing either 10 μM CNQX, or 1 μM TTX or 1 μM strychnine plus 20 μM bicuculline. At day 13, namely after 7 days in the presence of these drugs, the medium was replaced with fresh one without any blockers for 2-24 h before recordings. This variable washout period did not introduce significant changes to the effects induced by

chronic treatment. Synaptic changes induced by these chronic treatments progressively attenuated after 3 days from washout. Control culture, namely untreated cultures, were subjected to the same medium changes without addition of any blockers. Treated and untreated cultures coming from the same culture group are called 'sister cultures'.
To check whether the blockers after one week into the culture medium conserve their properties, they were diluted in standard Krebs at the appropriate final concentration and stored for 7 days at room temperature. These solutions were subsequently used during patch clamp experiments on control cultures and the efficacy of blockers was checked. In each case the solutions containing the blockers retained their pharmacological properties, namely they were able to induce the same changes in synaptic activity as acutely applied.

8. Data analysis

The analysis of spontaneous and miniature postsynaptic currents is performed using the Axograph 3.5.5 program (Axon Instrument). To identify the events the program uses a detection algorithm based on threshold in amplitude or on a sliding template (Clements and Bekkers, 1997). The 'template' function has a flat baseline region followed by an idealized synaptic time course consisting of an exponential rise time and decay time, and given amplitude. The 'template' function is fixed on the bases of kinetics of spontaneous currents, then it is moved along the data trace one point at a time and scaled to fit the data at each position. The detection criterion is calculated from the template scaling factor and how closely the scaled template fits the data. Detected events are captured and aligned at their onset. Moreover the program allows to reviewing selected events one by one, so events which appears as summated responses or are superimposed on a large event are discarded. On average 200-600 single PSCs and 50-100 miniature PSCs (mPSCs) are analyzed from each cell and the average time course is calculated. Usually from this average synaptic event rise time (from 10 to 90% peak amplitude) decay time and peak amplitude are calculated.
The analysis of rhythmic activity requires the definition of burst and its measurement. A burst is defined as a period of sustained inward current originating with rapid onset from baseline and having peak amplitude higher than 20 pA. Rhythmic activity is characterized by cycle period (CP) and burst duration (BD). Cycle period is defined as the time between two consecutive bursts, set at onset, and the duration is the time from the burst onset and 80-90% of its baseline recover (see fig. 1). The regularity of bursting activity is quantified

by two parameters, the coefficient of variation of cycle period (CV_{cp}) and the coefficient of variation of burst duration (CV_d). The coefficient of variation is defined as the ratio between the standard deviation and the mean. It is calculated for cycle periods and durations of each cell, mediated on a sample of cells and expressed as percentage.

Pooled data are expressed as mean ± standard deviation, with *n* indicating the number of cells. Statistical differences between groups of data are assessed using Student's t-test or ANOVA while to compare cumulative probability distributions, the Kolmogorov-Smirnov non-parametric test was used. For linear regression analysis, the Pearson Product Moment Correlation is used. Statistical differences are considered significant when $P<0.005$ (unless stated otherwise).

RESULTS

1. Spontaneous bursting activity in ventral interneurons

Spontaneous synaptic activity was routinely recorded from ventral interneurons that fulfill the morphological criteria for identification (see methods). Fig. 1 shows an example of such an activity when the membrane potential of the patched cell was held at -56 mV. At this potential value, synaptic currents mediated by glutamate or by glycine and GABA were detected as inward (see methods). In standard Krebs solution 47% of recorded ventral interneurons presented spontaneous bursting activity consisting of clusters of events (see fig. 1B) which lack a regular cycle period (2-10 s) and with variable duration (0.3-6 s) (fig. 1A). Between bursts single spontaneous postsynaptic currents (PSCs) were present (superimposed in fig. 1C) and shown variable amplitude and decay time course. The application of 1 μM TTX (not shown) always suppressed spontaneous bursts, suggesting that they were mediated by action potential-dependent release. Miniature post synaptic currents (mPSCs) were also detected in the presence of TTX.

Rhythmic bursts and spontaneous synaptic activity from ventral interneurons in the organotypic cultures have been investigated in the present thesis and will be described in the following sections.

2. Effects of pharmacological block of glycine and $GABA_A$ receptors

In the isolated spinal cord from neonatal rat, the block of glycine and $GABA_A$ receptors with strychnine and bicuculline, induces spontaneous rhythmic bursting in motoneurons (Bracci et al., 1996a). These rhythmic bursts are characterized by several intraburst oscillations and they are synchronous in left and right ventral roots (Bracci et al., 1996a). Intrinsic membrane properties of motoneurons seem not to be involved in the generation of this rhythmic pattern that relies on the activation of premotoneuronal spinal networks. Moreover it has been shown that bursting in the presence of strychnine and bicuculline requires the activation of spinal networks contained in a single ventral horn spanning over few lumbar segment (Bracci et al. 1996b).

These results raised the question about the expression of such a rhythmic activity in ventral horn interneurons in the organotypic spinal cultures and whether intersegmental connections were required to initiate and maintain this rhythmic activity. In fact, by use of the organotypic cultures, it was possible to assess the minimal spinal network sufficient to generate this disinhibited rhythm. Furthermore it was interesting to investigate the generation of the rhythmic activity in these interneurons during *in vitro* development. Glycine and GABA act as excitatory neurotransmitters on motoneurons during embryonic development (Nishimaru et al. 1996, Wu et al. 1992), however it is unknown to what extent ventral interneurons are inhibited by GABA and glycine and whether this phenomenon is developmentally regulated.

To address these issues, ventral interneurons were patch clamped at two different stages of development *in vitro*, at $\leq$ 9 days *in vitro* (8DIV) and at $\geq$ 13 days *in vitro* (14DIV). Experiments were carried out in voltage clamp conditions under whole cell configuration, with the membrane potential usually held at –56 mV. In 90% of ventral interneurons at 8DIV (fig. 2A top) and at 14DIV (fig. 2A bottom), bath coapplications of 1 µM strychnine and 20 µM bicuculline induced highly regular rhythmic activity composed by bursts of inward current with superimposed a background of intense spontaneous synaptic activity. Such a rhythm was preceded by an initial phase of irregular bursting summation, lasting 3-5 minutes after the application of strychnine and bicuculline. Once rhythmic activity developed it persisted as long as the drugs were applied. Cycle periods were significantly different ($p < 0.0001$) in the two groups of cultures (fig. 2B). Cycle periods were on average 83 ± 45 s (n = 25) and 54 ± 23 s (n = 70) at 8DIV and 14DIV, respectively (fig. 2B). Burst duration was not changed significantly (11 ± 5 s at 8DIV vs 14 ± 6 s at 14DIV) (fig. 2B). The average coefficient of variation of cycle period, CV_{cp}, during the application of strychnine and bicuculline was 8 ± 3 % and 10 ± 6 % at 8DIV and 14DIV respectively, while the coefficient of variation for burst duration, CV_d, was 12 ± 8 % and 15 ± 9 %. These low percentage values confirmed that rhythmic bursts induced by strychnine and bicuculline were remarkably regular.

These results indicate that rhythmic activity in ventral interneurons was reliably induced by block of glycine and $GABA_A$ receptors. This regular rhythm was generated at both stages of *in vitro* development studied although significant differences in terms of frequency were

consistently detected. This rhythmic pattern of activity when compared with that induced in motoneurons in the neonatal rat spinal cord in the same pharmacological conditions (fig. X) showed similar values of cycle periods. In particular at 14DIV cultures, the average cycle period is close to that recorded from motoneurons (31 ± 9 s) in the isolated spinal cord (Bracci et al, 1996).

3. Voltage dependence of rhythmic activity induced by coapplication of strychnine and bicuculline.

To investigate the involvement of intrinsic voltage-dependent properties of recorded neurons in rhythmic activity induced by strychnine plus bicuculline, the membrane holding potentials V_h were changed in a stepwise fashion within the -60/+20 mV range maintaining the imposed voltage level for more than 5 min (see fig 3B). When V_h was -60 mV each burst was detected as an inward current which disappeared at 0 mV and returned essentially unchanged but with opposite polarity at +20 mV; neither cycle period nor burst duration was significantly affected by membrane potential changes as shown in fig. 3C. The same result was obtained on a sample of 3 cells at 14DIV.

4. Effects of different pharmacological agents on bursts produced by strychnine and bicuculline

Fig 3B shows that 0 mV is the reversal potential for rhythmic bursts evoked by strychnine and bicuculline suggesting that such a pattern of activity is due to the activation of glutamate receptors. The effect of block of glutamate receptors on rhythmic activity induced by strychnine and bicuculline were studied at 8DIV as well as 14DIV.

On all 8DIV cells tested, the non-NMDA receptor blocker 6-cyano-7-nitroquinoxaline-2,3-dione (CNQX) (10μM) abolished both bursting and spontaneous synaptic activity without altering burst period prior to the block (n = 6; not shown). At 14DIV, CNQX fully suppressed bursting and ongoing spontaneous synaptic activity (Fig.3A, top) in 8/16 cells while, in the remaining 8 interneurons despite suppression of inter-burst spontaneous synaptic activity, bursting pattern persisted (albeit reduced in amplitude and duration, by 59±21 %, and 52±19

%; not shown). In this case subsequent co-application of 3-((RS)-2-carboxy-piperazine-4-yl)-propyl-1-phosphonate (CPP) (10μM), completely suppressed bursting activity.

The application of the N-methyl-D-aspartate (NMDA) receptor antagonist 3-((RS)-2-carboxy-piperazine-4-yl)-propyl-1-phosphonate (CPP) (10μM) had no effect neither on period nor on duration of rhythmic patterns at 8DIV (n = 4, not shown) while reduced burst duration (by 48±11 %) in 6/10 cells at 14DIV without altering cycle period (fig. 3A, middle).

The application of 1μM Tetrodotoxin (TTX) that block voltage-dependent Na^+ channels, completely eliminated bursting activity at 14DIV (n = 3) (Fig.3A, bottom), as well as 8DIV (n= 3, not shown) leaving only miniature postsynaptic currents. These findings show: (1) at 8DIV the rhythm in the presence of strychnine and bicuculline is mainly mediated by the activation of AMPA/Kainate receptors, (2) at 14DIV in 50 % of recorded cells it is mediated by both NMDA and AMPA/Kainate receptors, (3) such a pattern of activity is a network-driven phenomenon.

5. Effects of strychnine on spontaneous synaptic activity

To gain insight into the relative role of glycine at two distinct times in culture, strychnine was separately applied at 8DIV and 14DIV. In both culture conditions strychnine alone induced bursting activity only in 40% of cells tested (n = 9, 8DIV; n = 13, 14DIV) An example is given in fig. 4A for a cell at 14DIV. Note that the application of strychnine converts the spontaneous synaptic activity into irregular, large bursts. The lack of response (i. e. failure in generating bursts) to strychnine in 60 % of the patched interneurons was not due to insufficient concentration of this drug because further increments in the concentration of this agent (from 1 μM to 5 μM) also failed to elicit spontaneous bursting (n = 4). Whenever present, the strychnine-induced bursting was relatively irregular (CV_{cp}= 40±24 % and 54±18 % at 8 and 14 DIV, respectively), fast (CP = 30±22 s and 16±14 s) and consisted of short events (BD = 4±2 s and 3±2 s and CV_d= 15±6 % and 21±16%, see fig. 4B). No significant difference in neither cycle period nor burst duration, between 8DIV and 14DIV emerge (Fig. 4B). These rhythmic bursts had cycle period and duration significantly lower than those induced by coapplication of strychnine and bicuculline.

Strychnine increased the frequency (by 54±24%) of spontaneous postsynaptic currents (PSCs) in 3/5 cells at 14DIV (see example in fig. 4C), in 1/5 no change in spontaneous activity was found, and in one cell a reduction (20%) in spontaneous activity was detected. In the presence of strychnine an increase in frequency of spontaneous events was also observed in 4/7 cells at 8DIV (by 57±20%). Nonetheless 2/7 cells showed no change in the frequency of spontaneous events and in only one case a small (15%) reduction in spontaneous activity was present. The likelihood of observing a rise in synaptic activity was unrelated to the occurrence of bursting. Table 1 summarizes mean rise times or decay times of single spontaneous events detected in standard solution and in the presence of strychnine. Kinetics are measured on the average of all single events selected (when bursts were present, events were selected in the interburst interval). Note that there are no changes in either rise or decay time in control and in the presence of strychnine both for 8DIV and 14DIV cultures. The mean amplitude of spontaneous synaptic events was calculated for all cells tested: no differences were detected between the two groups (1.08±0.2 and 1.02±0.4, at 8DIV and 14DIV respectively, in the presence of strychnine, normalized to control values).

Block of glycinergic transmission, then, did not reliably elicit regular rhythmic activity in ventral interneurons, in fact only in 40 % of these cells, irregular bursting was detected at 8 DIV and 14DIV. The application of strychnine increased the frequency of PSCs at a similar rate at both ages of development *in vitro*.

6. Effects of bicuculline on spontaneous synaptic activity

Fig. 5A exemplifies on two cells (8DIV and 14DIV) the action of bicuculline *per se* which elicited irregular bursting activity. Such bursting activity was consistent in 98% of the cells (n = 11 8DIV, n = 6 14DIV) and characterized by CV_{cp}= 63±37 % and 41±14 %, and CV_d= 20±8 % and 25±11 % at 8DIV or 14DIV, respectively. No significant change in neither cycle period nor burst duration between the two groups emerged (fig. 5B). Those bursts were not significantly different in cycle period or burst duration from those recorded in the presence of strychnine alone. Bursts elicited by the application of bicuculline alone, showed a cycle period

significantly shorter than those induced by coapplication of strychnine and bicuculline at both stages of development.

At 14DIV bicuculline always increased the frequency of spontaneous events detected during quiescent periods (30±16 % in 4/5 cells) as shown in fig. 6B (top). Note that the frequency of synaptic currents is enhanced through the entire range of amplitude distribution (fig. 6A, top). Conversely, at the earlier stage of 8DIV, bicuculline reduced the frequency of spontaneous currents in 4/6 cells (fig. 6A, B, bottom) by 29±12%. In one cell bicuculline did not affect event frequency between bursts and in only one case a 20% increase in spontaneous activity appeared. Table 1 shows that there was no variation in both rise and decay time constants of the averaged spontaneous events at 8DIV and 14DIV in the presence of bicuculline. Mean amplitude of the averaged spontaneous events was unchanged after the application of bicuculline (0.99±0.35 and 1.03±0.20 at 8DIV and 14DIV, respectively, normalized to control values).

In summary, bicuculline consistently induced spontaneous, irregular bursts in ventral interneurons at both stages of development studied. Block of $GABA_A$ receptors differentially affected the frequency of PSCs depending on the time in culture: at 8DIV bicuculline predominantly decreased spontaneous events although at 14DIV it enhanced PSC frequency (an effect similar to that observed in the presence of strychnine at the same time *in vitro*).

7. Rhythmic activity induced by increasing extracellular K^+ concentration

Rhythmic activity is widely expressed by ventral interneurons in the organotypic slice cultures, following the application of strychnine and bicuculline, namely selectively blocking glycine and $GABA_A$ receptors. The following results were aimed at investigating whether rhythmic activity could be induced by increasing the excitability level of all neurons in the slice without suppressing inhibition. To this aim, the extracellular K^+ concentration was increased. This is a condition known to induce fictive locomotion in the neonatal rat spinal cord isolated *in vitro* (Bracci et al. 1998, fig. VII). In this group of experiments electrophysiological recordings were carried out on cultures at 14-21DIV.

On all ventral interneurons tested under voltage clamp conditions (n = 43) an increase in extracellular K^+ concentration from 4 mM (standard solution) to 7 mM induced a slow inward current as exemplified by the continuous trace in fig. 7A (right; see arrow for start of 7 mM K^+ superfusion) which on average peaked 30 ± 10 s from the onset of the application, reached a mean amplitude value of -36.4 ± 20.2 pA (measured at midpoint noise level), and then recovered to the baseline. Such a current was associated with a large enhancement in spontaneous synaptic activity. After 2 minutes the application of high K^+, in 35/46 neurons, spontaneous random synaptic activity turned into rhythmic bursts of inward current (see fig. 7B, left) and after 5 min this rhythm stabilized and became even more regular (fig. 7B, right). The induced patterned activity was abolished by washout to control solution, which was always accompanied by return to baseline current (not shown). The rhythm observed during the initial 2 min of 6-7 mM K^+ application consisted of events occurring at a cycle period of 1.58 ± 1.20 s (fig. 7C left, filled squares) and with average duration of 0.65 ± 0.21 s (fig. 7C right, filled squares). In a small minority of bursting neurons (6/35 cells) this rhythmicity disappeared within 5 min after the K^+ application. Nonetheless, in the majority of cells (n=29) this pattern persisted as long as high K^+ solution was applied (> 25 min) and it stabilized at a frequency value which was not significantly different from the one observed at 2 min application (fig. 7C left, filled triangles). Burst duration was also similar at 2 and 5 min application as indicated by the average plot of fig. 7C (right). These rhythmic currents were characterized by periodic bursts with cycle period and duration variable from cell to cell but very regular in each cell as indicated by CV_{cp} and CV_d mean values (20±5 % and 19±10 %, respectively).

The threshold concentration of K^+, sufficient to reliably induce rhythmic activity, was 6 mM (n=5). No significant difference in cycle period or burst duration was detected between 6 and 7 mM K^+, measured at both 2 and 5 min from application (fig. 7C). With higher doses of K^+ (8 mM; n = 3) a significant shortening of cycle period and burst duration was observed (fig. 7C), and rhythmic activity shows higher regularity. In 3 interneurons in which 6-8 mM K^+ was effective to induce bursting activity, the effects of 10 mM K^+ were also investigated (not shown). In these cells this high K^+ solution evoked a large inward current with reversible decrease in spontaneous synaptic activity which lacked any rhythmicity.

Ventral interneurons of the organotypic cultures consistently generated rhythmic activity following increases in extracellular K^+ concentration. This rhythmic activity displayed frequencies similar to that observed in the isolated spinal cord during fictive locomotion (Bracci et al., 1998; Kudo and Yamada, 1987; Cazalets et al., 1992).

8. Sensitivity of K^+ induced activity to pharmacological agents

Pharmacological tests were performed to find out the nature of the rhythmic activity evoked by high K^+. The application of CPP (10 μM) on rhythmic activity evoked by 7 mM K^+ reduced (to 45 ± 5 % of control) burst duration without affecting cycle period
(83 ± 10 % of control) (fig. 8A). Fig 8B (right) shows the superimposed average of 5 bursts, in the absence and in the presence (arrow) of CPP (same cell as in A). In the presence of the drug, burst amplitude is reduced, (-136 and -95 pA, respectively) rise time is slowed down (from 30.5 ms to 40.3 ms) and decay time constant became faster (55 ms in the presence of the drug versus 65 ms in control). The plot in fig. 8B (left) summarizes the results obtained from 5 ventral interneurons, in which CPP significantly reduced burst duration (to 60 ± 22 %) while it did not change the mean cycle period (105 ± 50%).

The non-NMDA ionotropic receptor blocker CNQX (10 μM) fully abolished the rhythmic pattern evoked by 7 mM K^+ (n = 4) (fig. 8C). Furthermore CNQX strongly decreased the frequency of spontaneous PSCs present among bursts. Attempts to replicate the bursting activity obtained in high K^+ solution by application of the glutamate receptor agonist AMPA were met with limited success. In fact, AMPA (1 μM) induced a slow inward current with superimposed intense synaptic activity which only transiently (after about 2-3 min) became organized into a rhythmic pattern (3/4 neurons) lasting at most 1-2 min. This short lasting rhythm has been observed also in the isolated rat spinal cord (E. Bracci, M. Beato and A. Nistri, unpublished observations) and its transient nature precluded studies on its features.

Application of TTX (2 μM) completely blocked bursts evoked by 7 mM K^+ while it did not abolish the slow inward current associated with this treatment (n = 3, not shown).

9. Ventral horn distribution of K^+ induced rhythmic activity

In order to investigate the distribution of high K^+ induced activity within the organotypic slice, simultaneous recordings were performed from single cells (under voltage (patch) clamp) located in a ventral horn and group of cells (with an extracellular field electrode) located in the contralateral ventral horn. The experimental set-up is depicted in the scheme in fig. 9. The extracellular electrode (EXTRA) was positioned in the contralateral ventral horn with respect to the patched ventral interneuron (WCR). The 7 mM K^+ concentration induced a patterned activity with a cycle period of 0.98 ± 0.4 s and 0.29 ± 0.1 s burst duration at 2 min (fig. 9Ab), which stabilized at values of 1.2 ± 0.1 s and 0.19 ± 0.04 s, respectively, at 5 min (fig. 9Bb). The field recording (fig. 9Aa, Ba) showed comparable rhythmic events in the controlateral ventral horn occurring 50-100 ms after the large events recorded from the patched neuron ($n = 4$). The occurrence of rhythmic activity in high K+ has been investigated at the level of DRG cells. In two different culture dishes after recording the regular pattern of activity from ventral interneurons in the presence of 7 mM K^+, a DRG cell was also patch clamped during K^+ superfusion. In both tests no spontaneous activity was detected in control condition and no bursting appeared after K^+ application, although an inward current was present, similar to that induced by K^+ in ventral interneurons (not shown).

The temporal phasing of the bursting pattern on either side of the slice was studied by simultaneous, extracellular field recording of bursting activity from two contralateral areas of the same slice culture after rhythmic activity pattern was established in high K^+ solution (not shown). Delay in the burst onset between the two contralateral ventral areas was 37 ± 15 ms ($n = 5$), a value relatively close to the latency of the excitatory inward currents (35 ± 4 ms; $n = 32$, in 4 different preparations), evoked by focal electrical stimulation of a DRG on a homolateral ventral interneuron.

10. Voltage dependence of rhythm elicited by high K^+

Voltage sensitivity of the bursting activity was assessed in voltage clamp (fig 10) or current clamp (fig 11) experiments. In voltage clamp conditions, after application of 6 or 7 mM K^+ V_h

was changed within the -66/+26 mV range (maintaining each value for >2 min) as indicated in fig. 10A (6 mM K^+ solution). At V_h = -66 mV, bursts appeared as multiphasic inward currents which were still inward at -36 mV even though reduced in amplitude. These responses disappeared around -18 mV (see data point in I/V of fig. 10B), and returned with opposite polarity at +16 mV (fig. 10A, bottom). Fig. 10B shows, on a sample of 6 interneurons, that neither cycle period nor burst duration were significantly affected by changes in holding potential.

The negative reversal potential (around -20 mV) for rhythmic activity evoked by high K^+ suggested a mixed contribution by glutamatergic as well as inhibitory, glycine and GABA mediated, Cl^- events. To question whether excitatory and inhibitory currents made discrete contributions to the rhythmic pattern, we pursued a different approach by performing current clamp experiments in which the intracellular solution was changed (see methods). The pipette solution differed from the standard intracellular solution in terms of a) low Cl^- concentration which shifted the reversal potential for Cl^- to more negative values to obtain a larger separation between inhibitory and excitatory reversal potentials, and b) presence of the Na^+ channel blocker, QX-314, that suppressed spiking in the patched cell. This approach improved the space clamp conditions of the neuron and avoided the possibility that synaptic responses were artifactually generated by inadequate space clamping of neurons. In these conditions, 7 mM K^+ induced a slow membrane depolarization that shifted the resting membrane potential from -54 ± 2 mV to -38 ± 6 mV (n = 5); after about a minute of high K^+ application, the membrane potential of the recorded cells, partially recovered toward the resting membrane potential (not shown). At -42 mV (fig. 11A, middle) bursting induced by 7 mM K^+ was expressed as a series of events with an initial depolarizing component (filled triangles) which is usually followed by hyperpolarizing events (open triangles) intertwined with smaller amplitude depolarizing components. Shifting the membrane potential to -66 mV (top traces in fig. 11A) by intracellular injection of -0.04 nA maintained a similar rhythmicity in which a large depolarizing response was followed by slower components of similar polarity with superimposed faster events (filled triangles) without change in periodicity. When the cell was depolarized to -12 mV by +0.07 nA injection (fig. 11A, bottom) each burst appeared to

comprise mainly a large inhibitory component (open triangles) with unchanged periodicity. These data indicate that rhythmicity consisted in a series of alternating excitatory postsynaptic potentials (EPSPs) followed by inhibitory postsynaptic potentials (IPSPs). It seemed interesting to examine if there was any tight relation between the temporal patterning of EPSPs and IPSPs. This possibility was tested at -42 mV membrane potential by correlating the cycle period of EPSPs and IPSPs. Fig. 11B shows that there was a linear relation between the period of the EPSPs (abscissa) and the one of the IPSPs (ordinate) with a Pearson correlation coefficient of 0.998 ($P<0.0005$). Similar results were obtained in five interneurons, while in two cells comparable shifts to depolarized potentials greatly attenuated the depolarizing events to reveal a tonic background of hyperpolarizing events. On 5 cells, plotting the peak amplitude of the burst events against membrane potential indicated that their estimated reversal potential was -30 mV.

These observations thus indicate that the K^+ induced rhythmic activity was made up by large, mixed synaptic events originating at network level and was expressed as a series of EPSPs usually followed by IPSPs or, in a minority of cells, superimposed upon tonic inhibition. The possibility of distinguishing these components was aided by recording them at different potentials and with a different intracellular solution. The membrane potential of the recorded cell thus determined their polarity but not their origin or temporal patterning.

11. Effects of increased K^+ concentration on strychnine and bicuculline induced bursts

Our observation of IPSPs following EPSPs during each burst episode suggested that excitation was apparently accompanied by inhibition but the nature of those inhibitory components could not isolated since blocking excitatory transmission with CNQX suppressed high K^+ evoked bursting. Suppression of glycine and $GABA_A$ receptor mediated activity has been investigated to ascertain whether they were responsible for the Cl^- dependent inhibition recorded under the present experimental conditions. As previously shown rhythmic bursting in lower frequency, developed spontaneously in the presence of 1 μM strychnine and 20 μM bicuculline and it was primarily supported by glutamate receptor activation (fig 2, fig 12A). Addition of 8 mM K^+ induced a slow inward current and, after 2-3 min, the burst frequency appeared consistently

increased (fig. 12A, right). On a sample of 5 ventral interneurons cycle period displayed a significant decrease to 47 ± 18 % of control as shown in fig. 12B (middle). High K^+ decreased also the burst duration of the rhythmic activity to 71 ± 15 % of control (fig. 12B, right).

During strychnine and bicuculline induced bursts V_h was changed in a stepwise fashion in the -66/+36 mV range as previously described. In fig 12C (left) the strychnine and bicuculline evoked burst amplitude decreased with membrane depolarization, disappeared at 0 mV and returned with opposite polarity at +36 mV (filled circles). Application of K^+ (8 mM) reduced burst amplitude uniformly throughout the voltage range although the same reversal potential value was retained (fig. 12C, filled triangles). Note however that the burst I/V relation remained non-linear at negative potentials despite the pharmacological suppression of GABA and glycine mediated components. One possibility is that voltage dependent block of NMDA receptors might have contributed to such non-linearity. This was explored (see fig. 12C, right) by measuring the I/V curve and reversal potential of strychnine and bicuculline bursts before (open squares) and after applying the NMDA receptor antagonist CPP (open triangles) which linearized the plot and gave it a steeper slope: for example, in the -46/-16 mV range the slope value was 0.007 in strychnine plus bicuculline solution (by linear regression analysis) and became 0.3 in the presence of CPP. Similar results were obtained in 3 cells. These observations thus indicate that after pharmacological block of glycine and $GABA_A$ receptors spontaneous inward currents were developed with a reversal consistent with the one of glutamate mediated responses in the spinal cord (Mayer & Westbrook 1987) and which were readily accelerated by external K^+. When the cell membrane was depolarized, a more consistent contribution by NMDA receptor activity to burst amplitude was manifested. These data thus expand those obtained under current clamp conditions and provide additional evidence about the multicomponent (glutamatergic, glycinergic and GABAergic) nature of bursting currents.

12. Sensitivity of K^+ induced activity to changes in external concentration of Mg^{2+} and Ca^{2+}

While the available data suggested a network origin of the rhythmic patterns, it seemed necessary to study whether the high K^+ solution actually facilitated transmitter release from

network cells. This issue was investigated indirectly by comparing K^+ induced rhythmic bursting in control and modified (Mg^{2+}/Ca^{2+} =5/1, see methods) solutions which should suppress synaptic transmission. Synaptic currents evoked by DRG electrical stimulation (see methods) were also monitored in these experiments to inspect the effectiveness of synaptic transmission block (see for instance the average of 5 evoked responses recorded from a ventral interneuron in control solution in fig. 13C, top). Fig. 13A shows that 6 mM K^+ changed spontaneous synaptic activity into bursting activity in a ventral neuron. After washout, and consequently disappearance of rhythmic bursting (not shown), subsequent superfusion with 5/1 solution largely reduced spontaneous synaptic activity, and fully prevented the K^+ (6 mM) induced rhythmic pattern (fig. 13B). Under the same conditions evoked responses were fully blocked (fig. 13C, middle) yet recovered after washout (fig. 13C, bottom).

High K^+ induced rhythmic bursts consisted of synaptic, widespread network-driven events and mainly mediated by the activation of non-NMDA receptors. Rhythmic bursts displayed similar periodicity in comparison to those recorded in the rat isolated spinal cord during locomotor-like activity.

13. Mg^{2+} free induced activity

Bath-application of NMDA is one of the primary tools to induce fictive-locomotion in the neonatal rat spinal cord *in vitro* (Kudo and Yamada 1987, Cazalets et al. 1992). In many studies NMDA is applied with 5-HT because coapplication of these two excitatory agonists together elicits a very stable pattern of activity (Sqalli-Houssaini et al. 1993; Kjaerulff and Khien, 1996). In order to investigate NMDA induced rhythmic activity in the organotypic slice cultures, increasing concentrations of this drug have been applied. The lowest concentration used was 4 μM that it is known to evoke fictive locomotion in the isolated rat spinal cord (Bracci et al., 1998). In n = 5 interneurons 2-4 μM NMDA did not produce any consistent change in spontaneous activity or in baseline current (not shown). Adding 5-HT (30 μM) to the NMDA solution did not help to elicit rhythmic bursting (not shown). The insensitivity to NMDA application was not a matter of insufficient concentration of this agent since 10 μM (n = 10 cells) or 20 μM (n = 3) NMDA also failed to elicited rhythmic patterns of activity. These

findings suggested that ambient Mg^{2+} might have functionally blocked NMDA receptors in a voltage dependent fashion (Mayer and Westbrooke, 1987). This was also suggested by the lack of linearity of I/V relation for rhythmic activity induced by high K^+ (fig. 10B).

To reduce the extent of any Mg^{2+}-block of NMDA glutamate receptors we used a nominally Mg^{2+} free solution (see methods). Removal of external Mg^{2+} evoked an inward current of -14±3 pA (in 8/13 cells) which peaked at 30 s. After 5-6 min from the onset of application of the Mg^{2+} free solution, at V_h = -56 mV a regular rhythmic pattern of activity developed and persisted as long as this divalent cation was absent from the bath solution (fig. 14A, left). The Mg^{2+} free induced pattern of activity was detected in all cells (n = 13), and was characterized by a mean cycle period of 4 ± 1 s and mean burst duration of 1.5 ± 0.7 s. The CV_{cp} and CV_d values 21 ± 6 % and 21 ±2 %, respectively, indicated regular occurrence of these bursts. During the Mg^{2+} free induced patterned activity, variations in V_h were imposed within the -66/+26 mV range with a procedure similar to the one described before. An example of this procedure is shown in Fig. 14A: each burst appeared as an inward current at -66 mV while it was outwardly directed at -10 mV. The graph of fig. 14B shows the I/V relation for burst amplitude with inversion of polarity at -20 mV. In this case the calculated slope which was 1.6 for the -46/-10 range , indicated a higher degree of steepness when compared with standard Mg^{2+} solution (see fig. 10B). On a sample of 6 cells cycle period and burst duration were not affected by changes in holding potential (data not shown). Bursting activity evoked by omitting Mg^{2+} from the bathing solution was not a mere consequence of increased membrane excitability due to a decreased divalent cation concentration. In fact, in 3 cells in which the total extracellular divalent cation concentration was kept constant by raising external Ca^{2+} to 3 mM (see methods), an analogous bursting pattern appeared when a Mg^{2+} free solution was applied.

Rhythmic currents evoked by Mg^{2+} free solution were similar to those induced by increasing extracellular K^+ in terms of periodicity, duration, shape and reversal potential, but not in terms of sensitivity to ionotropic glutamate receptor antagonists. In 3 cells out of a total of 5 cells on which 10 μM CPP was applied during Mg^{2+} free induced rhythmic activity this drug fully blocked the ongoing bursting activity, as depicted in the example of fig. 14C, top. In 2/5

neurons rhythmic activity was disrupted but irregular bursts of reduced amplitude still occurred (not shown). CNQX (10 μM) was added to the Mg^{2+} free solution in 7 neurons. Bursting activity persisted in 6/7 cells in the presence of CNQX, although reduced in amplitude (to 28.5±7 % of control; see example in fig. 14B, bottom). On average cycle period and burst duration were changed to 166 ± 44 % and 135 ± 25 % of control, respectively.

Bursting activity was reliably recorded from ventral interneurons in Mg^{2+} free solution. The periodicity, duration and reversal potential of the bursting activity were similar to those observed in the high K^+ ones. However it differed from high K^+ induced bursts, in terms of sensitivity to glutamate receptors block since its activation was mainly mediated by NMDA receptors.

14. Homeostatic plasticity in developing ventral interneurons

Ventral interneurons of the organotypic spinal cultures generate rhythmic synchronous activity by means of various manipulations of the network operation. In fact block of fast Cl^- mediated transmission by application of strychnine and bicuculline, or raise the extracellular K^+ concentration or removal of the extracellular Mg^{2+} although inducing bursting with different features, unmask a functional property of this circuit, namely the ability to express rhythmic activity using different neurotransmitter systems. These results led to investigate the presence of homeostatic plasticity as a mechanism that may influence network operation. To address this complex issue, three experimental protocols have been utilized (see methods): (I) chronic block of AMPA/Kainate glutamate receptors with CNQX to remove the main excitatory synaptic input to ventral interneurons, (II) chronic block of voltage-dependent Na^+ channels with TTX to mimic a systematic suppression of afferent inputs and (III) chronic block of glycine and $GABA_A$ receptors with strychnine and bicuculline to remove the Cl^- mediated transmission. The effects of these chronic manipulations on interneuronal activity were assessed by recording spontaneous and miniature PSCs together with the current responses evoked on the same cells by electrical stimulation of DRG cells. This combined assay measures three aspects of network synaptic function. In particular, spontaneous PSCs, should mainly reflect random firing of local neurons and thus provide an index of how changes in network activity can shape the function

of a single interneuron. On the other hand mPSCs are independent from action potential and should help to localize changes in synaptic activity at pre and/or post synaptic level. Finally, evoked DRG activity should assay synchronous activation of mono and polysynaptic projections to the recorded cell.

The database of the present study comprises 185 ventral interneurons (from 80 culture series prepared weekly) always recorded at 13-14DIV.

15. Properties of spontaneous postsynaptic currents (PSCs) in ventral interneurons

PSCs were recorded from 47 ventral interneurons in several different sets of cultures. An example of ongoing spontaneous activity in standard Krebs is given in fig 15A (left) in which PSCs are inward currents with a frequency of 13.1 Hz and variable amplitude. Single PSCs are detected (superimposed in fig. 15A, middle) and two PSC types are distinguished on the basis of decay time course: PSCs with a fast decay time and PSCs with slow decay time. The averaged fast PSCs and slow PSCs are shown at the right of fig. 15A (top and bottom respectively). On a sample of n = 30 ventral interneurons, average PSC frequency was 12.6 ± 3.5 Hz with -19 ± 5 pA mean peak amplitude. Control PSCs of the majority of these interneurons (70 %) decayed either rapidly (τ value = 2.1 ± 0.5 ms) or slowly (13.1 ± 5.6 ms), a difference statistically significant despite the similar rise time (0.9 ± 0.2 ms and 1.3 ± 0.3 ms, respectively). No correlation between rise time and half width of these events (fig. 15D), suggests that different decay values were unlikely to be due to electrotonic filtering. The mean amplitude of fast events was comparable with that of slow ones (-18.3 ± 5.2 pA and -21.1 ± 8.4 pA, respectively) and fast events ranging from 21 to 73 % of all events in each cell. On a minority (30 %) of cells only fast events (τ = 3.4 ± 0.7 ms) were recorded (rise time = 1.0 ± 0.3 ms).

The NMDA receptor antagonist CPP (10 μM) had either no effect on event frequency (in 4/10 cells) or slightly reduced it (15.6 ± 6.1 % reduction in 6/10 cells) without altering the proportion between fast and slow τ events. Mean amplitude (-19 ± 4 pA) was always unchanged like onset and decay of PSCs. As exemplified in Fig 15B (same cell as in Fig. 15A), the AMPA/kainate receptor antagonist CNQX (10 μM) fully suppressed fast τ PSCs and left

slow τ events (19.3 ± 8.3 ms; 1.9 ± 0.2 ms rise time; -12.8 ± 1.1 pA, mean amplitude) of reduced frequency (from 1.8 ± 1.5 Hz to 1.1 ± 0.5 Hz, n = 5). Further application of CPP did not affect these events, while, after washout of CPP, co-application of strychnine (1 μM) and bicuculline (20 μM) eliminated all events (n = 4, not shown).

In those cells in which only fast events could be identified in Krebs solution, application of CNQX fully abolished any spontaneous activity (n = 3).

To summarise, in control cultures (14DIV) spontaneous synaptic activity comprised in most cases both fast and slow τ PSCs. Fast events were abolished by CNQX and represented both AMPA/Kainate receptor mediated currents and Cl^- mediated PSCs with fast kinetics, whereas the slower ones (resistant to CNQX) were suppressed by co-application of antagonists of $GABA_A$ and glycine receptors suggesting that they are Cl^- mediated PSCs. Furthermore when rhythmic activity is induced by coapplication of strychnine and bicuculline, during interburst intervals, only fast τ events could be detected (n = 3) supporting the fact that slow τ PSCs are Cl^- mediated.

Given that block of NMDA receptors did not affect significantly spontaneous PSCs, the effect of the activation of these receptors to network activity has been studied on evoked currents (see methods). Polysynaptic currents were elicited by focal stimulation of the homolateral dorsal root ganglion (DRG; fig 15C, left) in 14 ventral interneurons. Evoked PSCs (n = 3) were completely inward at -56 mV V_h, biphasic (early inward current followed by an outward component) at -20 mV V_h, and fully outward at 0 mV V_h. In all cells tested (n = 5) application of CNQX completely removed any evoked event, which recovered upon 20 min washout (not shown). CPP reduced the area of the evoked currents by 34 ± 11 % (n = 3) as shown in the example of fig. 15 C.

16. Properties of synaptic activity in cultures chronically treated with CNQX

Spontaneous synaptic activity was recorded in 51 ventral interneurons from various cultures after 7 days of chronic incubation with CNQX (see methods). In all analysed cells (n = 25) an extensive and significant increase (61 % rise; compared to control cultures) in spontaneous

PSC frequency was detected (20.3 ± 4.1 Hz). This phenomenon was further consolidated by a qualitative change in spontaneous synaptic transmission as virtually all cells possessed fast PSCs only (τ = 3.6 ± 1.3 ms and 0.97 ± 0.27 ms rise time). Fig 16 A shows sample records from two interneurons from sister cultures, one in control condition (top traces) and one after chronic treatment (see methods) with CNQX (bottom traces). Fig 16 B shows the corresponding cumulative plots of PSCs where peak amplitudes for the chronically treated interneuron were distributed to the right of those of the control sister cell (a statistically significant difference). There was no linear relation between peak amplitude and rise time values of these currents (fig. 16C). Similar results were obtained from 3 different culture series (n=3). Note that if data were not compared between sister cultures, pooling together all responses yielded mean peak amplitude (-24.8 ± 8 pA) which was not significantly different from pooled controls (-19 ± 5 pA).

In 5/8 interneurons CPP reduced spontaneous synaptic event frequency by 24 ± 7 %, with a small insignificant reduction in mean amplitude (-17.3 ± 6.6 pA, not shown). Unlike the relatively small or even absent action of CPP, in all 13 neurons tested the effect of acute application of CNQX was characterized by a large change in synaptic transmission: in fact, while fast τ events disappeared, they were replaced with slow τ PSCs occurring at variable frequency (7.3 ± 4.3 Hz). This result is illustrated by comparing data in Fig. 17A and B. On average in the presence of CNQX slow τ was 27.2 ± 9 ms (PSCs had 2.22 ± 0.38 ms rise time and –14.4 ± 4.1 pA mean amplitude). Further application of CPP did not affect these events (n = 4), while, after washout of CPP, co-application of strychnine and bicuculline fully blocked slow τ PSCs (n = 5). On 7 cells displaying slow decay events after acute application of CNQX, subsequent addition of TTX evoked a dramatic reduction in the occurrence of spontaneous slow events which became very rare (0.03 Hz in four cells) or disappeared all together in three cells.

On 8 ventral interneurons PSCs elicited by DRG stimulation were inward at -56 mV (fig. 17C), became biphasic at -20 mV Vh and fully outward at 0 mV Vh like in sister cells (not shown). Acute application of CNQX completely and reversibly abolished evoked PSCs (n = 3) And they were partly reduced (44.4 ± 10.4 %, n=5) by CPP (see Fig. 17 C) .

17. Properties of synaptic activity in cultures chronically treated with TTX

Spontaneous events recorded from ventral interneurons (n = 24) after chronic TTX treatment had 15 ± 4 Hz of mean frequency and mean amplitude of -19.9 ± 4.8 pA. Both these values were similar to the ones observed in control cultures. In 60 % of recorded interneurons, only fast τ PSCs were detected (see example of cell fig. 18A middle and right; cumulative amplitude plot for this cell together with a control sister culture is shown in fig. 18D). On average fast τ values were 3.8 ± 0.6 ms with 0.9 ± 0.3 ms rise time. In 40 % of observed interneurons spontaneous PSCs were mixed with fast (2.7 ± 0.7 ms τ) and slow (12 ± 4 ms τ) values (rise time 0.9 ± 0.2 ms and 1.3 ± 0.2 ms, respectively) equally distributed in terms of occurrence (like in untreated cells). Superfusion with CPP reduced (by 37 ± 7 %) the frequency of all events in 4/6 cells. Application of CNQX (n = 3) suppressed fast events leaving no residual activity in those cells in which only fast events were detected (fig 18B). In interneurons with fast and slow events application of CNQX left only slow events as reported for control cultures (not shown).

Fig 18C (left) shows the average synaptic current evoked by DRG stimulation. Like in control cultures or in chronic CNQX treated ones, evoked currents were inward at -56 mV Vh, biphasic at -20 mV Vh and fully outward at 0 mV Vh (n = 3). Fig 18C (right) shows the area of the evoked PSC was reduced by 44% in the presence of CPP. On 5 interneurons the reduction in evoked PSCs brought about by CPP applications was 50.6 ± 13.7 %.

18. Properties of synaptic activity in cultures chronically treated with strychnine *plus* bicuculline

After 7 days of incubation in strychnine and bicuculline solution (see methods), 14/30 interneurons displayed spontaneous, irregular bursting activity (an example of these inward burst currents is shown in fig.19, left). In the majority of cells (18/30) the frequency of background synaptic activity (measured either during the quiescent period between bursts or at rest in those cells without spontaneous bursting) was significantly lower (8.2 ± 3.0 Hz) than in

control cultures (35 % decrease). Usually both fast (3.1 ± 1.0 ms) and slow (11 ± 3 ms) τ events could be detected with similar rise time (0.8 ± 0.2 ms and 1.0 ± 0.4 ms, respectively) as exemplified in fig. 19A (middle and right). Fast events were on average 70 ± 12 % of all measured events. Mean peak amplitude was smaller (-14.4 ± 3.4 pA) than in control cultures. In fig. 19D the cumulative amplitude distribution plot shows that data from a treated cell are significantly different from analogous ones in control and lay to the left of the standard curve. Similar results were obtained from 3 different culture series.

CPP significantly decreased the PSC frequency (41.1 ± 9.3 %, n = 9; not shown) while CNQX (fig. 19B) completely suppressed fast events (as reported for control cultures) leaving only slow events (15.6 ± 6.2 ms τ; 1.6 ± 0.4 ms rise time; n=5) the frequency of which was also reduced from 0.50 ± 0.35 to 0.23 ± 0.15 Hz.

Synaptic currents evoked by DRG stimulation appeared fully inward at -56 mV Vh (fig. 19C), became biphasic at - 20 mV Vh and outward at 0 mV Vh. CPP significantly reduced (by 60 ± 20 %, n= 5) the PSC area, as shown in fig. 19C (right). Application of CNQX fully blocked the evoked PSCs in 2/5 cells only as in 3 cells a residual evoked current (11 ± 8 % of control area) remained.

In 12/30 cells the spontaneous events had a frequency significantly higher (22.3 ± 10.1 Hz; $p < 0.0001$) than control and comprised only fast τ events (3.7 ± 1.1 ms, 1.0 ± 0.3 ms rise time, mean amplitude – 23.7 ± 12.1 pA, n=10, not shown) which were abolished by CNQX. CPP did not affect event frequency in 3 cells whereas reduced it by 40 ± 23 % in 2 cells. The probability of observing either an enhancement or a fall in the frequency of background synaptic activity bore no reference to the presence of irregular bursting in standard Krebs solution.

19. mPSCs in control and treated cultures

In control cultures acute application of TTX revealed mPSCs which could be classified in two groups on the basis of their τ decay values (2.6 ± 1.1 ms and of 11.5 ± 4.5 ms, respectively) although they all possessed similar rise times (fast: 1.0 ± 0.2 ms, slow: 1.6 ± 0.1 ms, respectively). As shown by the example of fig 20A a cell with fast PSCs only generated

exclusively fast τ mPSCs (on a sample of 4 cells τ = 3.9 ± 0.3 ms, 1 ± 0.1 ms rise time). The cumulative inter-event frequency plot for this cell is shown in fig. 20E (right, open circles) while its mPSC amplitude distribution is plotted in fig. 20E (left, open circles). On a sample of 9 cells the average frequency of mPSCs was 0.52 ± 0.12 Hz. The mean amplitude of mPSCs was -12.2 ± 3 pA (n = 9) and was not significantly changed by co-application of strychnine and bicuculline (106±35 %; n = 3) while their frequency were reduced (60±14 %). These results confirmed that in organotypic spinal culture neurons mPSCs are mediated by glutamate, GABA or glycine (Streit & Luscher, 1992).

Fig 20B shows a sample of mPSCs after applying TTX to a chronically CNQX treated interneuron. With this protocol mPSCs had a frequency significantly larger than the control condition (1.1 ± 0.3 Hz; see raw data example in fig. 20B and cumulative inter-event interval plot in fig. 20E, right, open squares) and comprised exclusively fast τ events (4.1 ± 0.9 ms, 1.0 ± 0.1 ms rise time) of amplitude comparable to control ones (see fig. 20E, left) which on average was -13.6 ± 3.5 pA (n = 11). Subsequent application of CNQX did not unmask slow mPSCs but simply blocked all activity (n = 7). Like in the case of the events recorded in control conditions, co-application of strychnine and bicuculline did not change the mPSCs amplitude (-11.3±2.0 pA; n = 4) but it simply reduced their frequency (46 ± 27 %).

In cultures previously subjected to chronic TTX treatment, subsequent acute application of TTX disclosed mPSCs occurring at high frequency (1.0 ± 0.4 Hz, $p<0.05$ *versus* control, n = 4, -13.5 ± 3.6 pA mean peak amplitude). Fig 20C shows raw data from a cell chronically treated with TTX with the corresponding inter-event frequency plot (fig. 20E, right, filled circles; note complete overlap with CNQX treatment data) and amplitude distribution similar to control (fig. 20E, left). In terms of shape of the activity, mPSCs reproduced the conditions observed in standard (untreated cells): namely fast τ events were detected (3.9 ± 0.9 ms, 1.0 ± 0.2 ms rise time) whenever in control solution a single PSC population had been present, or fast and slow τ events (2.0 ± 0.2 ms, 12 ± 2.3 ms, fast and slow, respectively) were detected whenever two PSC populations existed before adding TTX.

Fig 20D shows mPSCs after chronic treatment with strychnine and bicuculline: in this example the interneuron was representative of the majority group in which PSCs occurred at low

frequency before TTX application. The inter-event frequency plot (filled squares in fig. 20E, right) is found to the right of the control one indicating a lower event frequency while the amplitude scatter plot shows the events comprised between -5 and -15 pA (fig. 20E, left). On a sample of 4 such cells mPSC frequency was found to be very low (0.09 ± 0.01 Hz; $p<0.05$; mean peak amplitude was -9.1 ± 2.8 pA). Events with both fast (4.2 ± 1.3 ms τ) and slow (16 ± 4 ms τ) values were recorded (0.9 ± 0.1ms and 1.5 ± 0.2 ms rise time, respectively). The low frequency of these responses precluded their systematic pharmacological analysis. However, in two cases it was possible to observe a further reduction (by 53±18 %) in mPSC frequency after applying strychnine plus bicuculline.

As indicated above, a smaller sample (12/30) of cells chronically treated with strychnine and bicuculline displayed higher frequency PSCs. This enhanced occurrence was also observed when the same cells were subsequently exposed to TTX: in fact, their mPSC frequency (n = 4) was 1.1±0.2 Hz and was partly reduced (by 27±18 %) by acutely applied strychnine and bicuculline.

These results showed that long-lasting application of blockers for AMPA/Kainate receptors or $GABA_A$ and glycine receptors, induced opposite changes in the synaptic activity recorded from ventral interneurons during *in vitro* development. Chronic block of AMPA/Kainate receptors resulted in an increase in the rate of PSCs and mPSCs. Block of $GABA_A$ and glycine receptors induced decreased frequency of PSCs and mPSCs. Suppression of Na^+ dependent spike activity with TTX did not affect drastically interneuron spontaneous PSCs and induced an increase in spontaneous mPSC frequency.

20. Rhythmic activity and homeostatic plasticity.

Homeostatic changes induced by chronic treatment with CNQX on ventral interneurons included an increase in the rate of spontaneous and miniature PSC that displayed only fast decay times. Slow τ, Cl^- mediated PSCs appeared (at variable frequency) only when AMPA\Kainate receptor mediated activity was blocked in the network. The ability of chronic CNQX treated cultures to generate rhythmic activity has been investigated. To study this issue the three protocols known to generate rhythmic patterns in untreated cultures have been used:

(I) application of increased concentrations of extracellular K^+, (II) superfusion with nominally Mg^{2+} free solution and (III) coapplication of glycine and $GABA_A$ receptors blockers. All three experimental paradigms have been broadly investigated in untreated cultures in previous sections. The following data studied the effectiveness of these protocols to induce rhythmic activity in cultures chronically treated with CNQX. In order to assess plastic changes due to chronic treatment, always data from treated cultures have been compared with those from untreated sister cultures. All experiments have been carried out at 13DIV and 14DIV.

21. Rhythmic activity induced by high K^+ in cultures chronically treated with CNQX

Ventral interneurons in control, untreated cultures, displayed spontaneous synaptic activity with a mean frequency of 10.8 ± 4.8 Hz and as previously described, they usually presented both fast τ (2.6 ± 0.3 ms, 0.9 ± 0.2 ms rise time) and slow τ PSCs (17.2 ± 3.8 ms, 1.4 ± 0.1 ms, rise time). In these cultures, increasing the extracellular K^+ concentration to 7 mM induced a slow inward current (-35 ± 15 pA) in all cells tested (n = 25). After about 2 minutes of high K^+ superfusion, rhythmic bursts of inward current appeared (n = 18) with average cycle period of 2.8 ± 1.4 s and 0.7 ± 0.3 s duration. In fig. 21A it is shown an example of high K^+ induced activity in a control ventral interneuron: bursts displayed a rapid onset (38.6 ± 14.9 ms rise time) and an area of -28.6 ± 15.6 pAs (see fig. 21A, bottom). On a sample of 11 ventral interneurons, the average 5-90% rise time of rhythmic currents was 41 ± 16 ms and the average area was -42 ± 21.2 pAs. As previously described, rhythmic currents elicited by high K^+ were mainly mediated by AMPA/Kainate receptor activation. In fact, addition of CNQX (10 μM) completely abolished rhythmic bursting (n = 5). All these cells presented both fast τ (τ = 2.6 ± 0.3 ms, 0.9 ± 0.1 ms rise time) and slow τ PSCs (τ = 16.5 ± 2.6 ms and 1.3 ± 0.3 ms rise time) in standard solution and the application of CNQX on rhythm induced by high K^+ abolished both bursting and fast PSCs. Only slow τ events (τ = 22.3 ± 2.8 ms, 1.7 ± 0.4 ms rise time) were left with a mean frequency of 2.2 ± 1.6 Hz (1.9 ± 1 Hz was their frequency in standard solution).

In 34% of ventral interneurons chronically treated with CNQX, spontaneous synaptic activity in standard solution appeared organized into bursting currents (see fig. 21B, top). These irregular, synaptic clusters were characterized by a cycle period ranging from 1 s to 6 s and burst duration from 0.2 s and 3 s. Usually a background of high frequency PSCs was superimposed at such an activity. As previously described, in these chronic CNQX cultures a strong increase in PSC frequency was observed (22.1 ± 4.8 Hz) and only fast τ events were detected (τ = 3.4 ± 0.7 ms, 1.1 ± 0.2 ms rise time) in standard solution. The application of 7 mM K^+, induced a slow inward current (-60 ± 40 pA) in all cells tested (n = 45). In 75% of recorded interneurons, spontaneous synaptic activity developed into rhythmic currents after about 2 minutes of high K^+ superfusion. In 14 out 26 cells, the averaged cycle period (0.83 ± 0.56 s), and the mean duration (0.25 ± 0.14 s) of such bursts were significantly reduced in respect to untreated cells (compare fig. 21B to fig. 21A, middle). Fig. 21D-E shows cumulative distributions for cycle period and duration in control (circles) and chronically treated cultures (triangles). Note that for the chronically treated interneurons, cumulative distributions lie at the left of control ones. In the remaining ventral interneurons (n = 12), cycle period and duration were 3.1 ± 1.6 s and 1.1 ± 0.8 s respectively, these values were not significantly different from those recorded in control cultures.

Cycle period and duration of rhythmic bursts did not significantly change in response to different extracellular K^+ concentrations (6-8 mM) (not shown). The effects of chronic CNQX treatment on rhythmic activity generated by high K^+ consisted also in a radical change in the burst configuration (compare fig. 21A and 21B, bottom). In the majority (n = 10/16) of chronically treated cultures, either in the presence of high frequency oscillations (n = 5) or in slower ones (n = 5), single bursts had a very slow onset (309 ± 202 ms). Histograms in fig. 21C compare mean rise time in control (n = 9) and in treated cultures (n = 8).

In a set of cells (n = 6) the rise time of bursts (49 ± 21 ms) in high K^+ was similar to that recorded in control cultures. This rapid burst onset appeared not correlated to the appearance of rhythmic bursts with high (n = 3) or lower frequency (n = 3). In all cells tested (n = 6), addition of 10 μM CNQX to rhythmic currents evoked by high K^+ abolished rhythmic pattern, leaving an intense activity of spontaneous slow τ PSCs (7.1 ± 2.5 Hz).

22. Voltage dependence of high K^+ induced bursting in cultures chronically treated with CNQX

The voltage sensitivity of rhythmic bursts evoked by high K^+ has been studied with voltage clamp experiments. In fig. 22A a single burst induced by 8 mM K^+ is shown in a control cell at three different membrane potentials. At -56 mV V_h burst showed a rapid onset (24.3 ± 8.3 ms) and a gradual decay time course (fig. 22A, top). At V_h = -20 mV burst disappeared (fig. 22A, middle) even though inward and outward PSCs were still detectable. When the membrane potential was held at 0 mV, burst was entirely outward (fig. 22A, bottom). In fig. 22B (same cell as in A) the average peak burst amplitude is plotted against the membrane holding potential. A similar trend was observed in n = 4 interneurons.

In cultures chronically treated with CNQX, in 6 out of 12 cells, the voltage dependence of high K^+ induced bursts was similar to the control cells, the reversal potential was around -20 mV and all these cells expressed rhythmic bursts with a rapid rise time (50 ± 21 ms) (not shown). The other 6 interneurons in chronically treated cultures revealed a different behaviour. Fig. 22C gives an example of such a cell. When the membrane potential was held at -56 mV, burst was inward and it became fully outward at V_h = 0 mV. However at V_h = -20 mV, the burst current is made up by an initial outward component (open triangle) followed by a slow inward event (filled triangle). Fig. 22D illustrates the I/V relation in such a cell. In n = 4 of such ventral interneurons the outward component preceded the inward one while in two cases the situation was the opposite, namely the inward component temporally preceded the outward one (not shown). The presence of these two distinct components of different polarity at -20 mV, seemed not be related to the rise time of bursts, in fact 4/6 cells had slow rise time (301 ± 214 ms) and 2/6 possessed fast one (44.8 ± 19.2 ms).

Chronic CNQX treated cultures consistently generated rhythmic currents following increases in the extracellular K^+ concentration. In a half of ventral interneurons this rhythmic activity showed different features when compared to untreated sister cultures at the level of burst periodicity and burst shape.

23. Rhythmic activity induced by Mg^{2+} free in cultures chronically treated with CNQX

After 5-6 min from the onset of application of the Mg^{2+} free solution, at V_h = -56 mV a regular rhythmic pattern of activity developed and persisted as long as this divalent cation was absent from the bath solution (fig. 23A, middle). Rhythmic currents were observed in all cells studied (n = 3) and were characterised by a mean cycle period of 3.9 ± 1.3 s and mean duration of 1.5 ± 0.5 s. In fig. 23A (right), a single burst is shown which consisted of a sustained inward current originating with a fast onset and after reaching the peak, it gradually declined toward the baseline. Rhythmic currents in Mg^{2+} free solution exhibited an averaged rise time of (54 ± 15 ms).

In cells chronically treated with CNQX (n = 5), removal of external Mg^{2+} evoked a rhythmic pattern with a mean cycle period of 3.1 ± 1.3 s and duration 0.9 ± 0.3 s. An example is given in fig. 23B where removal of extracellular Mg^{2+} converted spontaneous, random PSCs (left) into bursts of inward current (middle). The regularity of such an activity was well maintained but the shape of every single burst presented a high variability (see fig. 23B). In 3 out of 5 cells, bursts revealed a slow onset with 264 ± 126 ms rise time (fig. 23B, left), while the other 2 cells had an averaged rise time similar to untreated cultures (47.7 ± 23.4 ms).

Mg^{2+} free solution induced rhythm activity in chronic CNQX ventral interneurons. Rhythmic bursts exhibited periods and durations comparable to those recorded from control untreated interneurons but (like in the case of high K^+ rhythmic activity) they presented irregular and slow rise time.

24. Block of Cl^- mediated transmission in cultures chronically treated with CNQX.

Rhythmic activity in the absence of fast Cl^- mediated transmission was preliminary studied in control and in chronic CNQX sister cultures. In the experiments (n = 3) with control cultures, block of glycine and $GABA_A$ receptors resulted in regular bursts of inward currents (fig. 24A). In average, cycle period and duration of the bursting activity were 62.2±15.1 s and 17.5 ± 1.8 s respectively. The burst in the presence of strychnine *plus* bicuculline was characterized by a rapid and regular rise time (38.2 ± 15.2 ms).

Ventral interneurons chronically treated with CNQX (n = 5) showed a similar pattern of rhythmic inward currents (fig. 24B) with an average cycle period of 54.8±15.7 s and an average duration of 16.3±5.2 s. The rise time of the single bursts in chronically CNQX treated ventral interneurons, was not significantly different to that of control experiments (38.2±15.2 ms) and showed an average of 48.8±16.4 ms.

Block of $GABA_A$ and glycine receptors induced rhythmic currents in chronically treated interneurons with periodicity, duration and burst shape comparable to those recorded from control cultures.

DISCUSSION

Organotypic cocultures of spinal cord and dorsal root ganglia represented a suitable tool for the study of rhythmogenesis and development of spinal circuits. A structure as organotypic slice, with only 3-4 cell layers, was able to express rhythmic events in different pharmacological conditions (block of Cl^- mediated transmission, high K^+ and Mg^{2+} free solutions) using diverse neurotransmitter systems. These rhythms possessed similarities with those observed in the rat isolated spinal cord *in vitro*, suggesting that some basic mechanisms underlying rhythmogenesis in the *in vitro* spinal cord was preserved in this minimal culture preparation. Homeostatic plasticity has been explored in *in vitro* developing spinal networks after long-term suppression of specific synaptic inputs. Chronic block of $GABA_A$ and glycine receptors induced a downregulation of spontaneous and miniature PSCs while chronic block of Na^+ spikes with tetrodotoxin did not induce radical changes in spontaneous PSCs. After block of AMPA/Kainate receptors for one week in culture, the frequency of spontaneous and miniature PSCs was almost doubled respect to untreated cultures and slow Cl^- mediated PSCs displayed a striking change in operativity and contribution to network activity.

1. Rhythmic activity in ventral interneurons

Block of glycine and/or $GABA_A$ receptors during in vitro development

In organotypic cultures of 8DIV and 14DIV, rhythmic, regular bursting activity was consistently observed in ventral interneurons following block of glycine and $GABA_A$ receptors. These rhythmic currents were always superimposed to a background of intense spontaneous synaptic activity. This patterned activity displayed differences when recorded at 8DIV and 14DIV in terms of cycle period and sensitivity to glutamate receptors antagonists. The frequency of bursting was higher at 14DIV than at 8DIV while burst duration was similar suggesting that different mechanisms regulated periodicity and duration, as observed in the neonatal rat spinal cord *in vitro* (Bracci et al., 1996b). The pharmacological sensitivity of bursts to ionotropic glutamate receptors was different at the two times in culture considered. At 8DIV, block of AMPA/Kainate receptor mediated transmission completely suppressed both bursts and ongoing spontaneous PSCs, while block of NMDA receptors did not affect bursting at all. These results suggested that after one

week in culture, rhythmic activity in the presence of strychnine and bicuculline is mainly mediated by non-NMDA receptors. At 14 DIV, NMDA receptor block reduced the duration of bursts without changing burst frequency. Block of AMPA/Kainate receptors, in half of the recorded cells left rhythmic currents with the same periodicity (although reduced in amplitude and duration) and in all cells recorded, abolished spontaneous PSCs. Block of both NMDA and non-NMDA receptors invariably suppressed rhythmic currents, indicating that they are generated by activation of glutamate receptors. This notion is also confirmed by the reversal potential of such an activity that is near 0 mV corresponding to the reversal potential for the multicationic current mediated by glutamate receptors activation (Mayer and Westbrook, 1987). The developmental changes in antagonist sensitivity might originate by alteration in the expression of different subtypes of glutamate receptors (Jakowec et al., 1995, Tölle et al., 1995a,b).

In the majority of cells, both at 8DIV and 14DIV, spontaneous PSCs increased in frequency in the presence of strychnine and bicuculline. Furthermore this ongoing spontaneous synaptic events were mediated by glutamate because they always were suppressed by coapplication of ionotropic glutamate receptor antagonists. Such an activity was uniformly distributed between bursts and no relationship emerged between burst length and EPSC frequency. In motoneurons in both the organotypic spinal cultures (Streit, 1993) and neonatal rat spinal cord (Bracci et al., 1996a, Ballerini et al., 1997), no spontaneous synaptic potentials emerged during the interburst intervals, suggesting that most of the excitatory interneurons that contribute to spontaneous synaptic activity in standard Krebs condition were synchronized to discharge together only during rhythmic activity (Bracci et al., 1996a).

Application of strychnine to block glycine receptors evoked bursting activity only in a minority of interneurons in both culture groups. These bursts were irregular when compared with those induced by coapplication of strychnine and bicuculline. The lack of reliable rhythmic activity was not due to an incomplete block of glycine receptors. In fact when 1 μM strychnine did not evoked any bursting activity, the concentration was raised to 5 μM and no bursts were observed. Furthermore, in several preparations in the presence of bicuculline, the concentration of strychnine was raised from 1 μM to 10 μM and no changes in burst frequency or duration were observed. In fact, in the neonatal rat spinal cord, it has been shown that the concentration of 1μM strychnine already saturate glycine receptors

(Bracci et al., 1996b). Although Streit (1993) observed a sustained and liable rhythmic bursting in motoneurons from organotypic spinal slices, following block of glycine receptors, it is important to notice that this author studied motoneurons rhythmic properties in cultures after 13-28DIV, namely in a later period respect to that considered in the present thesis. However the results of this thesis are similar to those described in the neonatal rat spinal cord *in vitro* where strychnine *per se* is not able to induce rhythmic patterns (Bracci et al., 1996a). Independently from the ability of strychnine to induce bursting, the block of glycine receptors increased the frequency of spontaneous PSCs recorded from ventral interneurons at both 8DIV and 14DIV without changes in rise time, peak amplitude and decay time of the detected PSC. Block of glycine receptors induced rhythmic, irregular bursts in a minor portion of ventral interneurons at both 8DIV and 14DIV and in any case increased the frequency of PSCs suggesting an inhibitory role of glycine in spinal networks at these stages of *in vitro* development.

Removing $GABA_A$ receptor mediated activity by application of bicuculline induced bursting in all interneurons tested at either times in culture. These bursts were highly irregular and separated by spontaneous, random PSCs. At 14DIV, block of $GABA_A$ receptors induced bursting activity and increased PSC frequency between bursts, suggesting that, at this age, GABA had mainly an inhibitory role. At 8DIV the frequency of PSCs in the presence of bicuculline was lower in respect to standard Krebs condition while it was higher at 14DIV, suggesting a different role of GABAergic transmission during development. At the embryonic day at which organotypic cultures are started (E13-14), glycine and GABA play a depolarizing role (Nishimaru et al., 1996) mediating spontaneous rhythmic activity in motoneurons (Nishimaru et al., 1996). At E17-18, block of $GABA_A$ receptors with bicuculline, blocks polysynaptic dorsal root-evoked potentials in motoneurons while at late embryonic ages (E20-21) block of $GABA_A$ receptors strongly increases the amplitude of such a polysynaptic potentials (Wu et al., 1992) suggesting that at the premotoneuronal level, GABA underwent a gradual change in its action. In line with this view removal of GABAergic activity in 8DIV organotypic cultures could unmask networks in which $GABA_A$ receptors already had an inhibitory role on certain synapses, as suggested by the presence of rhythmic bursts in bicuculline, while it was still excitatory on others, thus contributing to excitatory synaptic activity.

Application of bicuculline consistently induced rhythmic bursting (although irregular) at both stages of *in vitro* development. However its role in regulating ventral interneuron spontaneous activity changed during *in vitro* development since block of $GABA_A$ receptors at 8DIV downregulated spontaneous PSCs while at 14DIV increased PSC frequency. The different role that $GABA_A$ receptors played at 8DIV and 14DIV could be responsible for the different period of rhythm elicited by strychnine plus bicuculline at these two stages of development. In fact, assuming that synaptic efficacy was important for network oscillations (Streit, 1993), block of $GABA_A$ receptors at 8DIV would have removed an excitatory component to the recurrent circuits resulting in a burst frequency slower than at 14DIV when the action of GABA is primary inhibitory.

In three cells layered organotypic spinal cultures regular rhythmic activity is reliably expressed by ventral interneurons, following block of both glycine and $GABA_A$ receptors. Such a regular pattern was present after one, as well as two weeks in culture but with differences both in terms of periodicity and sensitivity to ionotropic glutamate receptor blockers. The periodicity was accelerated as the culture matured and after two weeks *in vitro*, it was near the values observed in the isolated neonatal rat spinal cord (Bracci et al., 1996a).

Mechanisms of bursting induced by strychnine plus bucuculline in ventral interneurons from organotypic cultures

Glutamatergic rhythmic currents evoked by removal of fast Cl^- mediated transmission were polysynaptic, and these network-driven events were widely expressed in organotypic cultures. The observations supporting the network origin of these patterns were: a) rhythmic bursts were blocked by TTX at both 8DIV and 14DIV b) the frequency of bursts was independent from the membrane potential of the recorded interneuron. Given the facts that intrinsic TTX-resistant membrane oscillations were not detected in recorded interneurons and NMDA receptor block did not abolished rhythmic activity, it was concluded that NMDA-receptor-dependent pacemaker cells (Hochman et al., 1994a, Khien et al., 1996) were not essential to the generation of spontaneous bursting activity. Thus the generation of rhythmic activity in strychnine plus bicuculline relies on reverberating properties of excitatory neuronal circuits and rhythmogenesis depends on the maintenance of a certain level of synaptic efficacy (Streit, 1993). In developing spinal cord, synaptic depression (co-

working with recurrent excitation) has been proposed as a possible mechanism responsible for burst frequency (Streit, 1993, Chub and O'Donovan, 1998, O'Donovan, 1998b). The lower burst frequency observed at 8DIV with respect to 14DIV could be explained by a prominent expression of such refractory mechanism. However the involvement of such a mechanism seemed unlikely because, in the presence of strychnine and bicuculline, spontaneous synaptic activity was uniformly increased during the intraburst interval at both 8DIV and 14DIV, with a frequency uncorrelated to the duration of the preceding burst. Alternatively, multisynaptic networks distinctly govern spontaneous, randomly occurring, PSCs and generation of rhythmic bursts. The latter working hypothesis could also explain 1) the differential action of bicuculline on spontaneous PSC frequency at 8DIV and 14DIV, and 2) the action of CNQX that, on half of the 14 DIV interneurons did not block bursting activity while abolishing spontaneous PSCs.

Rhythmic, regular bursts were consistently generated by ventral interneurons, after block of fast Cl^- mediated activity in the organotypic slice cultures. This network-driven pattern of activity was present after one as well as after two weeks of *in vitro* development with different frequency and sensitivity to glutamate receptor antagonists. These results revealed that, in a simplified spinal preparation containing few cell layers, ventral interneurons displayed 'disinhibited' bursts with network mechanisms close to that recorded in the rat isolated spinal cord.

Characterization and mechanisms of rhythmic activity induced by high K^+

Solution with high K^+ concentration (6-8 mM) was used to induce non-selective depolarization of spinal neurons in the slice. Such a strategy was sufficient to activate networks responsible for rhythmogenesis. Bursts had regular cycle period and duration, variable amplitude and were recorded simultaneously from a large population of cells in ventral horns. The frequency of such an activity was similar to that observed in motoneurons from neonatal rat spinal cord during high K^+ fictive locomotion (Bracci et al., 1998).

High K^+ induced rhythmic bursts were suppressed by block of AMPA/Kainate receptors, suggesting that they were mainly mediated by the activation of non-NMDA receptors in the network, although NMDA receptors also contributed to their amplitude and duration. Furthermore such an activity is blocked by TTX or low Ca^{2+} (high Mg^{2+}) extracellular

solution. All these results indicated the network origin of this rhythm. It is unlikely that activation of voltage dependent intrinsic properties in the recorded interneurons was responsible for such a rhythm since neither cycle period nor duration changed following membrane potential variations. Although the presence of intrinsic oscillatory neurons (Hochman et al., 1994, Kiehn et al., 1996) in the organotypic cultures could not be excluded, block of NMDA receptors did not abolished rhythmic activity in recorded ventral interneurons suggesting that NMDA-receptor dependent oscillators were not essential. Involvement of gap junctions in the propagation of K^+ induced activity is unlikely because the temporal interval between rhythm recorded from single patched ventral interneuron and the rhythmic events recorded from group of cells in the controlateral ventral horn, is similar to the latency of polysynaptic currents evoked by DRG electrical stimulation. However the presence of local gap junction-coupled interneuronal ensambles analogous to those detected among motoneurons in the isolated neonatal rat spinal cord (Tresch and Kiehn, 2000), could not be excluded.

The reversal potential for rhythmic events evoked by high K^+, was negative suggesting a mixed contribution of glutamate as well as Cl^- mediated transmission. The use of pharmacological tools to separate EPSPs and IPSPs was difficult since application of CNQX completely abolished rhythmic bursts while suppression of Cl^- mediated transmission with strychnine and bicuculline induced another kind of sustained rhythmic activity as previously described. To separate excitatory and inhibitory components, current clamp experiments were performed with a low intracellular Cl^- concentration (see methods) to obtain a larger separation between reversal potentials of inhibitory and excitatory transmission. This approach revealed that in a portion of ventral interneurons, for value near the resting membrane potential, individual bursts comprised EPSPs usually followed by IPSPs, while in other cells a tonic background of IPSPs was detected at 0 mV.

It appeared that organotypic cultures developed premotoneuronal networks able to generate rhythmic oscillations in the presence of high K^+ solution, with frequency comparable to that observed in motoneurons in the isolated neonatal rat spinal cord (Bracci et al., 1998). In some ventral interneurons, moreover, such rhythmic pattern consisted of temporally correlated EPSPs and IPSPs. A comparable temporal distribution of excitatory and inhibitory events is detected, with intracellular recordings, in motoneurons (Cazalets et al., 1996) and interneurons (Raastad et al., 1997) of the *in vitro* rat spinal cord during fictive

locomotion. It is noteworthy that such a rhythmic alternation of excitation and inhibition is a complex phenomenon to detect in the isolated spinal cord considering that it requires a complicated data analysis (Raastad et al., 1996, 1997). Furthermore not all interneurons show alternation between excitation and inhibition (Raastad et al., 1997) leaving the possibility that other pattern of excitation and inhibition could underlie locomotor-like activity. For example, a study on the mudpuppy spinal cord (Wheatley et al., 1994), reveals that the majority of interneurons involved in locomotion fire during the transition between excitation and inhibition of motor pools. These observations suggest that both the correlation between EPSPs and IPSPs and the presence of tonic inhibition are compatible with the operation of a CPG in the organotypic slice cultures. In summary, the present results suggested that organotypic cultures possessed the minimal wiring connections required to generate rhythmic activity in high K^+ with a frequency close to that observed during fictive locomotion in the isolated neonatal rat spinal cord. In such a simplified structure ventral interneurons display a complex organization of excitatory and inhibitory events, reminiscent of responses recorded from interneurons and motoneurons in the isolated preparation during fictive locomotion. A fundamental feature of fictive locomotion observed in the rat *in vitro* spinal cord, is the alternation between flexor and extensor motor pools and between left and right sides (Kudo and Yamada, 1987, Cazalets et al., 1992, Beato et al., 1997, Bracci et al, 1998). The organotypic cultures procedure did not allow the separation of flexor and extensor motor pools and they did not possess motor nerves, therefore this model could not generate pattern of alternation. Furthermore, at the embryonic age in which cultures were performed (E13-14), the isolated rat spinal cord displayed rhythmic activity synchronous at the left and right side of the spinal cord (Kudo et al., 1991). These observations were confirmed by simultaneous recordings from cell group in left and right ventral horns during high K^+ rhythmic activity. Bursting events displayed short temporal delay and they never appeared out of phase.

Effects of NMDA and AMPA on ventral interneuron activity

Attempts to induce bursts with AMPA or NMDA were of limited success even when high doses of 5-HT were added to these antagonists. The AMPA receptor desensitization is supposed to prevent stable rhythmic activity in the isolated neonatal rat spinal cord (Ballerini et al., 1995) and it is coherent with bursting activity evoked by cyclothiazide, a

blocker of AMPA receptor desensitization (Ballerini et al., 1995). In the isolated embryonic rat spinal cord, bath application of NMDA (or NMA) induces rhythmic activity in motoneurons (Kudo et al., 1991) starting from embryonic day E16. The absence of NMDA induced rhythm in the organotypic cultures could be explained by Mg^{2+} block of NMDA receptors since standard Krebs solution contained 1 mM Mg^{2+}. Coapplication of NMDA and 5-HT, a combination that reliably induces fictive locomotion in the isolated rat spinal cord (Cazalets et al., 1992, Sqalli-Houssaini et al., 1993, Bracci et al., 1998), did not favour rhythmic activity either. This could be due to an inadequate 5-HT receptor expression due to the loss of serotoninergic neurons coming from the brainstem (Streit, 1996) and removed during culture preparation.

Properties of Mg^{2+} free induced rhythmic activity

Rhythmic activity followed by removal of Mg^{2+} from the extracellular solution is similar to that induced by high K^+. Mg^{2+} free bursts were blocked by NMDA antagonists and they were only partially sensitive to the block of AMPA/Kainate receptors. This phenomenon suggested that the organotypic cultures could generate similar rhythmic patterns using either class of glutamate receptors as in the isolated neonatal rat spinal cord during fictive locomotion (Beato et al., 1997).

It seemed that, in organotypic spinal cultures rhythmicity crucially depended on the level of excitability in the network, as suggested by Bracci et al. (1996a) for the isolated rat spinal cord. Increasing the excitability of the network, triggers the activation of rhythmic outputs. This phenomenon has been elicited by several strategies: 1) block of inhibitory transmission with strychnine and bicuculline, 2) raising the extracellular K^+ concentration that promoted the depolarization of neurons in the slice or 3) removing the extracellular Mg^{2+}, that enhanced the NMDA receptor activation.

2. Homeostatic plasticity in organotypic spinal cocultures

Organotypic spinal cocultures from rat embryos preserved the basic neuronal organization of a spinal segment and contained the minimal neuronal circuitry involved in the generation of rhythmic activity. Furthermore, during *in vitro* development changes in rhythmic ability were observed suggesting that in the organotypic cultures, spinal networks underwent *in vitro* maturation. These features made the organotypic spinal culture a suitable model for the

study of compensatory mechanisms in response to external perturbations. In fact this culture system allowed performing drastic, long-term pharmacological suppression of certain synaptic inputs.

Properties of spontaneous synaptic activity in ventral interneurons

In standard Krebs solution PSCs of the majority of ventral interneurons were heterogeneous in their kinetics as they included events with fast ($\tau < 5$ ms) or slow ($\tau > 5$ ms) decay time. This distinction was preserved when recording mPSCs. There was no correlation between PSC rise time and peak amplitude or between rise time and half width, suggesting that different τ values were not due to cable attenuation (Wyllie et al., 1994, Gao et al., 1998). Furthermore PSCs with different τ values had a comparable rise time, then it seemed unlikely that they were simply related to different synaptic locations (Hestrin, 1993, Wyllie et al., 1994, Nusser et al., 1997).

The slow τ PSCs always disappeared following strychnine and bicuculline application. They were Cl^- mediated events and they were partially driven by the activation of AMPA/Kainate receptors in the slice since CNQX lowered their frequency. All fast events were blocked by CNQX and presumably represented both AMPA/Kainate receptors mediated currents and Cl^- mediated PSCs driven by the activation of AMPA/Kainate receptors in the network. The use of glycine and $GABA_A$ receptor blockers on spontaneous fast PSCs to find out the relative contribution of these receptors to fast events, was not suitable. In fact, block of fast Cl^- mediated transmission generated sustained bursting activity altering excitatory transmission in the network. Recording miniature PSCs helped to overcome this problem and revealed that 30-60 % (depending on the cell) of fast mPSCs were suppressed by coapplication of strychnine and bicuculline. However it is difficult to distinguish which Cl^- mediated events (with fast or slow τ) were due to GABA or glycine receptor activation since it is known that, on cultured rat spinal neurons, inhibitory mPSCs display τ ranging from 5 to 40 ms and they are all decreased in frequency by strychnine and bicuculline (Lewis and Faber, 1996).

Fast PSCs which were resistant to the application of strychnine and bicuculline displayed a τ value consistent with AMPA receptor activation (Hestrin, 1993, Wyllie et al., 1994) and always lacked any biexponential decay implicative of a late NMDA receptor mediated

component. Besides block of NMDA receptors did affect neither the amplitude nor the kinetics of spontaneous PSCs. The negative membrane holding potential and the presence of 1 mM Mg^{2+} in the standard solution probably avoided detection of any NMDA component in PSCs. The block of NMDA receptors did not alter the frequency of spontaneous PSCs either, suggesting that they did not participate to spontaneous network activity. Nevertheless, CPP reduced the area of evoked polysynaptic PSCs, elicited by DRG electrical stimulation suggesting that, whenever strong excitatory inputs synchronized polysynaptic contacts, NMDA receptor contribution emerged.

CNQX treated cultures

Block of AMPA/kainate receptor activity during the first week *in vitro* implicated the suppression of the main excitatory synaptic input to ventral interneurons. After one week of chronic CNQX treatment all cells recorded in standard solution displayed a significant and very large increase in the frequency of PSCs which had fast decay only. These fast events had similar τ values and pharmacology to those observed in untreated cultures. Comparing PSC cumulative amplitude distribution among CNQX treated cultures and control sister ones, a significant shift of the curve towards larger values was detected. Summation of larger excitatory signals within a network with extensive connectivity might have been responsible for the increased frequency of spontaneous synaptic activity. A similar explanation excluded an up-regulation of NMDA receptors because CPP had minimal effects on spontaneous event frequency and amplitude. Furthermore, this possibility contrasted with the fact that evoked PSCs appeared similar as found in control cultures. Chronic treatment with CNQX induced also a significant increase in mPSC frequency that possessed only fast decay times. Despite the raise in frequency, mPSC mean amplitude was not changed, suggesting a presynaptic locus of action, like for example, increased number of functional release sites or increased release probability at certain strategic sites which not necessarily were implicated in polysynaptic pathways excited by DRG electrical stimulation. It is noteworthy that in organotypic cultures of the hippocampus analogous electrophysiological effects on mPSCs are induced by chronic block of NMDA receptors and are associated with increased number of functional synaptic connections formed by newly sprouted axons (McKinney et al., 1999).

There are several possible hypotheses concerning the absence of slow PSCs in chronic CNQX cultures: in particular 1) functional lack of some GABA or glycine receptors, 2) change in location of slow event synapses. The former hypothesis was denied since neurons were still capable of expressing GABA or glycine receptor mediated slow responses, as these were unmasked after acute block of AMPA/kainate receptors. The latter hypothesis also seemed improbable as these slow events, which instantly emerged after the acute application of CNQX, had standard amplitude and rise time. Lack of slow events might then require a different interpretation. Slow τ PSCs required a network drive to be detected, since in the presence of TTX they were rare or were not present at all. Such a drive did not require the activation of AMPA/Kainate receptors. The detection of slow τ PSCs could have been obscured by the dramatic rise in network-mediated fast synaptic events. In fact one could imagine that single slow τ events were superimposed to high-frequency fast PSC activity and summated events were usually excluded from data analysis (see methods). In this context, only after silencing AMPA/Kainate receptor mediated activity slow τ PSCs emerged.

A variant of this interpretation would be that, after chronic treatment with CNQX, a considerable change in circuit operation took place whereby fast synaptic transmission was so strongly upregulated that somehow it even inhibited slow synaptic events that could be detected only after blocking AMPA/kainate receptor activity.

In summary, long-term application of CNQX resulted in a massive increase in frequency of spontaneous and miniature PSCs that possessed exclusively fast τ decay times. Slow τ events emerged only when the AMPA/Kainate receptor mediated activity was abolished. This chronic treatment induced profound changes in the spinal network activity, transforming synapses mediating slow τ events into low releasing probability synapses.

TTX treated cultures

Although interneurons treated with chronic TTX could express fast and slow events like in control cultures, the majority of them generated fast events only with frequency, kinetics and pharmacological properties unchanged. Note that, in analogy with the data obtained following chronic CNQX treatment, there was a significant increase in frequency of mPSCs without a parallel change in peak amplitude. These observations suggested that at the level

of mPSCs, chronic TTX and chronic CNQX shared similar presynaptic effects manifested as increased event frequency. Nevertheless, at network level, studied in terms of PSCs, long-term block of Na^+ action potentials was apparently compensated by mechanisms that must have affected excitation as well as inhibition to leave the fundamental properties of circuit operation intact. This condition clearly differed from the effect of chronic removal of AMPA/kainate inputs.

Strychnine plus bicuculline treated cultures

$GABA_A$ and glycine receptors were blocked by chronic incubation of slices in strychnine and bicuculline. In this case cultures exhibited two opposite behaviours: 1) In the majority of cells an overall decrease in frequency of synaptic activity was present (together with a decrease in mPSC frequency) without a global change in spontaneous event kinetics. The relative contribution by glutamate or glycine and GABA to mPSC activity was apparently the same as observed in control cultures. On these cultures depressant effects by CPP on spontaneous and evoked synaptic activity were clearly observed, implying a larger contribution of NMDA receptors to synaptic activity. 2) In a smaller group of cells a strong increase in spontaneous synaptic activity (both PSCs and mPSCs) was present and usually included fast events only, thus reminiscent of chronic CNQX treated cells, although slow events were never detected even after acute CNQX application. The less frequent occurrence of this pattern of activity prevented its systematic investigation. Nevertheless, the sensitivity of such mPSCs to strychnine and bicuculline was not significantly different from the one tested in any other chronically treated culture.

It is unclear whether the different pattern of synaptic activity induced by strychnine and bicuculline reflects the existence of distinct classes of interneuron or the differential sensitivity to bicuculline treatment previously observed at 8DIV when the chronic treatment was started. The non-normal distribution of PSC frequency across the entire neuronal population justified their grouping into two separate classes although their functional significance remains uncertain.

Thus, on most cells incubation with blockers of $GABA_A$ and glycine receptors affected the network operation in terms of frequency of spontaneous and miniature events in a manner opposite to the phenomenon observed with chronic CNQX application.

In addition, on these cells the role of NMDA receptors in mediating electrically evoked synaptic transmission was enhanced by chronic strychnine plus bicuculline treatment.

Homeostatic plasticity and spinal networks

Recently, homeostatic plasticity have been studied using different culture models from various CNS areas chronically treated with various blockers of synaptic transmission (hippocampus, Rao & Craig, 1997; Lissin *et al.*, 1998; visual cortex, Turrigiano *et al.*, 1998; spinal cord, O'Brien *et al.*, 1998). The emergent evidence was that glutamate receptors undergo a form of long-term activity dependent regulation primarily based on postsynaptic changes.

The present study provided little evidence for postsynaptic increase or decrease in AMPA/kainate receptors as the mPSC amplitude remained essentially unchanged after various chronic treatments. There were, however, consistent variations (enhancement or depression) in the rate of spontaneous release estimated from the frequency of mPSCs and PSCs. This result supported the possibility that, in this model, homeostatic plasticity was based on presynaptic mechanisms within the spinal network, perhaps including receptors for glutamate, GABA and/or glycine. A postsynaptic increase in synaptic efficacy could, nevertheless, be manifested as a straightforward increase in mPSC frequency if it were caused by activation of silent synapses (Malenka and Nicoll, 1997, Feldman et al., 1999, Atwood and Wojtowicz, 1999). In the latter case one would, however, expect to observe a larger synaptic response to electrical stimuli unless the formerly silent receptors were totally inaccessible to evoked transmitter release, a possibility that so far has no experimental support.

The present investigation indicates that in a structurally well preserved mammalian spinal cord culture which could express network rhythmicity, homeostatic plasticity was not simply due to a series of postsynaptic changes in glutamate receptor activity occurring at single cell level but it included a complex rearrangement of network operation which also involved other neurotransmitters like GABA and glycine.

Rhythmic activity in CNQX treated cultures in high K^+ or Mg^{2+} free solutions

To explore the effects of chronic block of AMPA/Kainate receptor activity on spinal rhythmogenesis, chronic treated cultures were studied in parallel with sister control ones at 13-14DIV.

In control cultures rhythmic currents induced by raising the extracellular K^+ concentration, displayed features similar to those previously described. However in this set of experiments rhythmic bursts were characterized by a slightly higher cycle period, with comparable duration. This discrepancy could be related to the different stage of *in vitro* development studied in the two sets of experiments. In fact, previous results on high K^+ (6-7 mM) induced rhythmic bursts have been collected on cultures after 14-21DIV, namely in a DIV range wider respect to that studied now. Therefore, it was possible that the frequency of high K^+ rhythm increased during *in vitro* maturation of the slice. This was consistent with the different burst frequency (but not duration) observed in the rhythm induced by strychnine and bicuculline between 8DIV and 14DIV cultures: at 14DIV such a 'disinhibited' rhythmic activity displayed a frequency higher than at 8DIV, although burst duration was similar. The relation between K^+ concentration and the frequency of bursting was not systematically studied for this earlier time of growth *in vitro* therefore it could not be excluded that higher K^+ concentrations could elicit bursts with higher frequencies.

In cultures chronically treated with CNQX, spontaneous clusters of PSCs were observed in a minority of ventral interneurons in standard solution. The percentage of cells displaying such a spontaneous bursting activity and the features of these bursts were comparable to that found in control cultures. Bursts were highly irregular both in periodicity and duration and always associated with an intense background of spontaneous synaptic activity consisting of only fast τ PSCs. Raising the extracellular K^+ concentration, induced regular rhythmic activity in the majority of ventral interneurons. However burst period and duration displayed large variability. In most ventral interneurons high K^+ elicited fast oscillations at a very high frequency, whereas a portion of interneurons expressed rhythmic currents with periodicity and duration similar to control cultures. The significant increase in burst frequency observed could be related to homeostatic changes induced by chronic treatment with CNQX.
The high K^+ burst profile was characterized by a slow rise time in most of treated cells; single bursts consisted in summation and overlap of spontaneous events apparently without a marked synchronization as enlightened by the slow burst rise time. This feature was not related to the frequency of high K^+ rhythm and it was never observed in control cultures.

Rhythmic currents were blocked by acute application of CNQX, suggesting that, as for control cultures, activation of AMPA/Kainate receptors within the network was fundamental for the occurrence of this rhythmic activity.

In half of ventral treated interneurons, the reversal potential for rhythmic currents induced by high K^+ was near -20 mV suggesting that, as in control cultures, such a pattern of activity was mediated by both glutamate and Cl^- mediated transmissions. In the other group of interneurons, for holding potential close to -20 mV, bursts were present and were composed by two distinct types of events with opposite polarity: usually outward components preceded the inward ones. Such a temporal separation of excitatory and inhibitory events that built up high K^+ bursts was not found in voltage clamped interneurons from control sister cultures. Chronic treatment with CNQX might have changed the degree of synchrony between excitatory and inhibitory events, therefore IPSCs and EPSCs were temporally correlated to made up a burst, but they were not simultaneously expressed. The lack of synchronization between excitatory and inhibitory components during high K^+ rhythmic activity might support also the slow burst onset observed in a part of chronic CNQX treated interneurons. Nonetheless the distinction of EPSCs and IPSCs within single bursts during high K^+ rhythm, was observed also in two treated neurons expressing rapid burst onset. Another hypothesis, was that in chronically treated ventral interneurons, the reversal potential for Cl^- was shifted toward values more negative respect to untreated cultures. If that was the case, the separation between inhibitory and excitatory reversal potentials was more pronounced in treated cultures making the dissection of EPSCs and IPSCs easier. The direction of Cl^- flux depends on the Cl^- gradient across the cell membrane and the regulation of the Cl^- homeostasis is due to K^+/Cl^- co-transporters (Jarolimek et al., 1999, Rivera et al., 1999). Recently it has been shown that the expression of a type of Cl^--extruder K^+/Cl^- co-transporters is upregulated during neuronal development and it plays an important role in the change of GABA action from depolarizing to hyperpolarizing in the rat hippocampal neurons (Rivera et al., 1999). It might be the case that in chronic CNQX treated cultures an overexpression of K^+/Cl^- co-transporters took place. This hypothesis required the assumption that the intracellular Cl^- concentration was not determined exclusively by the Cl^- contained in the patch pipette (Sernagor et al., 1995).

After chronic block of AMPA/Kainate receptors, rhythmic bursts were consistently observed in organotypic spinal cultures following increases in the extracellular K^+ concentration.

Chronic treatment had no effect on the ratio of interneurons expressing high K^+ rhythmic activity, nonetheless the majority of these ventral interneurons expressed fast rhythmic currents at a very high frequency with a less tight temporal correlation among different components.

Removal of Mg^{2+} from the extracellular solution, induced rhythmic bursts in ventral interneurons chronically treated with CNQX. These bursts were similar to those observed in control sister cultures in terms of periodicity and duration. In chronic cultures no cells displayed Mg^{2+} free rhythmic events with higher frequency (as in high K^+), suggesting that homeostatic plasticity manifested differently in Mg^{2+} free and high K^+ induced rhythms.
In a number of interneurons from chronically CNQX treated cultures, rhythmic bursts in Mg^{2+} free and high K^+ shared a common feature: they were composed by events that summated into bursts but without the temporal synchronization observed in control cultures.

Rhythmic activity in CNQX treated cultures induced by coapplication of strychnine and bicuculline

Block of glycine and $GABA_A$ receptors induced regular, rhythmic bursts in all ventral interneurons from chronic CNQX cultures. These rhythmic currents were comparable to that observed in untreated sister cultures at the level of periodicity, duration and burst shape.
Therefore silencing the Cl^- mediated transmission in chronic CNQX cultures revealed a purely excitatory rhythmic activity identical to that observed in control cultures. This result suggested that the Cl^- mediated transmission might play a major role in the expression of the different rhythmic features observed in chronic treated interneurons.

CONCLUSIONS

The present study has investigated the operation of spinal premotoneuronal networks in organotypic cocultures of spinal cord and dorsal root ganglia from rat embryos. Ventral horn interneurons in the organotypic slice cultures consistently generated rhythmic activity. Rhythmicity crucially depended on the level of excitability in the network. Increasing the excitability of the network triggered the activation of rhythmic outputs. This phenomenon had been elicited by: a) block of Cl^- mediated transmission, b) raising the extracellular K^+ concentration that promoted the depolarization of all the cells in the slice, c) eliminating Mg^{2+} from the extracellular solution which enhanced the NMDA receptor activation in the network.

In the case of rhythmic activity induced by block of Cl^- mediated transmission, after two weeks in culture, cycle period and duration were similar to those recorded in motoneurons from the rat isolated spinal cord *in vitro* in the same pharmacological conditions. Likewise, rhythmic bursts in the presence of high K^+ or Mg^{2+} free displayed a frequency close to that observed during locomotor-like rhythmic patterns in the isolated neonatal rat spinal cord. Furthermore, during high K^+ bursting activity, ventral interneurons displayed a complex temporal organization of excitatory and inhibitory events reminiscent of responses recorded from motoneurons and interneurons in the isolated preparation during fictive locomotion. These observations suggested that a well-preserved structure such as organotypic spinal cultures that had few cell layers, contained the basic circuitry responsible for the generation of rhythmic activity and some mechanisms underlying rhythmogenesis in the isolated *in vitro* spinal cord were also present.

Ionotropic glutamate receptors played a fundamental role in mediating these rhythms. Rhythmic activity induced by block of Cl^- mediated transmission, after two weeks in culture, was the expression of synchronous activation of both NMDA and non-NMDA receptors. High K^+ oscillations were mainly dependent on AMPA/Kainate receptor activation while Mg^{2+} free rhythm was suppressed by NMDA receptor antagonist, suggesting that ventral interneurons could generate similar rhythms using either class of glutamate receptors (as observed in the intact spinal cord preparation). Rhythmic activity induced by block of Cl^- mediated

transmission was studied after one as well as after two weeks in culture and it showed different features both in terms of burst periodicity and sensitivity to glutamate receptors antagonist. In particular the frequency of these rhythmic bursts increased during *in vitro* development suggesting that in the organotypic spinal cultures, rhythmogenic networks underwent *in vitro* maturation.

Another important property of ventral interneurons in organotypic spinal cultures consisted in their ability to compensate for drastic, prolonged changes in the network excitability. Homeostatic mechanisms regulated spinal network activity during *in vitro* development. Chronic block of AMPA/Kainate receptors during the first week in culture, induced a significant increase in the frequency of spontaneous postsynaptic currents (PSCs) or miniature currents (mPSCs) respect to control, untreated cultures. Chronic block of Cl^- mediated transmission induced an effect opposite to that induced by chronic block of non-NMDA receptors, in fact the frequency of both PSCs and mPSCs were strongly reduced. Chronic suppression of Na^+ dependent spiking activity did not drastically affect the spontaneous activity of the interneuron. The amplitude of miniature events presented no significant changes after these chronic treatments, supporting that, in these *in vitro* spinal networks, homeostatic plasticity was manifested mainly at the presynaptic level changing the operation of the network at the level of the frequency of spontaneous and miniature synaptic activity. Preliminary results on cultures chronically treated with the AMPA/Kainate receptor blocker, suggested that also the rhythmogenic properties of ventral interneurons were homeostatically regulated. In fact ventral interneurons consistently generated rhythmic activity increasing the extracellular K^+ concentration, but such an activity showed a frequency higher than in control cultures and the burst shape was characterized by a very slow rise time. A similar burst profile was observed also in Mg^{2+} free rhythmic activity. Block of Cl^- mediated transmission induced a pattern of activity comparable to that observed in control cultures.

References

Avignone, E., and Cherubini, E., 1999. Muscarinic receptor modulation of GABA-mediated giant depolarizing potentials in the neonatal rat hippocampus. *J. Physiol.* 518, 97-107.

Atwood, H. L., and Wojtowicz, J. M. 1999. Silent synapses in neural plasticity: current evidence. *Learning and Memory*. **6**, 542-71.

Bacci, A., Verderio, C., Pravettoni, E., and Matteoli, M. 1999. Synaptic and intrinsic mechanisms shape synchronous oscillations in hippocampal neurons in culture. *EJN* 11, 389-97.

Ballerini, L., Bracci, E., and Nistri, A. 1995. Desensitization of AMPA receptors limits the amplitude of EPSPs and the excitability of motoneurons of the rat isolated spinal cord. *Eur. J. Neurosci.* 7, 1229-34.

Ballerini, L., Bracci, E., and Nistri, A. 1997. Pharmacological block of the electrogenic sodium pump disrupts rhythmic bursting induced by strychnine and bicuculline in the neonatal rat spinal cord. *J. Neurophysiol.* 77, 17-23.

Barbeau, H., and Rossignol, S. 1991. Initiation and modulation of the locomotor pattern in the adult chronic spinal cat by noradrenergic, serotoninergic and dopaminergic drugs. *Brain Res.* 546, 250-60.

Barry, M. J., and O'Donovan, M.J., 1987. The effects of excitatory amino acids and their antagonists on the generation of motor activity in the isolated chick spinal cord. *Dev. Brain Res.* 36, 271-77.

Beato, M., Bracci, E., and Nistri, A. 1997. Contribution of NMDA and non-NMDA glutamate receptors to locomotor pattern generation in the neonatal rat spinal cord. *Proc. Roy. Soc.* B 264, 877-84.

Bekoff, A., Stein, P. S., and Hamburger, V., 1975. Coordinated motor output in the hindlimb of the 7-day chick embryo. *PNAS* 72, 1245-48.

Ben-Ari, Y., Cherubini, E., Corradetti, R., and Gaiarsa J-L., 1989. Giant synaptic potentials in immature rat CA3 hippocampal neurons. *J. Physiol.* 416, 303-25.

Berridge, M.J. 1998. Neuronal calcium signaling. *Neuron.* 21, 13-26.

Bormann, J., Hamill, O. P., and Sakmann, B. 1987. Mechanism of anion permeation through channels gated by glycine and γ-aminobutyric acid in mouse cultured spinal neurones. *J. Physiol.*, 385, 243-86.

Bracci, E., Ballerini, L., and Nistri, A., 1996a. Localization of rhythmogenic networks responsible for spontaneous bursts induced by strychnine and bicuculline in the

rat isolated spinal cord. *J. Neurosci.* 16, 7063-76

Bracci, E., Ballerini, L., and Nistri, A., 1996b. Spontaneous rhythmic bursts induced by pharmacological block of inhibition in lumbar motoneurons of the neonatal rat spinal cord. *J. Neurophysiol.* 75, 640-47.

Bracci, E., Beato, M., and Nistri, A., 1998. Extracellular K+ induces locomotor-like patterns in the rat spinal cord in vitro: comparison with NMDA or 5-HT induced activity. *J. Neurophysiol.* 79, 2643-52.

Braschler, U. P., Iannone, A., Spenger, C., Streit, J., and Lüscher, H.-R. 1989. A modified roller tube technique for organotypic cocultures of embryonic rat spinal cord, sensory ganglia and skeletal muscle. *J. Neurosci. Meth.* 29, 121-29.

Brown, A.G. 1981. Organization in the spinal cord. The anatomy and the physiology of identified neurons. Berlin:Springer-Verlag.

Butts, D. A, Feller, M. B., Shatz, C. J., and Rokhsar, D. S.. 1999. Retinal waves are governed by collective network properties. *J. Neurosci.* 19, 3580-93.

Calvo, S., Stauffer, J., Nakayama, M., and Buonanno, A. 1996. Transcriptional control of muscle plasticity: differential regulation of troponin I genes by electrical activity. *Dev. Genet.* 19, 169-81.

Cazalets, J.-R., Sqalli-Houssaini, Y., and Clarac, F. 1992. Activation of the central pattern generators for locomotion by serotonin and excitatory amino acids in neonatal rat. *J. Physiol.* 455, 187-204.

Cazalets, J.R., Sqalli-Houssaini, Y., and Clarac, F., 1995. GABAergic inactivation of the central pattern generators for locomotion in isolated neonatal rat spinal cord. *J. Physiol. (Lond)* 474, 173-81.

Cazalets, J.R., Borde, M., and Clarac, F., 1995. Localization and organization of the central pattern generator for hindlimb locomotion in newborn rat. *J. Neurosci.* 15, 4943-51.

Cazalets, J.R., Borde, M., and Clarac, F., 1996. The synaptic drive from the spinal locomotor network to motoneurons in the newborn rat. *J. Neurosci.* 16, 298-306.

Cherubini, E., Gaiarsa, J.L., and Ben-Ari, Y., 1991. GABA: an excitatory transmitter in early postnatal life. *Trends Neurosci.* 14, 515-9.

Chub, N., and O'Donovan, M. J., 1998. Blockade and recovery of spontaneous rhythmic activity after application of neurotransmitter antagonists to spinal networks of the chick embryo. *J. Neurosci.* 18, 294-306.

Chub, N., Moore, L. E., and O'Donovan, M. J., 1998. Comparison of NMDA–induced membrane potential oscillations and spontaneous rhythmic activity in the chick spinal cord. *NY. Acad. Sci.* 860, 467-69.

Clements, J. D., and Bekkers, J. M. 1997. Detection of spontaneous synaptic events with an optimally scaled template. *Biophys. Journal* 73, 220-9.

Cowley, K. C., and Schmidt, B. J., 1995. Effects of inhibitory amino acid antagonists on reciprocal inhibition interactions during rhythmic motor activity in the *in vitro* neonatal rat spinal cord. *J. Neurophysiol.* 74, 1109-17.

Craig, A. M. 1998. Activity and synaptic receptor targeting:the long view. *Neuron* 21, 459-62.

Crain, S. M. 1976. Neurophysiologic studies in tissue culture. Raven press, New York

Crair, M.C., 1999. Neuronal activity during development: permissive or instructive? *Curr. Opin. Neurobiol.* 9, 88-93.

Davis, G. W., and Goodman, C. S. 1998. Synapse-specific control of synaptic efficacy at the terminals of a single neuron. *Nature*. 392, 82-6.

Delfs, J., Friend, J., Ishimoto, S., and, Saroff, D. 1989. Ventral and dorsal horn acetylcholinesterase neurons are maintained in organotypic cultures of postnatal rat spinal cord explants. *Brain Res.* 488, 31-42.

Desai, N. J., Rutherford L. C., and Turrigiano, G. G. 1999. Plasticity in the intrinsic excitability of cortical pyramidal neurons. *Nat. Neurosci.* 2, 515-20.

Fedirchuk, B., Wenner, P., Whelan, P. J., Ho, S., Tabak, J., and O'Donovan, M.J., 1999. Spontaneous network activity transiently depresses synaptic transmission in the embryonic chick spinal cord. *J.Neurosci.* 19, 2102-12.

Feldman, D. E., Nicoll, R. A., and Malenka, R. C. 1999. Synaptic plasticity at thalamocortical synapses in developing rat somatosensory cortex: LTP, LTD, and silent synapses. *J. Neurobiol.* **41**, 92-101.

Feller, M. B., Wellis, D. P., Stellwagen, D., Werblin, F. S., and Shatz, C. J., 1996. Requirement for cholinergic synaptic transmission in the propagation of spontaneous retinal waves. *Science* 272, 1182-87.

Feller, M. B., Butts, D. A., Aaron, H. L., Rokhsar, D. S., and Shatz, C. J., 1997. Dynamic processes shape spatiotemporal properties of retinal waves. *Neuron* 19, 293-306.

Fields, R. D., and Itoh, K. 1996. Neural cell adhesion molecules in activity-dependent

development and synaptic plasticity. *Trends Neurosci.* 19, 473-80.

Fischer, K. F., Lukasiewicz, P. D., and Wong, R. O. L., 1998. Age-dependent and cell class-specific modulation of retinal ganglion cell bursting activity by GABA. *J. Neurosci.* 18, 3767-78.

Franklin, J. L., and Johnson, E., 1992. Suppression of programmed neuronal death by sustained elevation of cytoplasmic calcium. *Trends Neurosci.* 15, 501-08.

Gähwiler, B. H. 1981. Organotypic monolayer cultures of nervous tissue. *J. Neurosci. Meth.* 4, 329-42.

Gähwiler, B. H. 1984. Dvelopment of the hippocampus in vitro: cell types, synapses and receptors. *Neuroscience* 11, 751-60.

Gaiarsa Jl, Corradetti R, Cherubini E, Ben-Ari Y., 1990. Modulation of GABA-mediated synaptic potentials by glutamatergic agonists in neonatal CA3 rat hippocampal neurons. *Eur J. Neurosci.* 3, 301-09.

Galli, L., and Maffei, L., 1988. Spontaneous impulse activity of rat retinal ganglion cells in prenatal life. *Science* 242, 90-91.

Gao, B.-X., Cheng, G., and Ziskind-Conhaim, L. 1998. Development of spontaneous synaptic transmission in the rat spinal cord. *J. Neurophysiol.* 79, 2277-87.

Garaschuk O., Hanse E., and Konnerth A., 1998. Developmental profile and synaptic origin of early network oscillations in the CA1 region of rat neonatal hippocampus. *J. Physiol.* 507, 219-36.

Garcia-Castro, M., and Bronner-Fraser, M. 1999. Induction and differentiation of the neural crest. *Curr. Opin. Cell Biol.* 11, 695-98.

Gomez, T. M., and Spitzer, N. C. 1999. *In vivo* regulation of axon extension and pathfinding by growth-cone calcium transients. *Nature* 397, 350-55.

Goodman, C. S., and Shatz, C. J., 1993. Developmental mechanisms that generate precise patterns of neuronal connectivity. *Cell* 72, 77-98.

Greer, J. J., Smith, J. C., and Feldman, J. L., 1992. Respiratory and locomotor patterns generated in the fetal rat brain stem- spinal cord *in vitro. J Neurophysiol.* 67, 996-99.

Grillner, S. 1981. Control of locomotion in bipeda, tetrapods and fish. *In:* Handbook of Physiology (ed. Brooks VB). *American Physiological Society:MD*, 1179-1236.

Grillner, S., and Matsushima 1991. The neural network underlying locomotion in

lamprey--synaptic and cellular mechanisms. *Neuron* 7, 1-15.

Grillner, S., and Zangger, P. 1979. On the central generation of locomotion in the low spinal cat. *Exp. Brain Res.* 34, 241-61.

Gurantz, D., Harootunian, A. T., Tsien, R. Y., Dionne, V. E., and Margiotta, J. F. 1994. VIP modulation neuronal acetylcholine receptor function by cyclic AMP-dependent mechanism. *J.Neurosci.* 14, 3540-47.

Hestrin, S. 1993. Different glutamate receptor channels mediate fast excitatory synaptic currents in inhibitory and excitatory cortical neurons. *Neuron* 11, 1083-91.

Ho, S, and O'Donovan, M. J., 1993. Regionalization and intersegmental coordination of rhythm-generating networks in the spinal cord of the chick embryo. *J. Neurosci.* 13, 1354-71.

Hochman, S., Jordan, L. M., and MacDonald, J. F. 1994. N-methyl-D-aspartate receptor- mediated voltage oscillations in neurons surrounding the central canal in slices of rat spinal cord. *J. Neurophysiol.* 72, 565-77.

Iizuka, M., Nishimaru, H., and Kudo, N., 1998. Development of the spatial pattern of 5-HT-induced locomotor rhythm in the lumbar spinal cord of rat fetuses in vitro. *Neurosci Res* 31, 107-11.

Jakowec, M. W., Fox, A. J., Martin, A. J., and Kalb, R. G. 1995. Quantitative and qualitative changes in AMPA receptor expression during spinal cord development. *Neuroscience* 67, 893-907.

Jarolimek, W., Lewen, A., and Misgeld, U. 1999. A furosemide-sensitive K^+-Cl^- cotransporter counteracts intracellular Cl^- accumulation and depletion in cultured rat midbrain neurons. *J. Neurosci.* 19, 4695-4704.

Jarvis, J. C., Mokrusch, T., Kwende, M. M., Sutherland, H., and Salmons, S. 1996. Fast-to-slow transformation in stimulated rat muscle. *Muscle Nerve* 19, 1469-75

Kaila, K. 1994. Ionic basis of GABAA receptor channel function in the nervous system. *Progr. Neurobiol.* **42**, 489-537.

Kandel, E. R., Schwartz, J. H., and Jessell, T. M. 2000. Principles of neural science, IV edition. McGraw-Hill: NY.

Kater, S.B., Mattson, M.P., Cohan, C., and Connor, J., 1988. Calcium regulation of the neuronal growth cone. *Trends Neurosci.* 11, 315-21.

Katz L.C., and Shatz C.J., 1996. Synptic activity and construction of cortical circuits. *Science* 274, 1133-38.

Khazipov R., Leinekugel X., Khalilov I., Gaiarsa J.L., and Ben-Ari Y., 1997. Synchronization of GABAergic interneuronal network in CA3 subfield of neonatal rat hippocampal slices. *J. Physiol.* 498, 763-72.

Kiehn, O., Johnson, B. R., and Raastad, M. 1996. Plateau properties in mammalian spinal interneurons during transmitter-induced locomotor activity. *Nuroscience* 75, 263-73.

Kremer, E., and Lev-Tov, A., 1997. Localization of the spinal network associated with generation of hindlimb locomotion in the neonatal rat and organization of its transverse coupling system. *J. Neurophysiol.* 77, 1155-70.

Kjaerulff, O., Barajon, I., and Kiehn, O., 1994. Sulphorhodamine-labelled cells in the neonatal rat spinal cord following chemically induced locomotor activity in vitro. *J. Physiol. (Lond)* 478, 265-73.

Kjaerulff, O., and Kiehn, O., 1996. Distribution of networks generating and coordinating locomotor activity in the neonatal spinal cord *in vitro*: a lesion study. *J. Neurosci.* 16, 5777-94.

Kudo, N., and Yamada, T., 1987. Morphpological and physiological studies of development of the monosynaptic reflex pathway in the rat lumbar spinal cord. *J. Physiol.* 389, 441-59.

Kudo, N. Ozaki, S., and Yamada, T. 1991. Ontogeny of rhythmic activity in the spinal cord of the rat. *In:*Neurobiological basis of human locomotion.(eds.Shimamura, M., Grillner, S., and Edgerton, V. R) PUBLISHER: Tokyo, 127-136.

Landmesser, L., 1978. The development of motor projection patterns in the chick hind limb. *J. Physiol.* 284, 391-414.

Landmesser, L. T., and O'Donovan, M. J., 1984. Activation patterns of embryonic chick hindlimb muscles recorded *in ovo* and in an isolated spinal cord preparation. *J. Physiol.* 347, 189-204.

Leinekugel, X., Medina, I., Khalilov, I., Ben-Ari, Y., and Khazipov, R., 1997. Ca2+ oscillations mediated by the synergistic excitatory action of GABAA and NMDA receptors in the neonatal hippocampus. *Neuron* 18, 243-55.

Leinekugel, X., Tseeb, V., Ben-Ari, Y., and Bregestovski, P., 1995. Synaptic $GABA_A$ activation induces Ca++ rise in pyramidal cells and interneurons from rat neonatal hippocampal slices. *J. Physiol.* 487, 315-22.

Lev-Tov, A., and O'Donovan, M. J. 1995. Calcium iumaging of motoneuron activity in the en-bloc spinal cord preparation of the neonatal rat. *J. Neurophysiol.* 74, 1324-34.

Lewis, C. A., and Faber, D. S. 1996. Properties of spontaneous inhibitory synaptic currents in cultured rat spinal cord and medullary neurons. *J. Neurophysiol.* 76, 448-460.

Lissin, D. V., Gomperts, S. N., Carroll, R. C., Christine, C. W., Kalman, D., Kitamura, M., Hardy, S., Nicoll, R. A., and Malenka, R. C. 1998. Activity differentially regulates the surface expression of synaptic AMPA and NMDA glutamate receptors. *Proc. Natl. Acad. Sci.* 95, 7097-7102.

Malenka, R. C. ,and Nicoll, R. A. 1997. Silent synapses speak up. *Neuron*, **19**, 473-75.

Mayer, M. L., and. Westbrook, G. L. 1987. The physiology of excitatory amino acids in vertebrate central nervous system. *Progr. Neurobiol.* 28, 197-276.

McAllister A.K., Katz L.C., and Lo D.C., 1996. Neurotrophin regulation of cortical dendritic growth requires activity. *Neuron* 17, 1057-64.

McKinney, R. A., Lüthi, A., Bandtlow, C. E., Gähwiler, B. H., and Thompson, S. M. 1999. Selective glutamate receptor antagonists can induce or pervent axonal sprouting in rat hippocampal slice cultures. *Proc. Natl. Acad. Sci.* 96, 11631-36.

Meister, M., Wong, R.O., Baylor, D.A., and Shatz, C. J. 1991. Synchronous bursts of action potentials in ganglion cells of the developing mammalian retina. *Science* 252, 939-43.

Milner, L. D., and Landmesser, L. T. 1999. Cholinergic and GABAergic inputs drive patterned spontaneous motoneuron activity before target contact. *J. Neurosci.* 19, 3007-22.

Ming, G.L., Song, H.J., Berninger, B., Holt, C.E., Tessier-Lavigne, M., and Poo, M. M. 1997. cAMP-dependent growth cone guidance by netrin-1. *Neuron* 19, 1225-35

Nakayama, K., Nishimaru, H., Iizuka, M., Ozaki, S., and Kudo, N. 1999. Rostrocaudal progression in the development of periodic spontaneous activity in fetal rat spinal motor circuits *in vitro*. *J. Neurophysiol.* 81, 2592-95.

Narayanan, C. H., Fox, M. W., and Hamburger, V. 1971. Prenatal development of spontaneous and evoked activity in the rat (*Rattus norvegicus albinus*). *Behaviour* 40, 100-34.

Nishimaru, H., Iizuka, M., Ozaki, S., and Kudo, N. 1996. Spontaneous motoneuronal activity mediated by glycine and GABA in the spinal cord of rat fetuses *in vitro*. *J. Physiol* 497, 131-43.

Nornes, H. O., and Das, G. D. 1974. Temporal pattern of neurogenesis in spinal cord of rat. I. An autoradiographic study-time and sites of origin and migration and settling patterns of neuroblasts. *Brain Res.* 73, 121-38.

Nusser, Z., Cull-Candy, S., and, Farrant, M. 1997. Differences in synaptic GABAA receptor number underlie variation in GABA mini amplitude. *Neuron* 19, 697-709.

O'Brien, R. J., Mammen, A. L., Blackshaw, S., Ehlers, M. D., Rothstein, J. D., and Huganir, R. L. 1997. The development of excitatory synapses in cultured spinal neurons. *J. Neurosci.* 17, 7339-50.

O'Brien, R. J., Kamboj, S., Ehlers, M. D., Rosen, K. R., Fischbach, G. D., and Huganir, R. 1998. Activity-dependent modulation of synaptic AMPA receptor accumulation. *Neuron* 21, 1067-78.

O'Donovan, M. J., and Landmesser, L. T. 1987. The development of hindlimb motor activity studied in an isolated preparation of the chick spinal cord. *J. Neurosci.* 7, 3256-64.

O'Donovan, M. J. 1989. Motor activity in the isolated spinal cord of the chick embryo: synaptic drive and firing pattern of single motoneurons. *J Neurosci.* 9, 943-58.

O'Donovan, M. J., Ho, S., and Yee, W. 1994. Calcium imaging of rhythmic network activity in the developing spinal cord of the chick embryo. *J. Neurosci.* 14, 6354-6369.

O'Donovan, M. J., Wenner, P., Chub, N., Tabak, J. and Rinzel, J. 1998a. Mechanisms of

spontaneous acitivty in the developing spinal cord and their relevance to locomation. *NY. Acad. Sci.* 860, 130-41.

O'Donovan, M. J., Chub, N., and Wenner, P. 1998b. Mechanisms of spontaneous activity in developing spinal networks. *J. Neurobiol.* 37, 131-45.

O'Donovan, M. J. 1999. The origin of spontaneous activity in developing networks of the vertebrate nervous system. *Curr. Opin. Neurobiol.* 9, 94-104.

Oppenheim, R. W., Chu Wang, I. W. and Foelix, R.F. 1975. Some aspects of synaptogenesis in the spinal cord of the chick embryo: a quantitative electorn microscopic study. *J. Comp. Neurol.* 161, 383-418.

Ozaki, S., Yamada, T:, Iizuka, M., Nishimaru, H., and Kudo, N. 1996. Development of locomotor activity induced by NMDA receptor activation in the lumbar spinal cord of the rat fetus studied *in vitro. Dev. Brain Res.,* 97, 118-25.

Penn, A. A., Riquelme, P. A., Feller, M. B., and, Shatz, C. J. 1998. Competition in retinogeniculate patterning driven by spontaneous activity. *Science* 279, 2108-12.

Provine, R. R. 1972. Ontogeny of bioelectric activity in the spinal cord of the chick embryo and its behavioral implications. *Brain Res.* 41, 365-78.

Raastad, M., Johnson, B. R., and Kiehn, O. 1996. The number of postsynaptic currents necessary to produce locomotor-related cyclic information in neurons in the neonatal rat spinal cord. *Neuron* 17, 729-38.

Raastad, M., Johnson, B. R., and Kiehn, O. 1997. Analysis of EPSCs and IPSCs carrying rhythmic, locomotor-related information in the isolated spinal cord of the neonatal rat. *J. Neurophysiol.* 78, 1851-59.

Rao, A., and Craig A. M. 1997. Activity regulates the synaptic localization of the NMDA receptor in hippocampal neurons. *Neuron* 19, 801-12.

Rexed, B. 1952. The cytoarchtectonic organization of the spinal cord in the cat. *J. Comp. Physiol.* 78, 1851-59.

Rivera, C. Voipio, J., Payne, J. A., Ruusuvuori, E., Lahtinen, H., Lamsa, K., Pirvola, U., Saarma, M., and Kaila, K. 1999. The K^+/Cl^- co-transporter KCC2 renders GABA hyperpolarizing during neuronal maturation. *Nature* 397, 251-55.

Rossignol, S. 1996. Neural control of stereotypic limb movement. *In* Handbook of Physiology, Section 12. Exercise: Regulation and Integration of Multiple Systems. Edited by Rowell, L. B., and Sheperd, J. T. *American Physiological Society:MD*, 13-216.

Schmidt, J. T., and, Eisele, L. E. 1985. Stroboscopic illumination and dark rearing block the sharpening of the regenerated retinotectal map in goldfish. *Neuroscience*. 14, 535-46.

Senn, W., Wyler, K., Larkum, M., Lüscher, H.-R., Mey, H., Müller, L., Stainhauser, D., Vogt, K., and Wannier Th. 1996. Dynamics of a random neural network with synaptic depression. *Nural Net.* 9, 575-88.

Sernagor, E., Chub, N., Ritter, A., and O'Donovan, M. J. 1995. Pharmacological characterization of the rhythmic synaptic drive onto lumbosacral motoneurons in the chick embryo spinal cord. *J. Neurosci.* 15, 7452- 64.

Shatz, C. J. 1990. Impulse activity and the patterning of connections during CNS development. *Neuron* 5, 745-56.

Snider, W. D., Zhang, L., Yusoof, S., Gorukanti, N., and Tsering C. 1992. Interactions between dorsal root axons and their target motor neurons in developing mammalian spinal cord. *J. Neurosci.* 12, 3494-3508.F.

Sqalli-Houssaini, Y., Cazalets, J-R., Clarac, F. 1993. Oscillatory properties of the central pattern generator for locomotion in neonatal rats. *J. Neurophysiol.* 70, 803-13.

Stellwagen, D., Shatz, C. J., and Feller, M. B. 1999. Dynamics of retinal waves are controlled by cyclic AMP. *Neuron* 24, 673-85.

Stoppini, L., Buchs, P. A., and Muller, D. 1991. A simple method for organotypic cultures of nervous tissue. *J. Neurosci. Meth.* 37, 173-81.

Streit, J., and, Lüscher, H. R. 1992. Miniature excitatory postsynaptic potentials in embryonic motoneurons grown in slice cultures of spinal cord, dorsal root ganglia and skeletal muscle. *Exp. Braib Res.* 89, 453-58.

Streit, J. 1993. Regular oscillations of synaptic activity in spinal networks *in vitro*. *J. Neurophysiol.* 70, 871-78.

Streit, J. 1996. Mechanisms of pattern generation in co-cultures of embryonic spinal cord and skeletal muscle. *Int. J. Developm. Neurosci.* 14, 137-48.

Suzue, T. 1992. Physiological activities of late-gestation rat fetuses *in vitro*. *Neurosci. Res.* 14, 145-57.

Tabak, J., and O'Donovan, M. J. 1998. Statistical analysis and intersegmental delays reveal possible role of network depression in the generation of spontaneous activity in the chick embryo spinal cord. *NY. Acad. Sci.* 860, 428-31.

Tabak, J., Senn, W., O'Donovan, M. J., and Rinzel, J. 2000. Modeling of spontaneous activity in developing spinal cord using activity-dependent depression in an excitatory network. *J. Neurosci.* 20, 3041-56.

Tanabe, T., and Jessell, T. M. 1996. Diversity and pattern in the developing spinal cord. *Science* 274, 1115-22.

Taylor M., and Reh T.A. 1990. Induction of differentiation of rat retinal, germinal, neuroepithelial cells by dbcAMP. *J Neurobiol.* 21, 470-81.

Tölle, T. R., Berthele, A., Laurie, D. J., Seeburg, P. H., and Zieglgänsberger, W. 1995b. Cellular and subcellular distribution of NMDAR1 splice variant mRNA in the rat lumbar spinal cord. *Eur. J. Neurosci.* 7, 1235-44.

Tölle, T. R., Berthele, A., Zieglgänsberger, W., Seeburg, P. H., and Wisden, W. 1995a. Flip and Flop variants of AMPA receptors in the rat lumbar spinal cord. *Eur. J. Neurosci.* 7, 1414-19

Tresch, M. C., and Kiehn, O. 2000. Motor coordination without action potentials in the mammalian spinal cord. *Nature Neurosci.* 3, 593-99.

Turrigiano, G. G., Leslie, K. R., Desai, N. S., Rutherford, L. C., and Nelson, S. B. 1998.

Activity-dependent scaling of quantal amplitude in neocortical neurons. *Nature* 391, 892-96.

Verderio, C., Bacci, A., Coco, S., Pravettoni, E., Fumagalli, G., and Matteoli, M. 1999. Astrocytes are required for the oscillatory activity in cultured hippocampal neurons. *EJN* 11, 2793-2800.

Wheatley, M. Javanovic, K., Stein, R. B., and Lawson, V. 1994. The activity of interneurons during locomotion in the in vitro *Necturus* spinal cord. *J. Neurophysiol.* 71, 2025-32.

Wong, R. O. L., Chernjavsky, A., Smith, S. J., and Shatz, C. J. 1995. Early functional neuronal networks in the developing retina. *Nature* 374, 617-18.

Wong, R. O. L. 1999. Retinal waves and visual system development. *Annu. Rev. Neurosci.* 22, 29-47.

Wyllie, D. J. A., Manabe, T., and, Nicoll, R. A. 1994. A rise in postsynaptic Ca^{2+} potentiates miniature excitatory postsynaptic currents and AMPA responses in hippocampal neurons. *Neuron* 12, 127-38.

Wu, W. L., Ziskind-Conhaim, L., and Sweet, M. A. 1992. Early development of glycine- and GABA-mediated synapses in rat spinal cord. *J. Neurosci.* 12, 3935-45.

Zhou, Z. J. 1998. Direct participation of starbust amacrine cells in spontaneous rhythmic activities in the developing mammalian retina. *J. Neurosci.* 18, 4155-65.

Ziskind-Conhaim, L. 1990. NMDA receptors mediate poly- and monosynaptic potentials in motoneurons of rat embryos. *J. Neurosci.* 10, 125-35.

APPENDIX

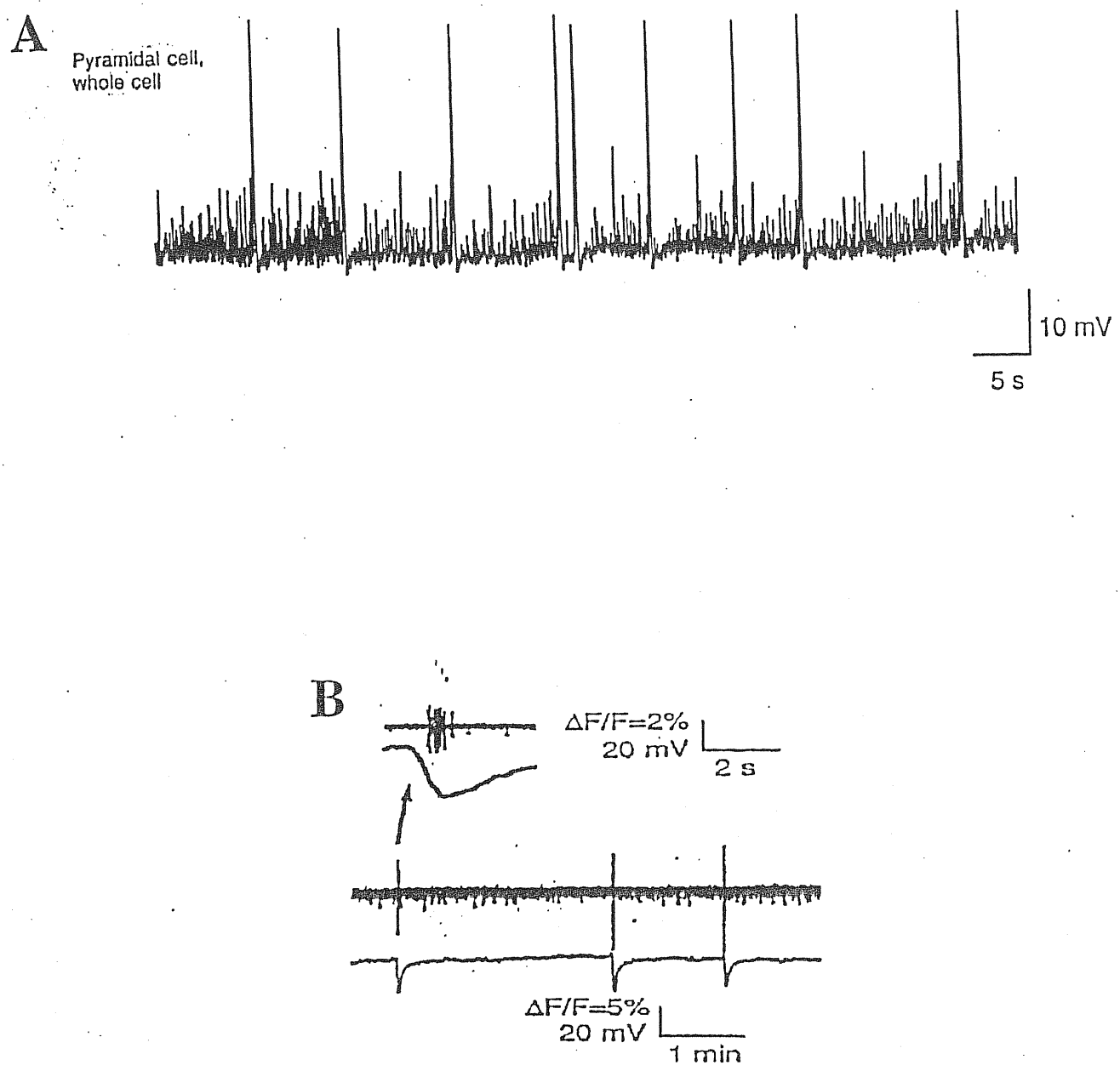

Figure I. Spontaneous GDPs from a CA3 pyramidal neuron in the rat at postnatal day P5. The resting membrane potential is -55 mV (**A**) (adapted from Avignone and Cherubini, 1999). **B**: Simultaneous extracellular recordings (upper trace) and Ca^{2+} imaging recordings (lower trace) from ganglion cells in the retina of neonatal ferret. Bursts of action potentials occur simultaneously with retinal waves measured with fura-2AM ($\Delta F/F$ averaged over an area of tissue 50 by 50 μm^2). The arrow indicates a burst (top) and a Ca^{2+} wave (bottom) shown on an expanded time scale. (Adapted from Penn et al., 1998).

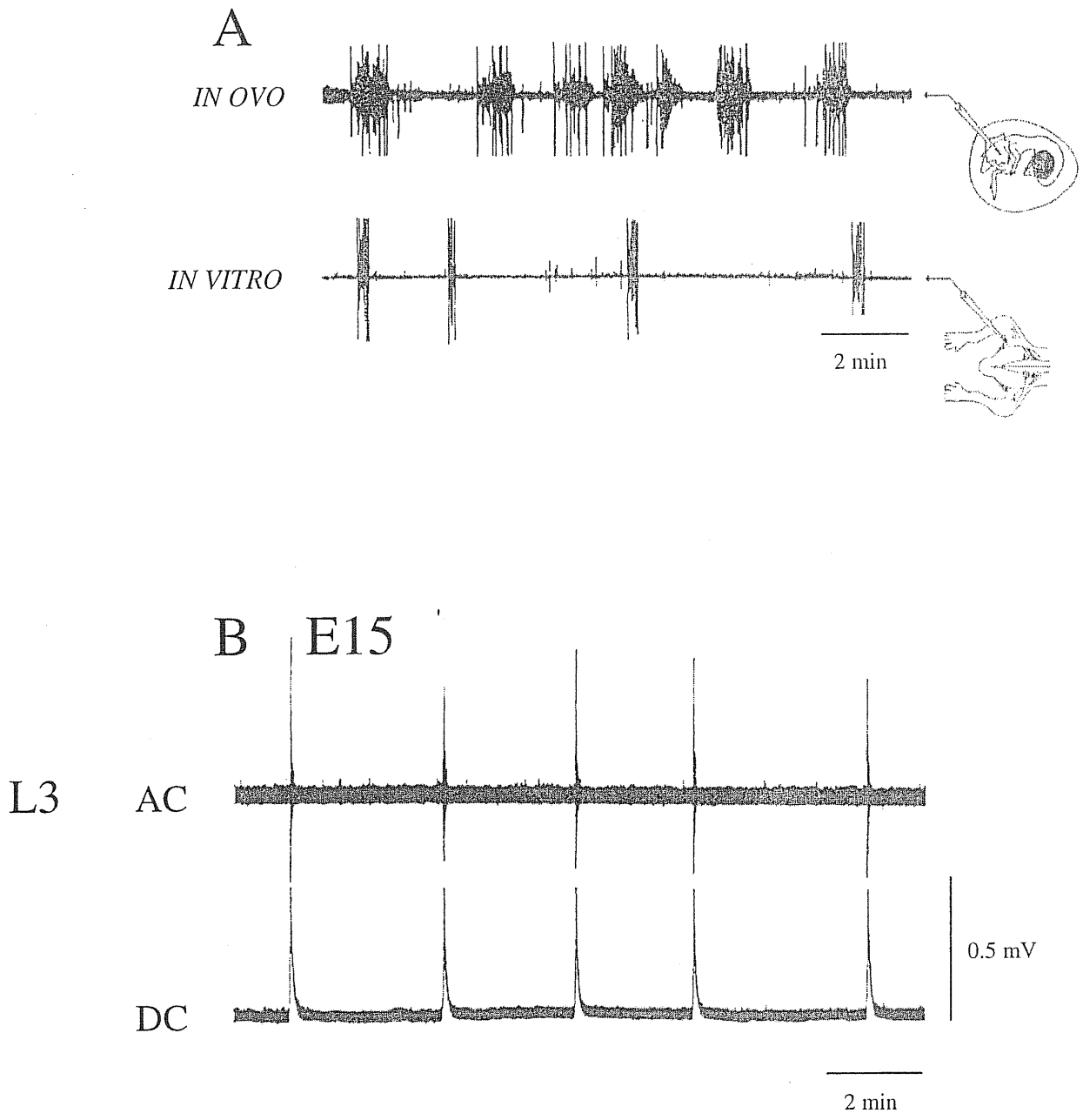

Figure II. A: Comparison of spontaneous rhythmic activity generated by hindlimb muscles in the egg (*in ovo)* or in the isolated spinal cord/hindlimb preparation (*in vitro).* Electromyographic recordings from the sartorius muscle *in ovo* and in an isolated spinal cord preparation with hindlimb attached from chick embryos at stage 36. (Adapted from O'Donovan et al., 1998). **B**: Spontaneous rhythmic activity from the L3 ventral root in rat embryo (E15). Upper and lower traces are recorded from the same extracellular electrode and show respectively nerve discharges recorded by high gain AC amplifier and ventral root potentials by a DC amplifier. (Adapted from Nishimaru et al., 1996).

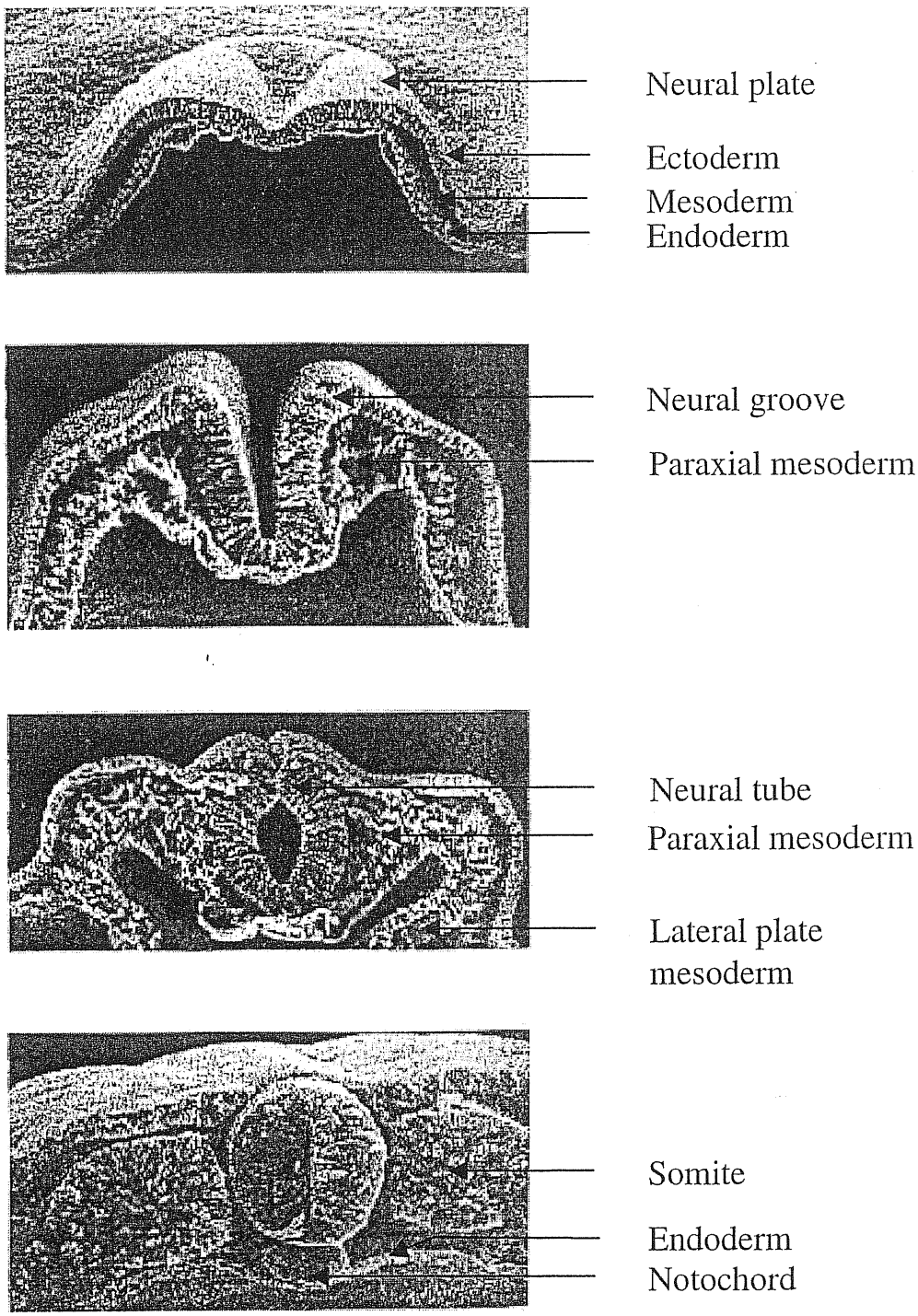

Figure III. Scanning electron micrographs of chick embryo spinal cord during development. **A**: Position of the neural plate in relation to non-neural cell layers, the mesoderm and the endoderm. **B**: After the neural plate has formed it begins to fold into a tubular structure, the neural groove. **C**: Dorsal closure of the neural groove to form the neural tube. **D**: Maturation of the neural tube and its position relative to the axial mesodermal structure, notochord and somites. (Adapted from Kandel et al., 2000)

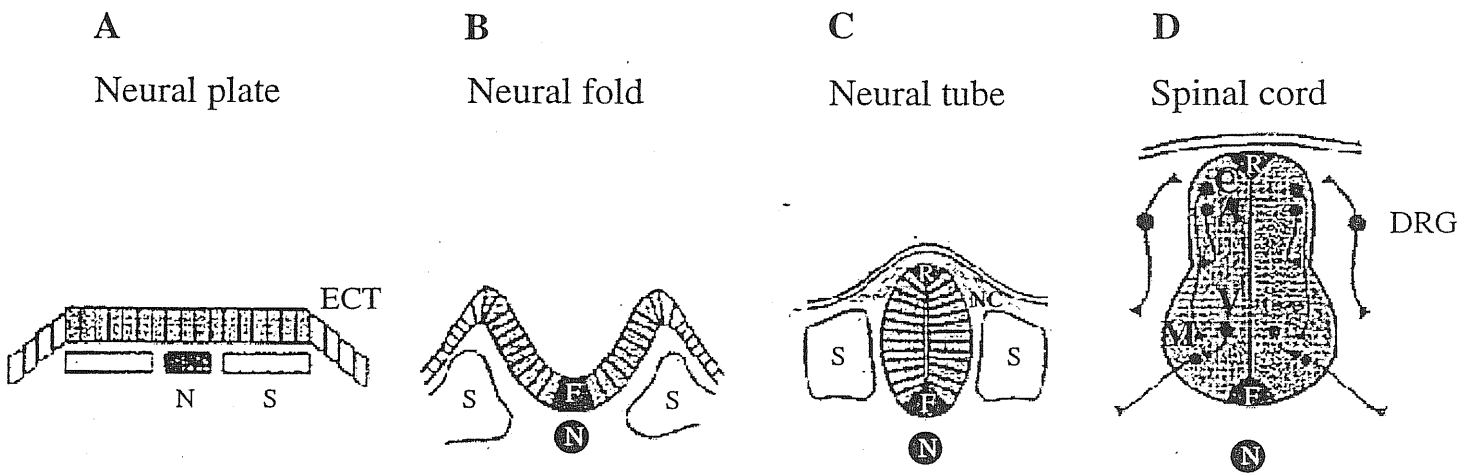

Figure IV. A: the neural plate is formed as a columnar epithelium and is underlain by axial mesoderm cells of the notochord (N) and paraxial mesoderm (later somites, S) and flanked by epidermal ectoderm (ECT). **B**: The neural plate buckles at its midline (floor plate, F) to form the neural folds. **C**: The neural tube forms by fusion of the dorsal tips of the neural folds, generating roof plate cells and neural crest cells (NC)which emigrate from the dorsal neural tube. **D**: Cells proliferate and differentiate into neurons located at different dorsoventral positions. Subclasses of commissural (C) and association (A) neurons differentiate dorsally, whereas motoneurons (M) and ventral interneurons (V) differentiate ventrally near F. Dorsal root ganglion (DRG) neurons are generated from post-migratory neural crest cells. (Adapted from Tanabe and Jessell, 1996).

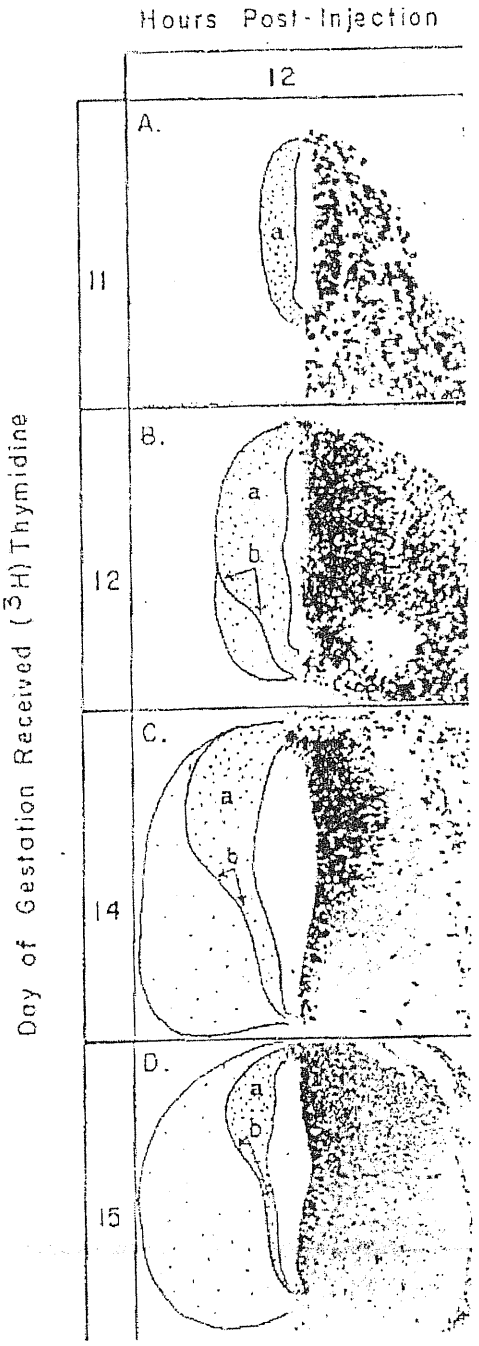

Figure V. Changes in the ventricular zone in autoradiograms from the cervical regions of rat embryos that had received [^{3}H] thymidine at several stages of gestation and were sacrificed 12 h post-injection. On day E11, labeled, proliferating cells are located throughout the entire neural tube (**A**). **B**: By E12, the ventricular zone (a) in the ventral quarter of the tube starts to regress (b indicates the region of regression). As development progresses, the ventricular zone continues to exhibit a progressive regression in the dorsal direction (**C**, **D**). (Adapted from Nornes and Das, 1974).

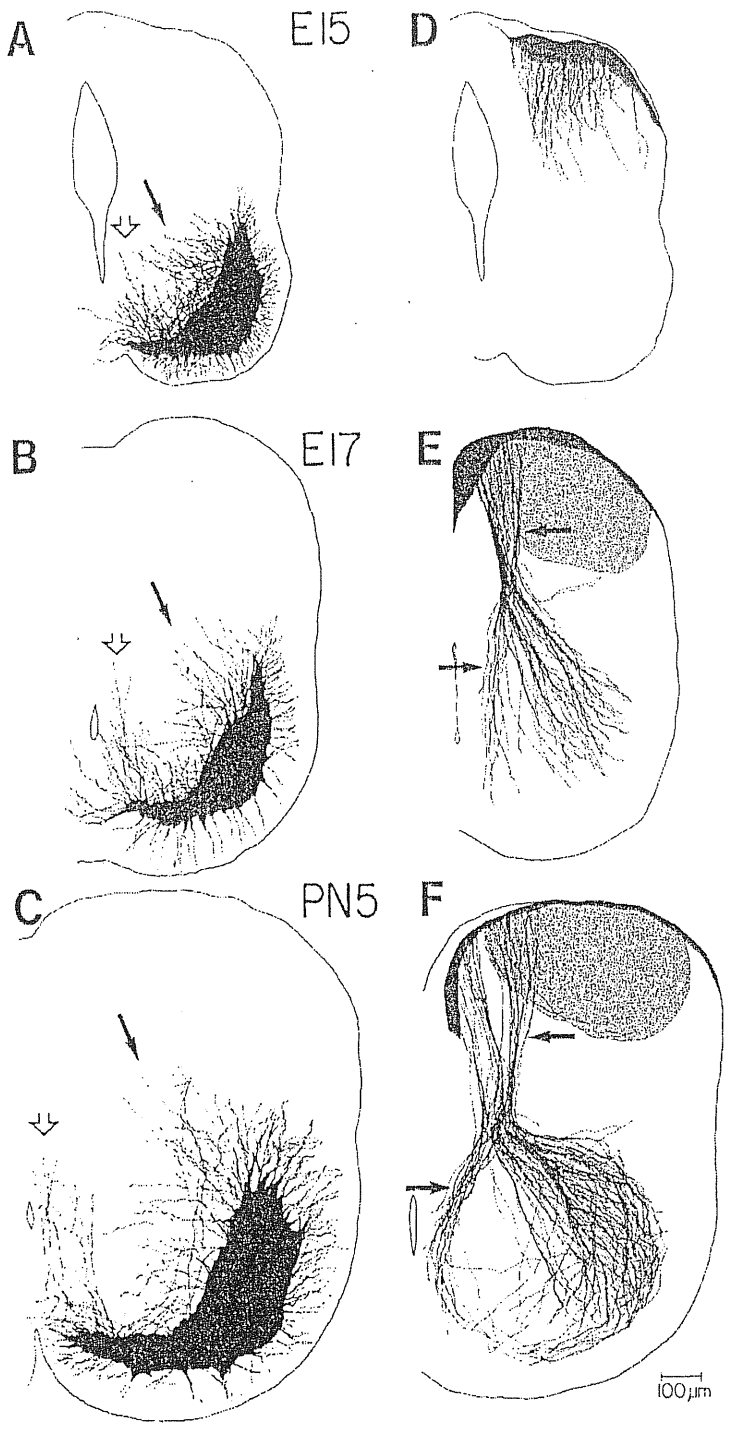

Figure VI. A-C: Camera lucida tracing of motoneuron dendrites in the cervical segment C5 in the rat. Motoneuronal pools are tightly clustered at early ages and individual pools are not distinguished. By E15 (**A**), motoneurons project dendrites into the gray matter (solid arrow). **B**: At E17 dendrites of lateral motoneurons (solid arrow) project directly in the path of incoming Ia afferents. Dendrites of medial motoneurons project dorsally along the midline (open arrow). This pattern of dendritic outgrowth of motoneurons is maintained at P5 (**C**). **D-F**: Development of the Ia projection in C5. **D**: At E15 dorsal root afferents first penetrate gray matter. **E**: the afferents grow in fascicles toward the motor pool, they converge in the intermediate zone and axons destined for the medially located motor pools (arrows) segregate from others in the intermediate zone and grow along the midline toward their target neurons. **F**: at P5 the overall arrangement is similar to that at E17. (Adapted from, Snider et al., 1992).

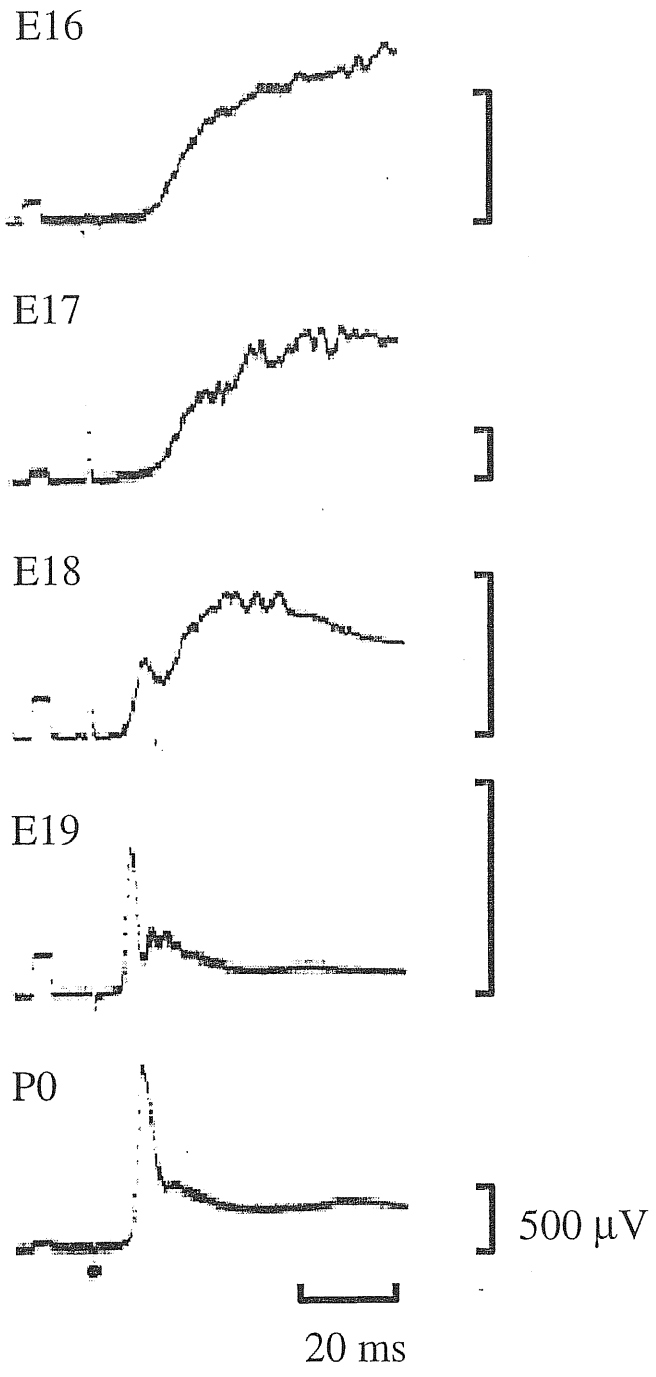

Figure VII. Evoked ventral root potentials from L4 elicited by L4 dorsal root stimulation in the rat isolated spinal cord. Slow, long-lasting responses are evoked in ventral roots at E17-18. A response with a steep rise and a shorter latency appears at E19 and it is even more pronounced with age (E20, P0) revealing a monosynaptic component (• indicates the stimulus artifact). (Adpted from Kudo and Yamada, 1987)

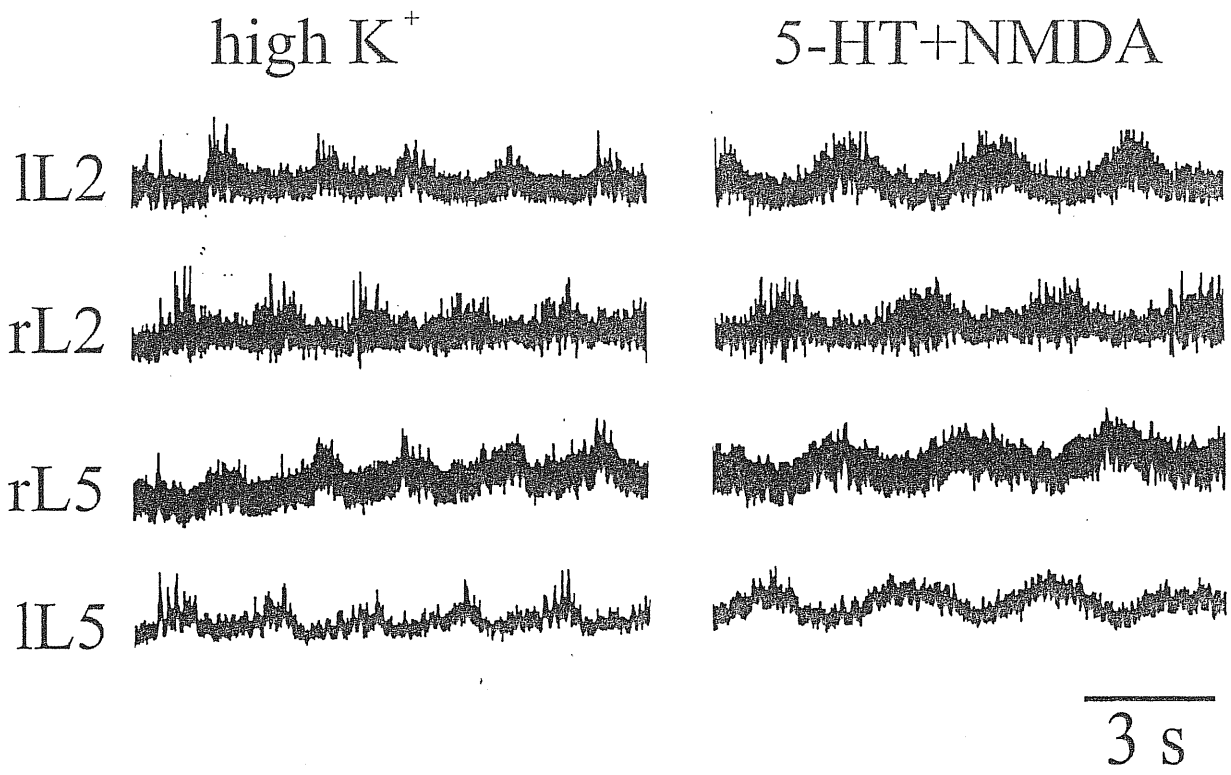

Figure VIII. Simultaneous DC recording from four lumbar ventral roots of the *in vitro* neonatal rat spinal cord. Top to bottom: Responses from left L2 (lL2) and right L2 (rL2) ventral roots and from right L5 (rL5) and left L5 (lL5) ventral roots in the presence of 9 mM extracellular K^+(left) or a mixture (right) of 5-HT (30 μM) and NMDA (6 μM). Note alternation between left and right ventral roots and between L2 and L5 ventral roots of the same side in both conditions. Note the similar frequencies of the two rhythmic patterns. (Adapted from Bracci et al., 1998).

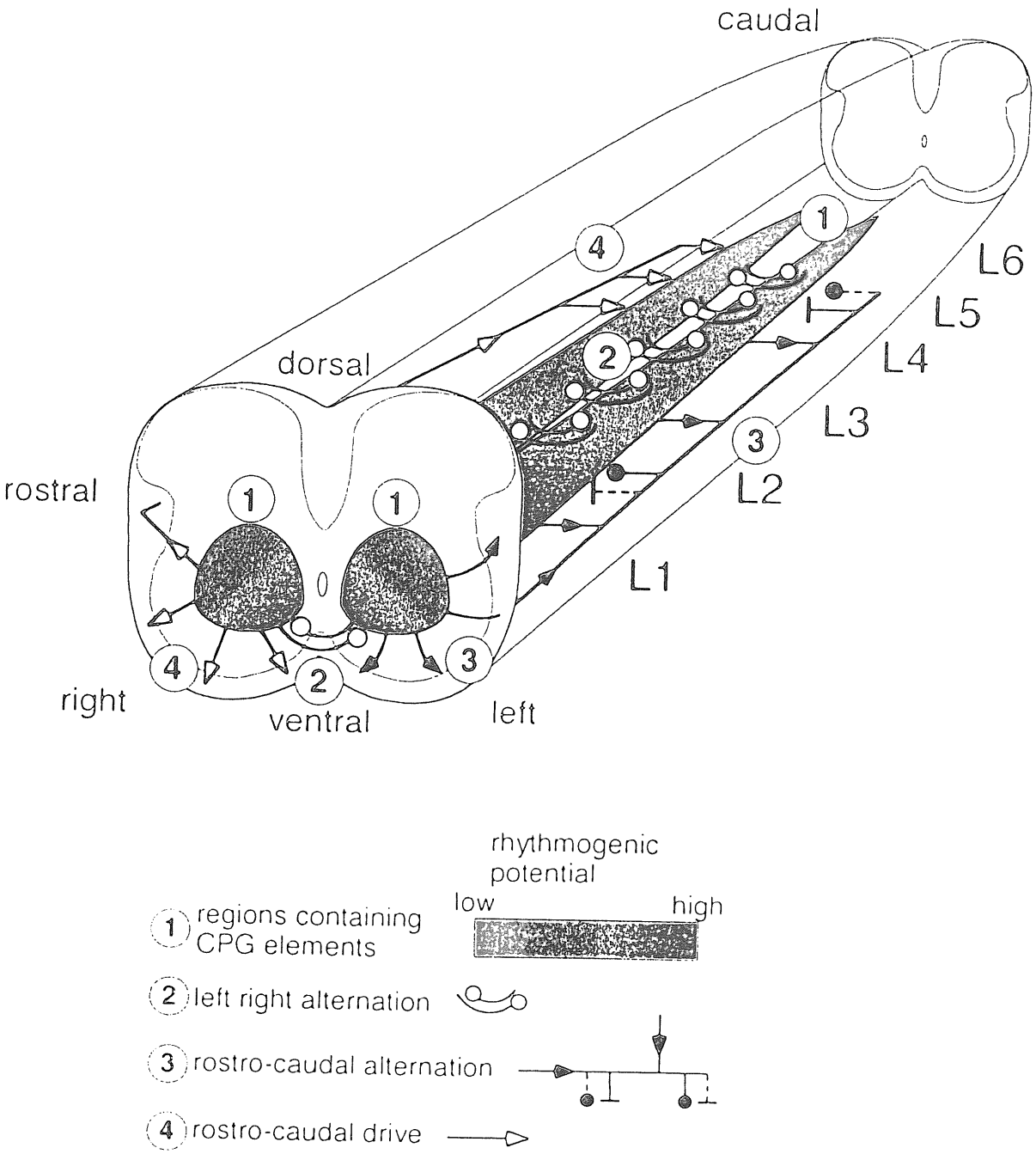

Figure IX. Rhythm generating networks are distributed along the lumbar rat spinal cord as two medial columns. The taper and the color gradient indicate the high rostral and lower caudal ability to generate rhythmic activity. In the rostral end, the columns are shown in cross section, indicating that the rhythmogenic networks extend rostrally into the thoracic segments. The mediolateral color gradient indicates the lower rhythmogenic potential in the lateral direction. The area below the central canal (1) contains part of the CPG for locomotor-related activity. The pathways mediating the left-right alternation are located in the ventral commissure (2). The pathways mediating rostrocaudal alternation are widely distributed in the lateral and ventral funiculus on the left side of the preparation (3). The rostrocaudal drive is indicated on the right side of the preparation (4). (Adapted from Kjaerulff and Kiehn, 1996).

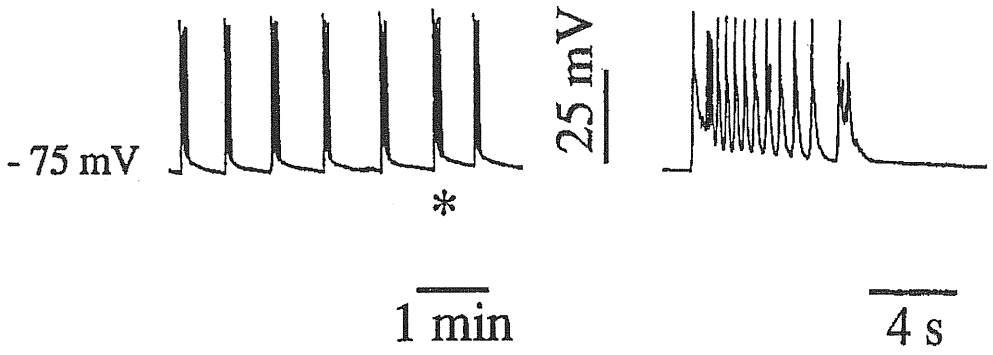

Figure X. Intracellular recordings from a lumbar motoneuron in the rat isolated spinal cord in the presence of strychnine (1 μM) and bicuculline (20 μM). Rhythmic and regular bursts of action potentials are elicited by the application of these drugs. A single burst (*) is shown in an expanded time scale at the right to reveal intraburst oscillations. (Adapted from Ballerini et al., 1997).

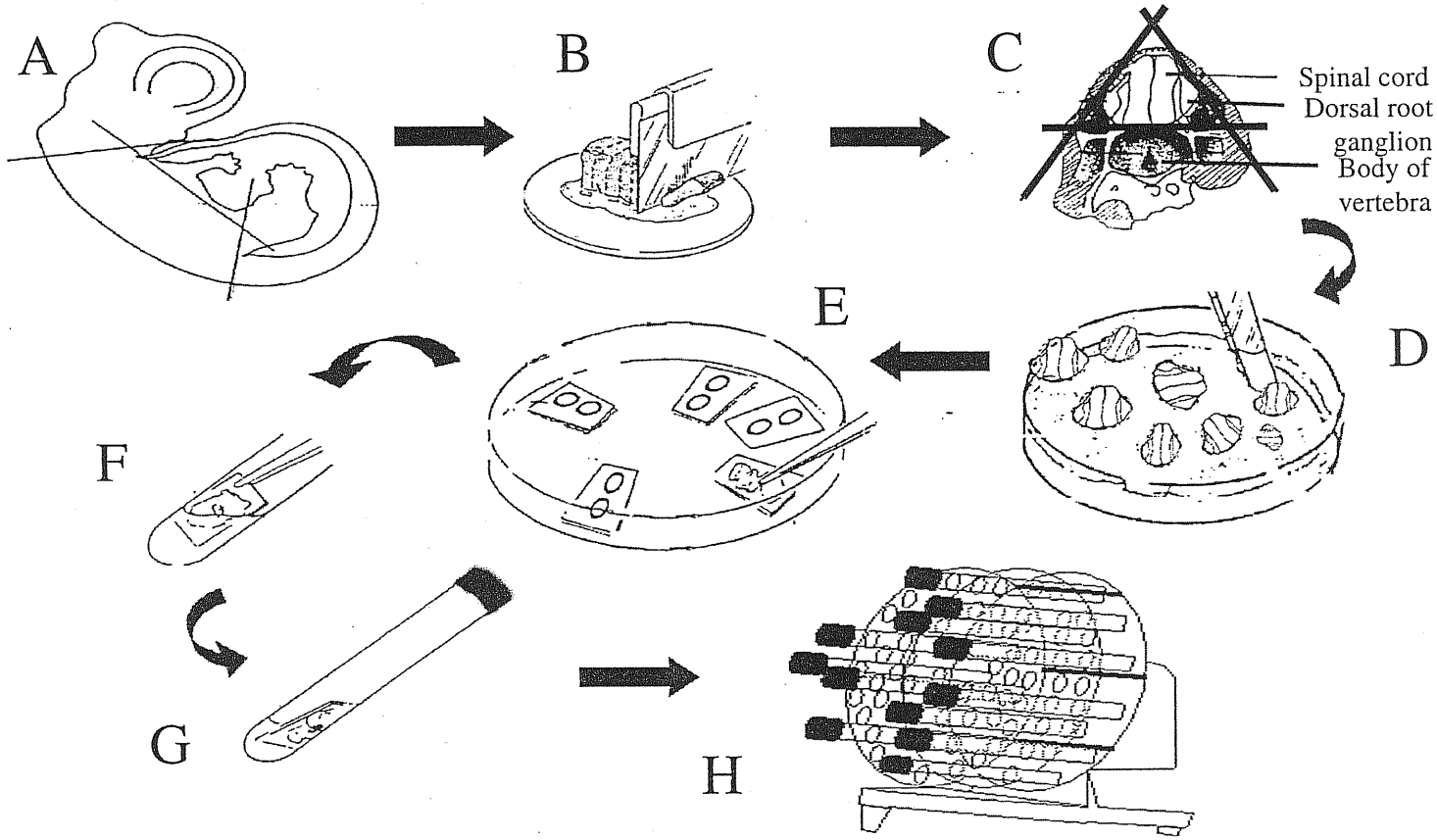

Figure XI. Preparation of organotypic cocultures of embryonic rat spinal cord and dorsal root ganglia. **A**: Dissection of the embryo back occurs at the level of the lines. **B**: The tissue is chopped in transverse slices. **C**: Transverse section of the back: spinal cord with dorsal root ganglia attached is isolated from the body of vertebra and from the rest of the slice following the lines. **D**: Slices are maintained in Petri dishes containing Hanks. **E**: Preparation of coverslips. **F-G**: Coverslips with slices are kept in plastic tubes containing nutrient medium. **H**: Tubes are inserted in the roller drum. (Adapted from Delfs et al., 1989).

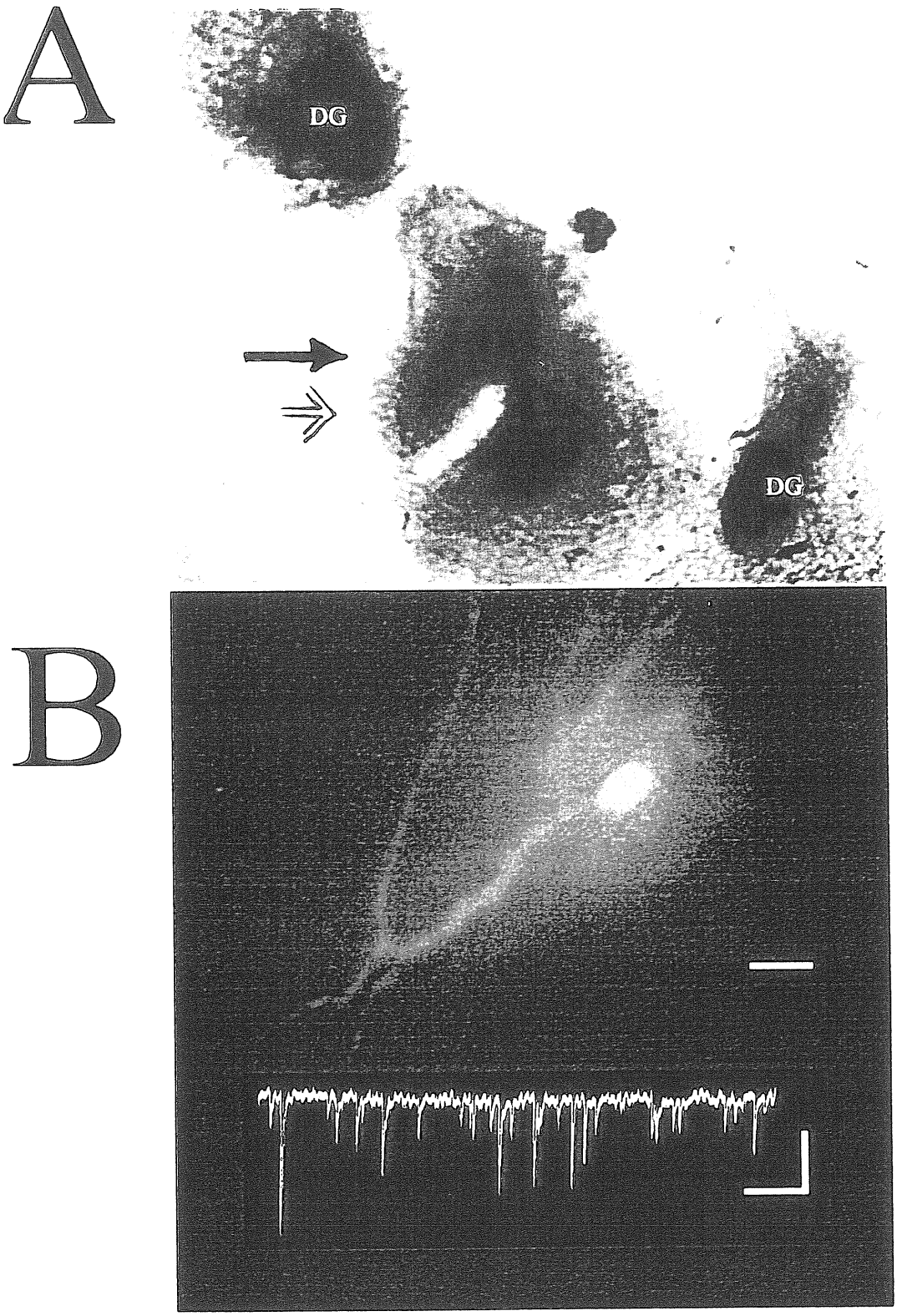

Figure XII. A: Organotypic spinal cord and dorsal root ganglia (DG) coculture at 14DIV. Ventral horns (one is indicated by the closed arrow) are identified by the presence of the central fissure. Calibration bar 1 mm, objective 2.5X. B: Ventral interneuron visualized by intracellular injection of Lucifer Yellow (1.5 mg/ml) in the same slice as in A (open arrow). Note the small, round-shaped cell body. Calibration bar, 15 µm, epifluorescence microscope, objective 40X. Superimposed tracing shows spontaneous synaptic currents from the same interneuron in standard solution. Calibrations 50 pA, 100 ms.

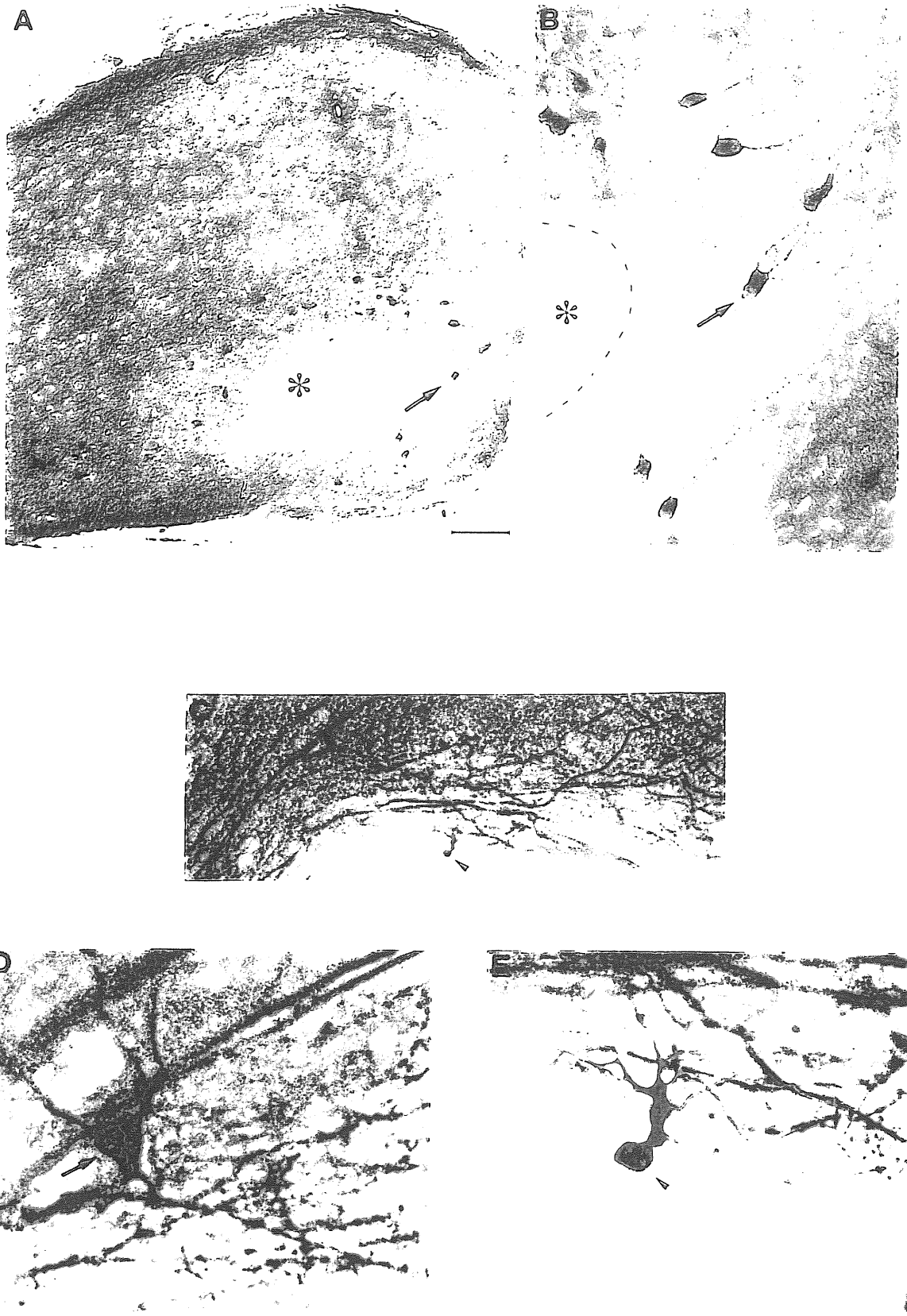

Figure XIII. A: Choline acetyltransferase (ChAT) immunocytochemical staining in a 14DIV organotypic culture. ChAT-positive cells are distributed around the central fissure (*), calibration bar 200 µm, objective 5X. B: Same slice as in A, presumed motoneurons show a large, multipolar cell body. Calibration (see bar in A) 75 µM, objective 20X. C: ChAT immunocytochemical staining and biocytin staining in a spinal coculture at 14DIV. Note the ChAT-negative neuron (arrow) and the ChAT-negative neuron (arrowhead). Calibration (bar in A) 50 µm, objective 20 X. D: ChAT-positive cell (same as in C) show a large, triangle-shaped soma. Calibration (see bar in A) 25 µm, objective 40X. E: ChAT-negative neuron (same as in C), filled with biocytin. Note the small, oval cell body. Calibration (see bar in A) 25 µm, objective 40X.

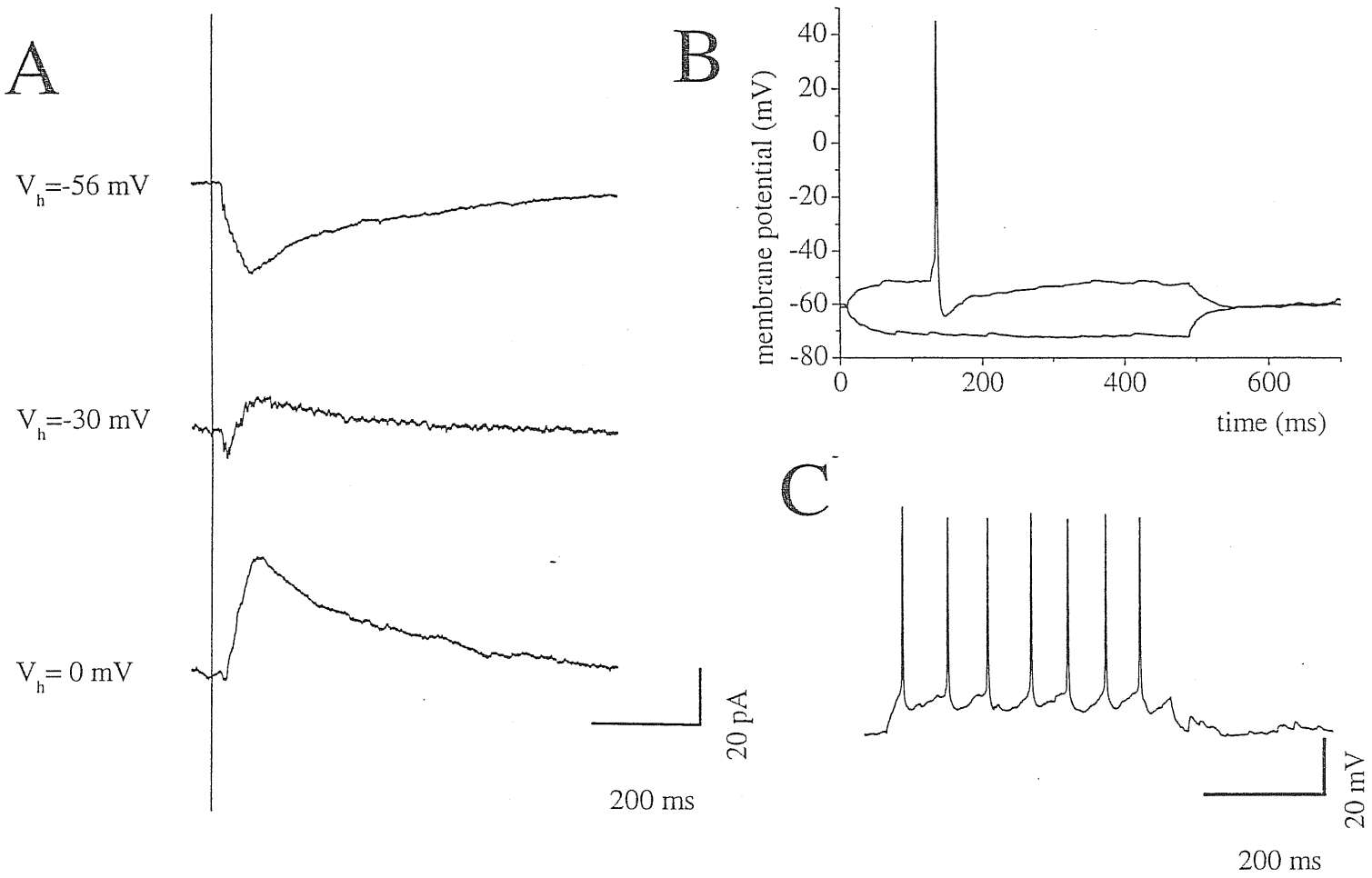

Figure XIV. A: Evoked currents in a ventral interneuron at 14DIV elicited by focal electrical stimulation of the omolateral dorsal root ganglion. Short voltage pulses (100 μs) of 10 V amplitude are delivered at a frequency of 0.05 Hz. Evoked currents are inward at membrane holding potential (V_h) -56 mV, they show an inward component followed by an outward one at -30 mV and are completely outward at V_h = 0 mV. Each trace represents the average of 5 consecutive evoked currents. **B**: Injecting a current pulse of +0.04 nA for 500 ms in a ventral interneuron, the membrane potential reaches the threshold and an action potential is generated. Note the spike overshoot. Injection of a negative current pulse (-0.05 nA, 500 ms duration) induces a membrane hyperpolarization in the patched cell. **C**: Train of spikes elicited by injection of a current pulse (+ 0.04 nA, 500 ms) in a ventral interneuron. Note the superimposed spontaneous synaptic activity.

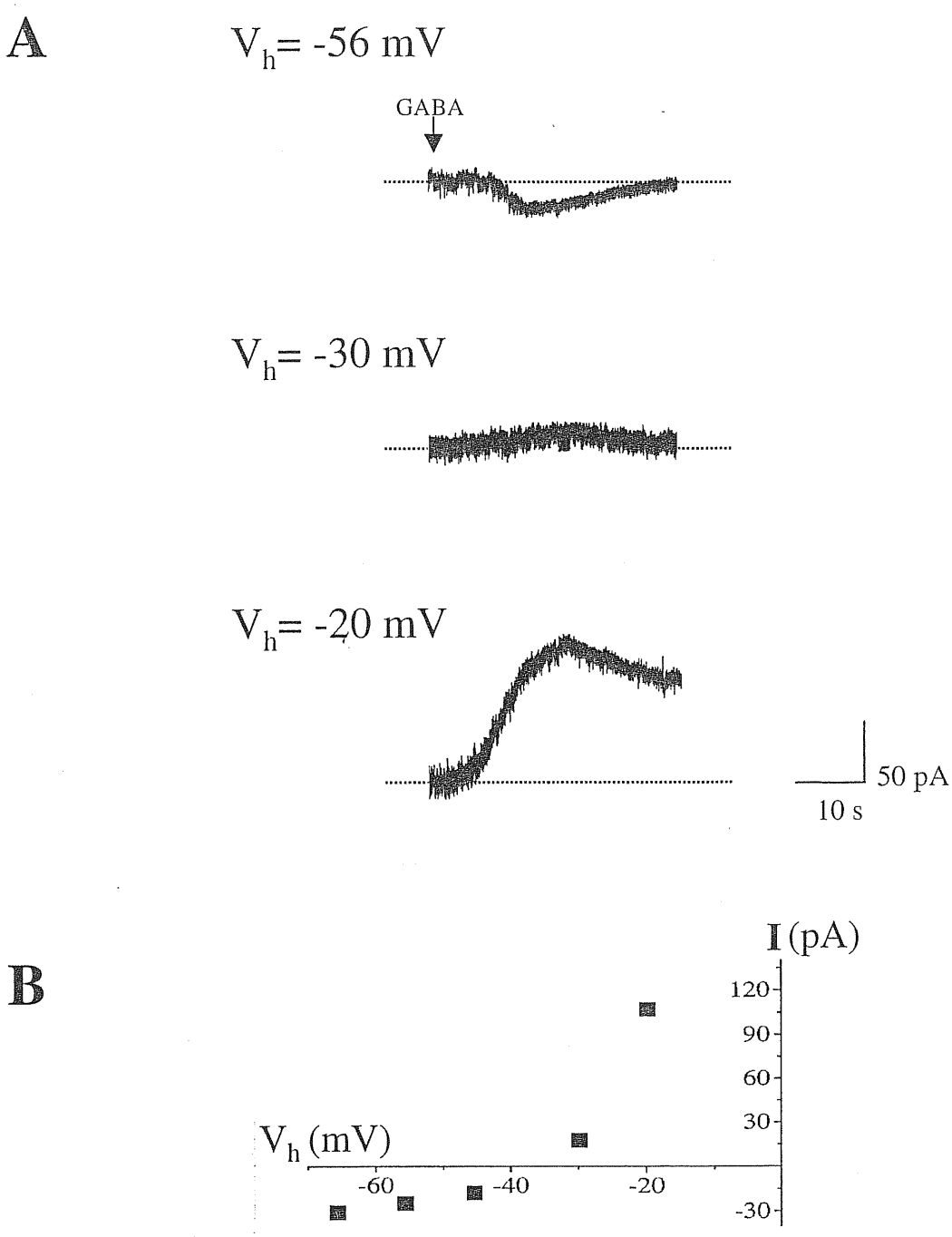

Figure XV. A: Voltage clamp recordings from a ventral interneuron (14DIV) in the presence of TTX (1 μM). The application of 0.1 mM GABA (arrow) induces an inward current at –56 mV, at V_h –30 mV the GABA-induced current is outward and at –20 mV the outward current is more pronounced. **B**: plot of the amplitude of the GABA-induced current against the membrane holding potential in the same cell as in **A.**

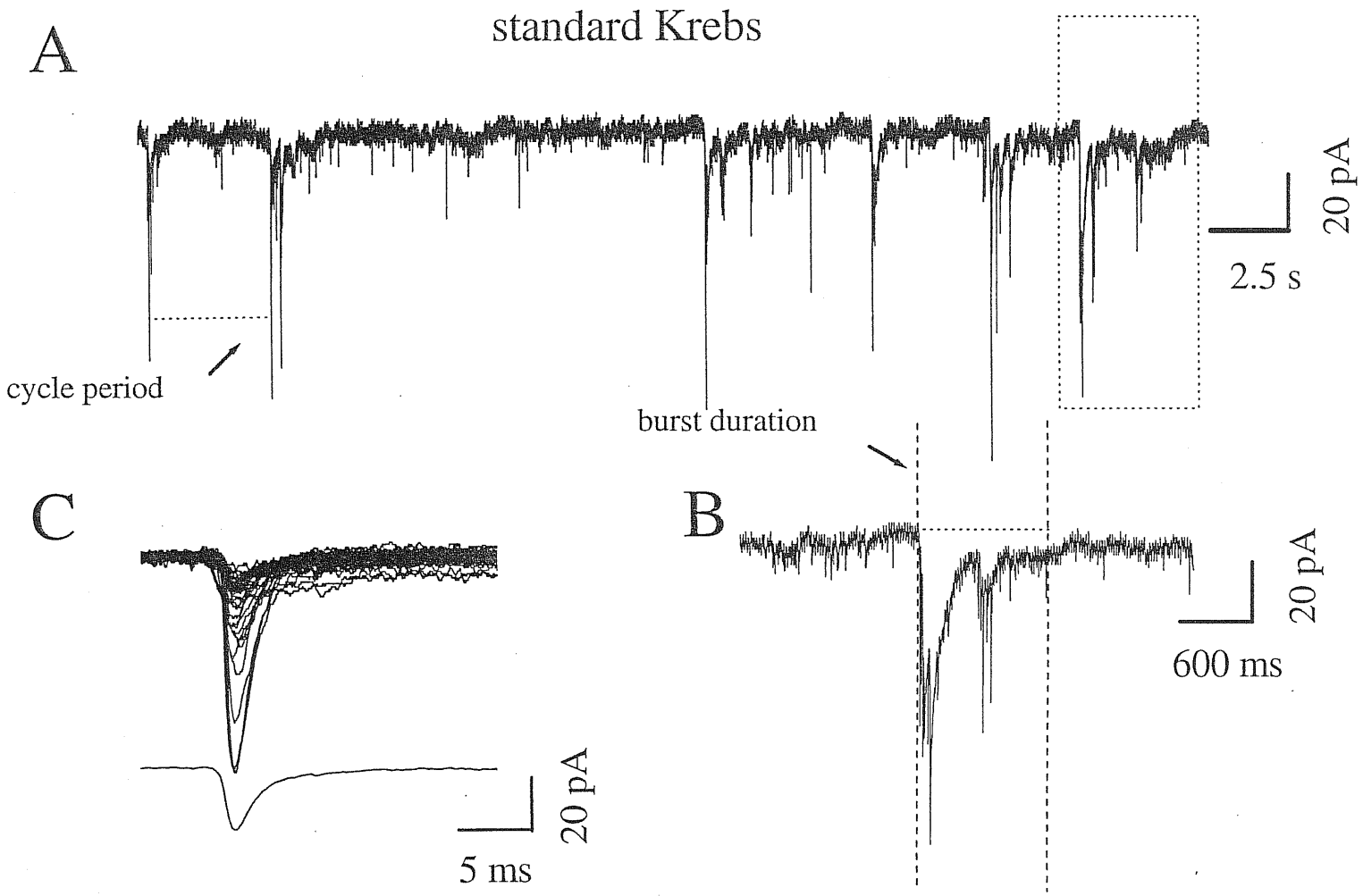

Figure 1. A: Spontaneous synaptic activity from a ventral interneuron at 14DIV that displays clusters of events with irregular cycle period and variable duration. Membrane potential was held at -56 mV. **B**: The single burst outlined in **A** is rescaled. **C**: Single spontaneous postsynaptic currents (PSCs) are present (superimposed in C, top) between bursts and show variable amplitude and decay time course. Decay time (τ = 2.5 ms), rise time (0.9 ms) and peak amplitude (–22 pA) are measured on the average PSC (C, bottom).

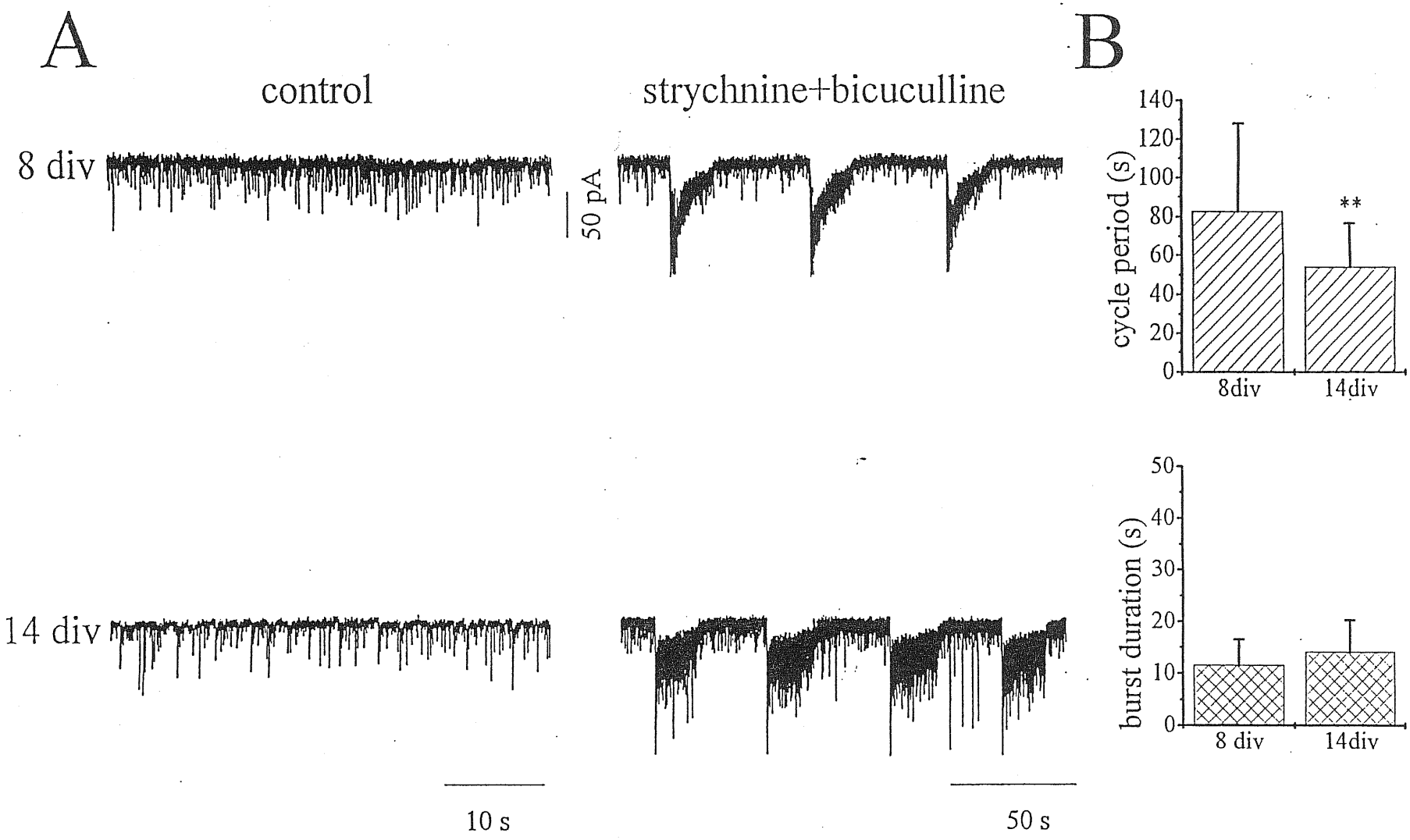

Figure 2. A: Spontaneous synaptic activity in control solution (left) is shown at both one (8DIV, top tracings) and two weeks in culture (14DIV, bottom tracings). Coapplication of strychnine and bicuculline (right) induces the appearance of rhythmic bursts of inward current on a background of spontaneous activity, both at 8DIV and 14DIV (top and bottom respectively). Note the regularity of such an activity. **B**: Cycle period (top) or burst duration (bottom) in the presence of strychnine and bicuculline are depicted against time in culture. At 14DIV frequency of bursting is higher (**) than at 8DIV while burst duration is similar at both times in culture. Data are from a group of cells and at least 7 bursts/cell are measured.

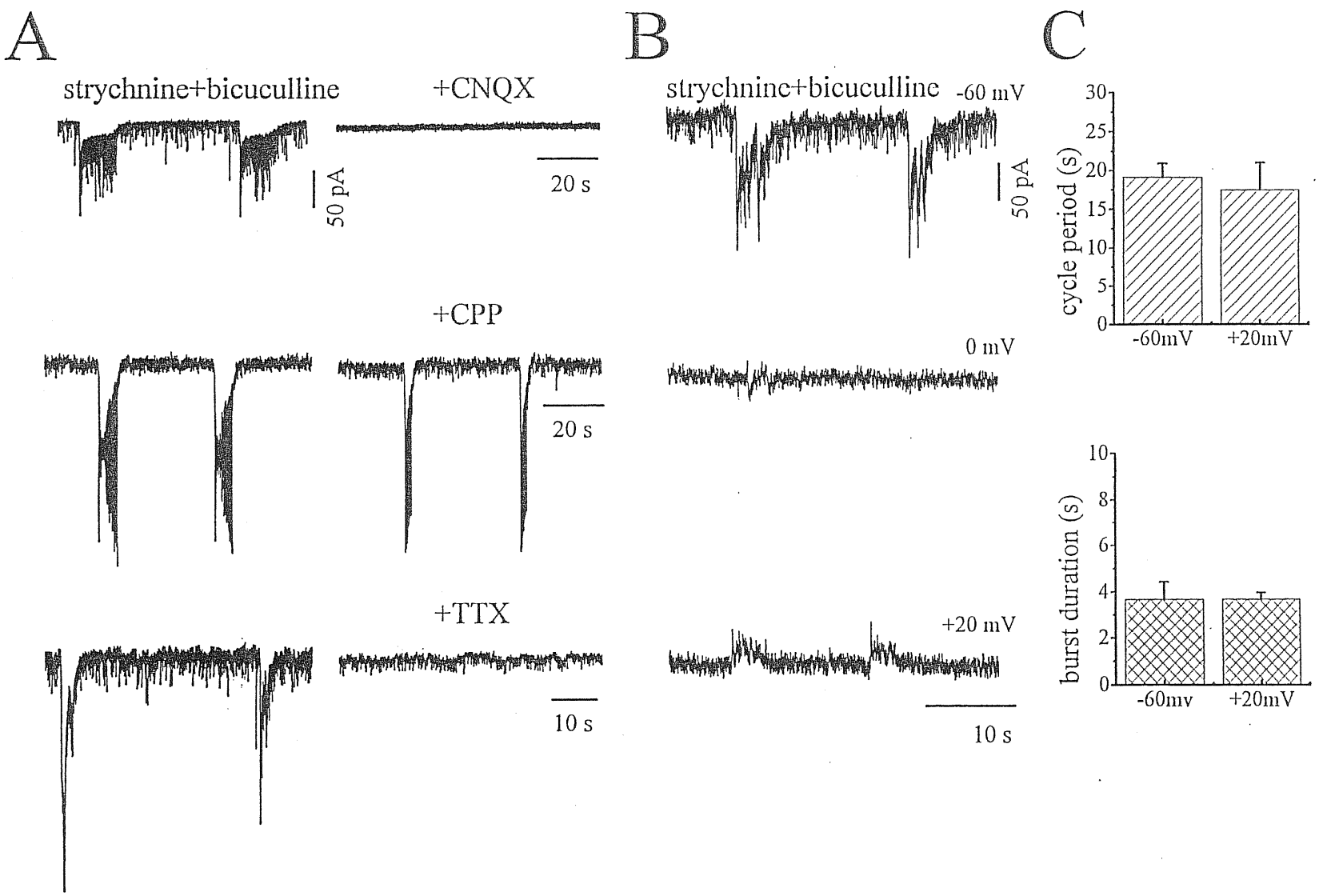

Figure 3. **A**: In the presence of strychnine and bicuculline (top, left) spontaneous bursts are suppressed by CNQX (top, right). Middle tracings: in the presence of strychnine and bicuculline (left) burst duration is reduced when CPP is superfused (right). Bottom tracings: spontaneous bursting in the presence of strychnine and bicuculline (left) is abolished by addition of TTX (right). Data are from 3 different cells at 14DIV. **B**: Bursting currents are inward at V_h of -60 mV (top), disappear at V_h of 0 mV (middle), and are outward at V_h = +20 mV (bottom). **C**: cycle period and burst duration are measured for each burst and averaged for each level of holding potential (same cell as in B, 14DIV).

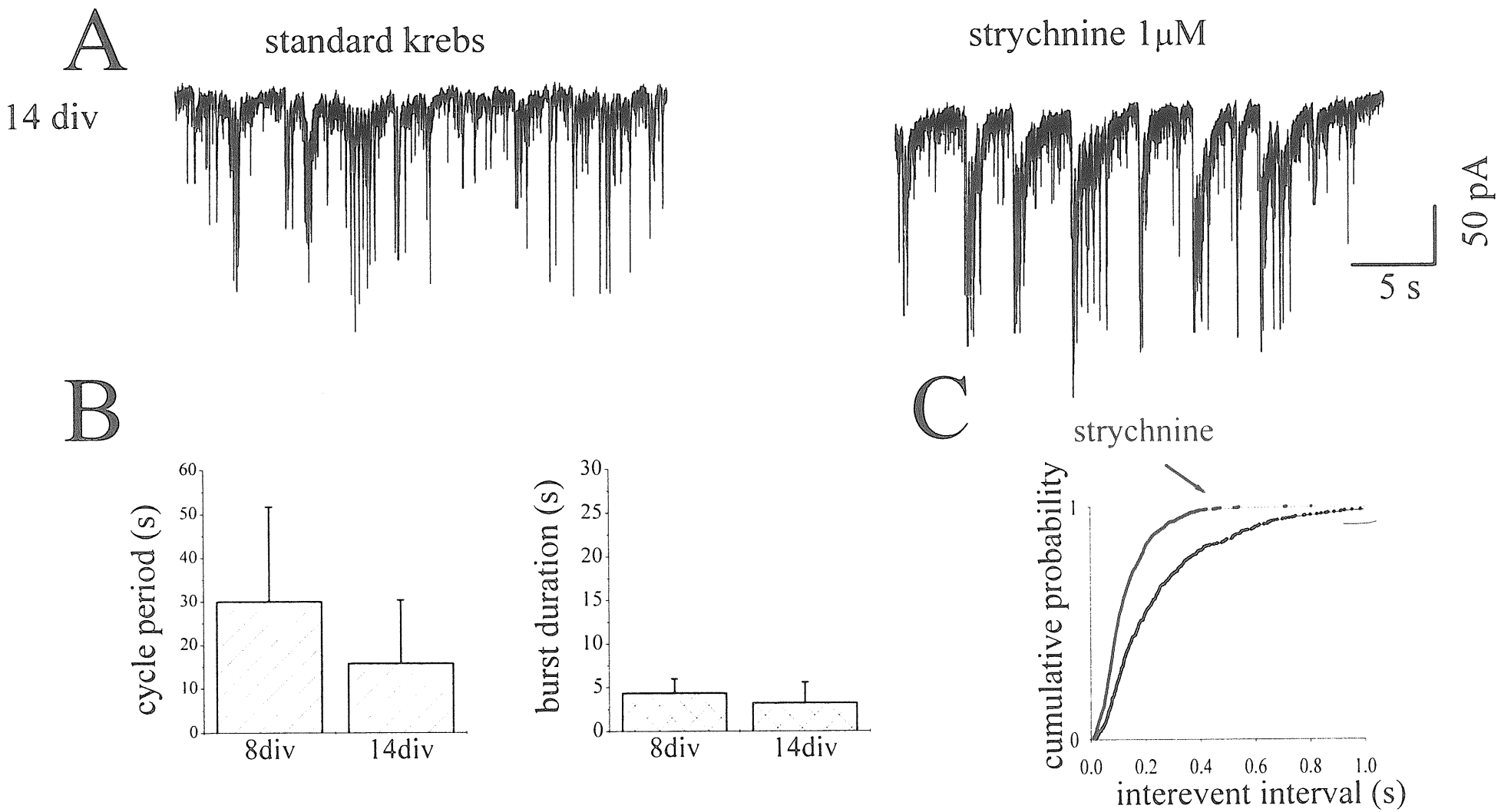

Figure 4. A: Spontaneous synaptic activity in control solution (left) at 14DIV is changed into irregular bursting patterns by the presence of strychnine (right). B: Cycle period (left) and burst duration (right) are shown at 8DIV and 14DIV and no significant differences are detected between the two groups of cultures. C: Cumulative probability distribution of interevent intervals of PSCs detected from a ventral interneuron in the presence (see arrow) and in the absence of strychnine.

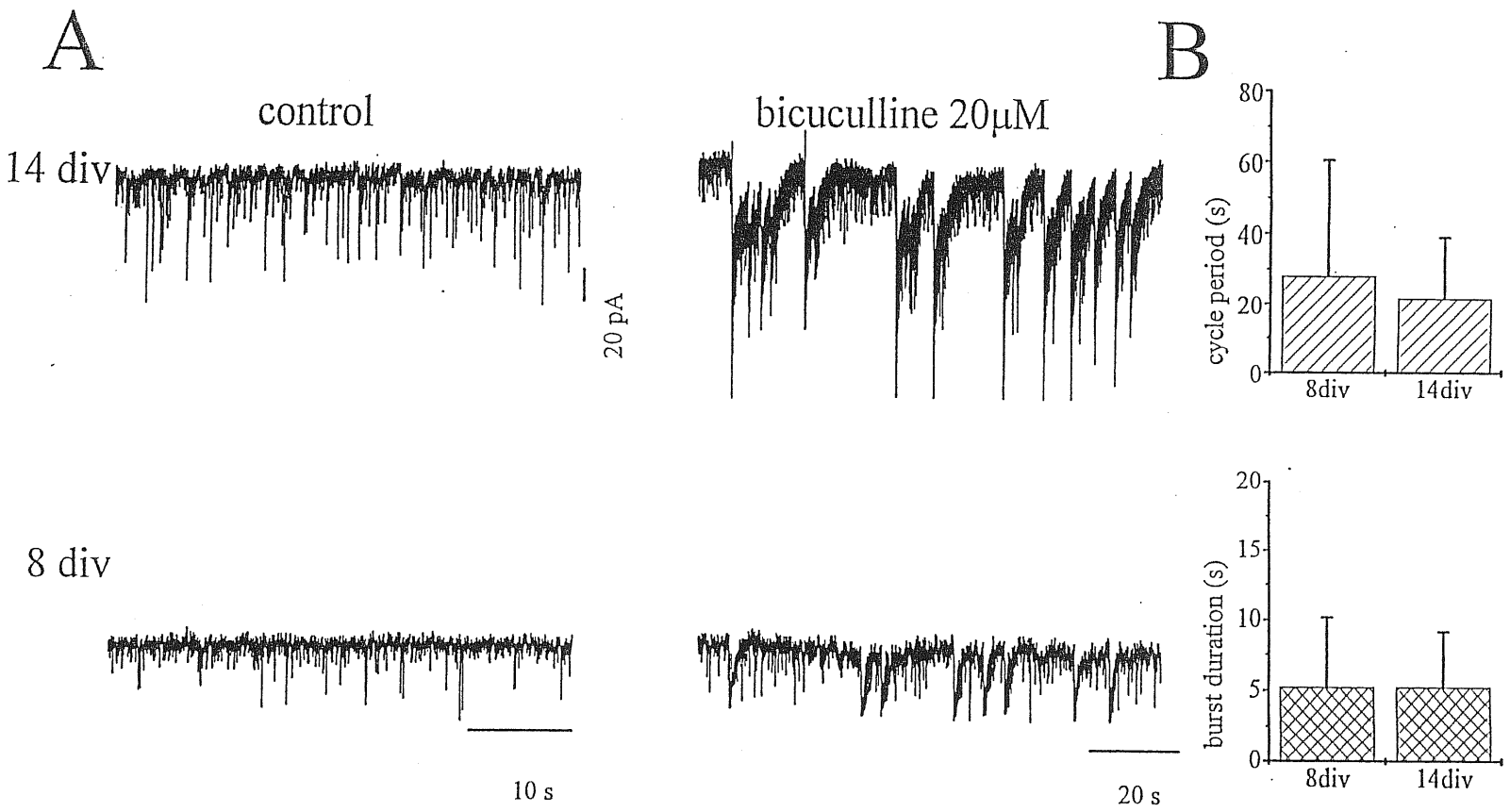

Figure 5. A: Application of bicuculline changes spontaneous synaptic activity in control solution (left) into irregular bursts (right) at both 14DIV (top) and at 8DIV (bottom). **B**: Cycle period (top) and burst duration (bottom) against time in culture. Note the similarity in burst cycle period and in burst duration between the two groups of cultures.

Tab. 1

	control			bicuculline			strychnine		
	rise time (ms)	decay time (ms)	N	rise time (ms)	decay time (ms)	N	rise time (ms)	decay time (ms)	N
14 div	1,13±0,25	5,22±2,59	9	1,09±0,18	5,52±1,46	4	1,25±0,09	6,2±1,9	3
8 div	1,01±0,26	3,32±1,12	9	1,17±0,31	4,57±1,25	4	0,97±0,26	3,54±1,23	4

Table 1. Effects of strychnine and bicuculline on rise time and decay time constant of spontaneous PSCs. Synaptic currents are detected in control solution or in the presence of strychnine or bicuculline in cultures of both 8DIV and 14DIV. In each ventral interneuron, the rise time and the monoexponential decay time constant are measured on the average PSC. No significant variations are detected between different treatments and times in culture.

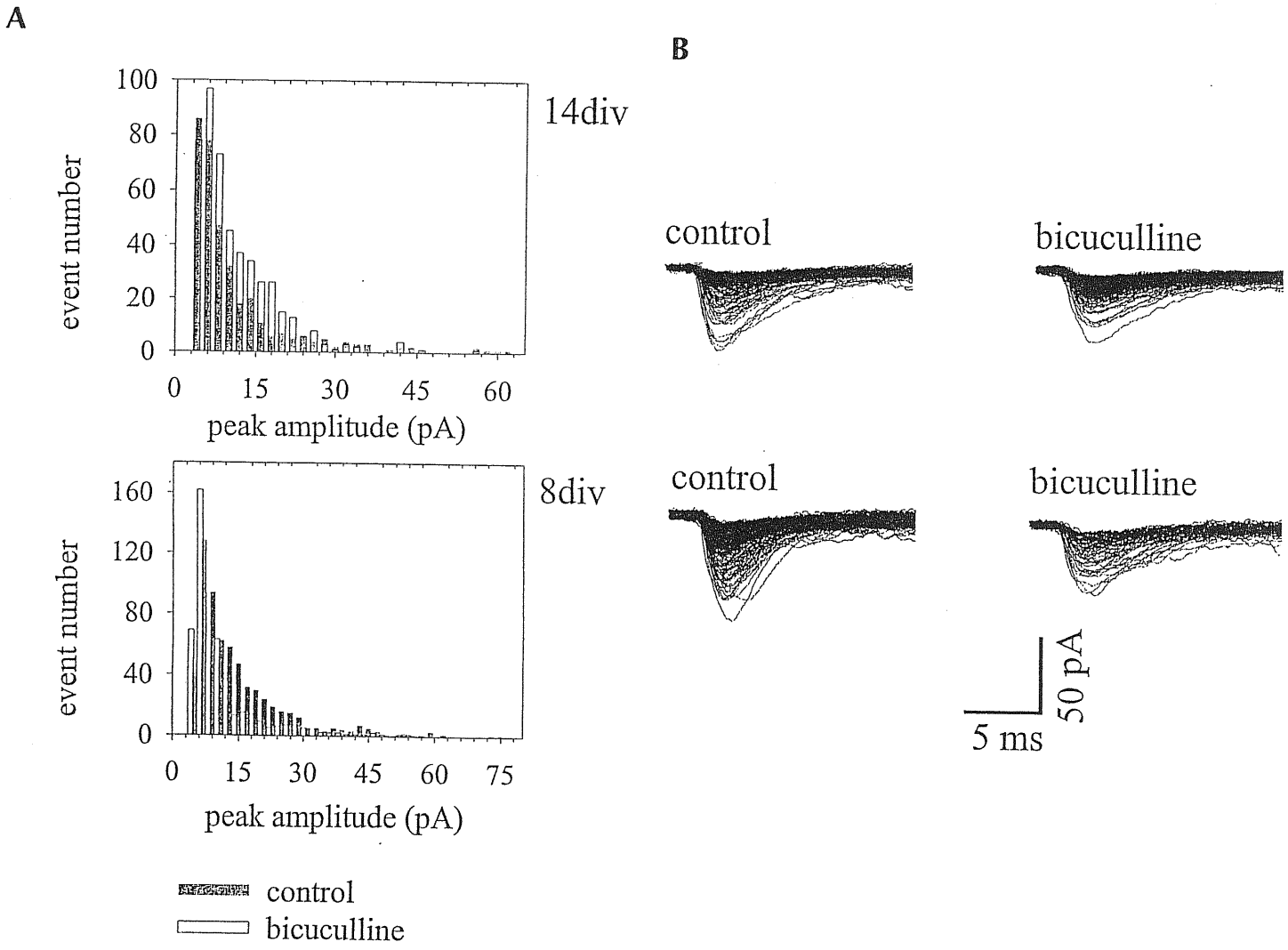

Figure 6. A: Distribution of PSC amplitude in a ventral interneuron at 14DIV (top) and at 8DIV (bottom), histograms represent the number of PSCs in control solution (close bar) and in the presence of bicuculline (open bar) against the amplitude. Spontaneous synaptic events are detected during quiescent interburst periods of 30s in both cases, the detected events are superimposed in **B**. **B**: Top tracings: superimposed events in control (left) and in the presence of bicuculline (right), at 14DIV, same cell as in **A**. Bottom tracings: superimposed events in control (left) and in the presence of bicuculline (right), at 8DIV, same cell as in **A**. Note that at 8DIV, in the presence of bicuculline, there is a reduction in the PSC frequency in the entire amplitude range.

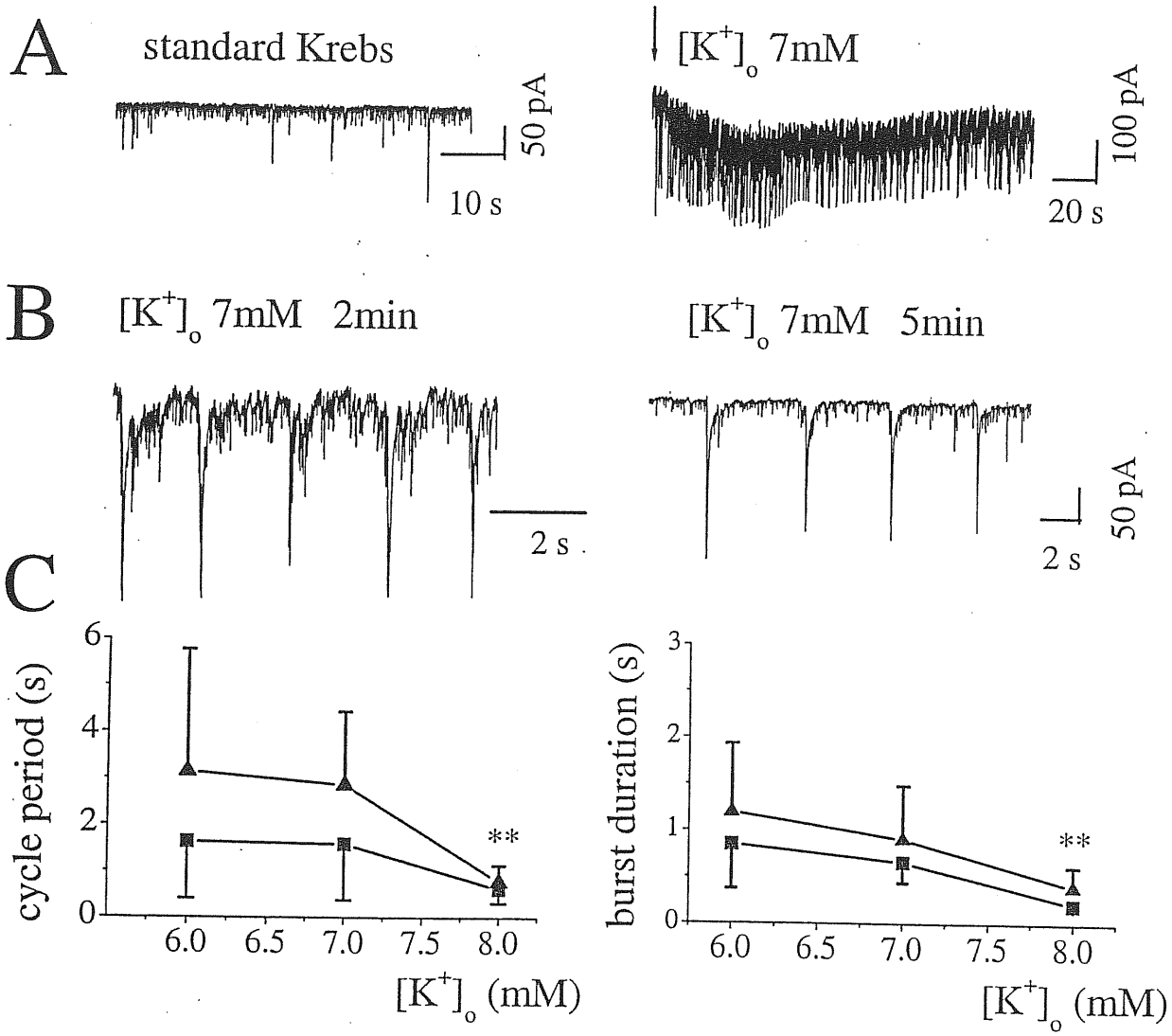

Figure 7. A: Spontaneous synaptic activity in control solution (left). Increased extracellular K^+ (7 mM, see arrow for start of application) induces a slow inward current which, 40 s later, reaches a peak value of -65 pA. This response is accompanied by a large increase in spontaneous synaptic activity and a gradual decline of the inward current towards baseline during continuous K^+ superfusion. **B**: In the presence of high K^+ spontaneous synaptic activity turns into a patterned activity within 2min from K^+ application (left), consisting of rapid bursts of inward current. This pattern persists with a regular although slower rhythm at 5 min of K^+ superfusion (right). **C**: In the two graphs burst cycle period (left) and duration (right) values are plotted against three different concentrations of extracellular K^+. Cycle period and burst duration values were collected at 2 min (filled squares) or at 5 min (filled triangles) of the K^+-induced patterned activity. Note the significant (**) shortening in cycle period and burst duration with 8 mM K^+. Data are pooled from a population of ventral interneurons.

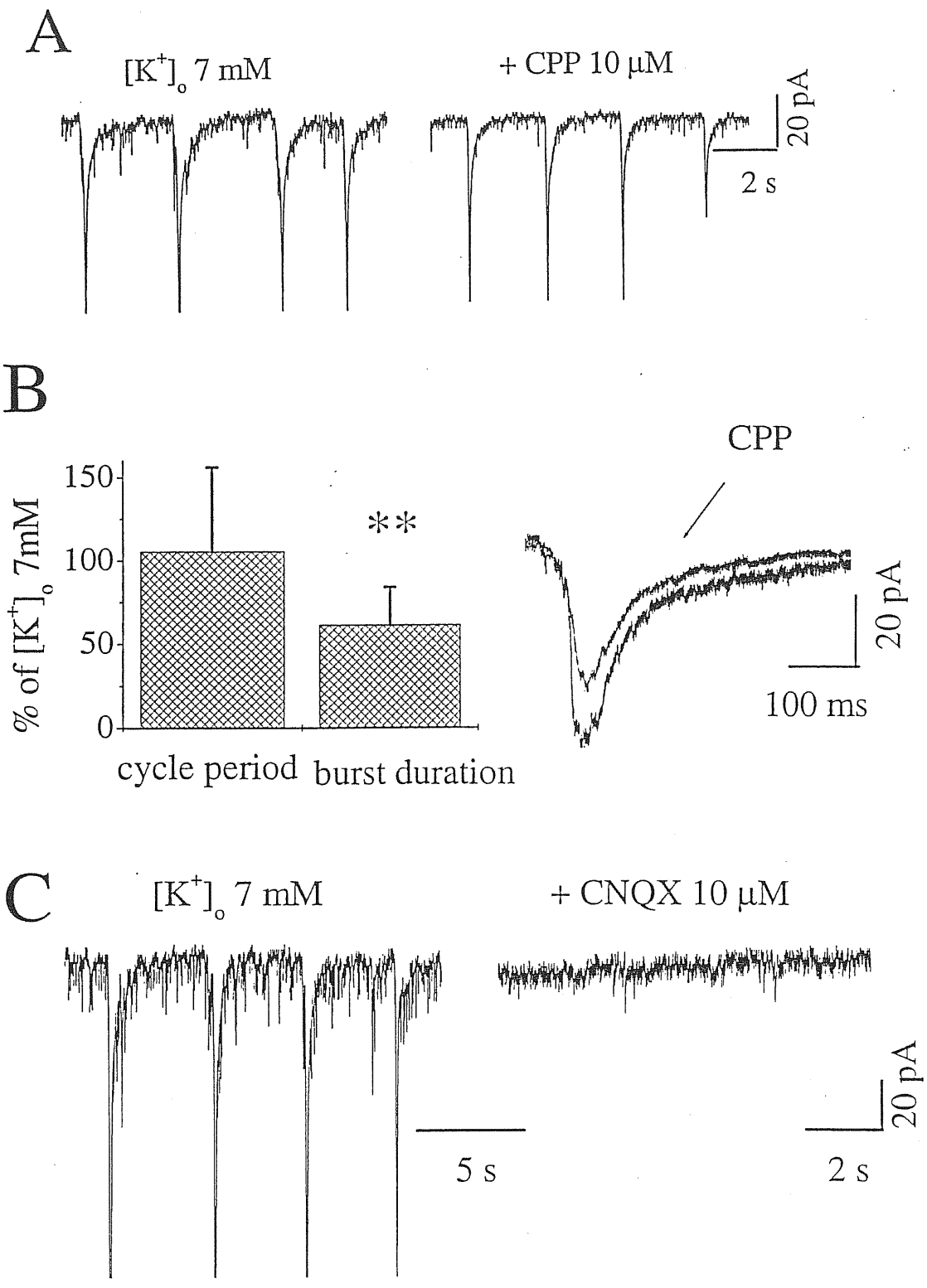

Figure 8. A: 7 mM K^+ induced rhythmic activity (left) is reduced in burst duration and amplitude by CPP (right). **B**: histograms of cycle period and burst duration recorded in the presence of CPP in 5 interneurons and expressed as % of rhythm observed in high K^+ solution (left). A significant reduction (**) in burst duration is observed. Right: averaged traces of 5 consecutive burst events in the absence or in the presence (arrow) of CPP are superimposed. Note the reduction in amplitude and duration brought about by CPP. **C**: rhythmic bursts induced by 7 mM K^+ are suppressed by addition of CNQX.

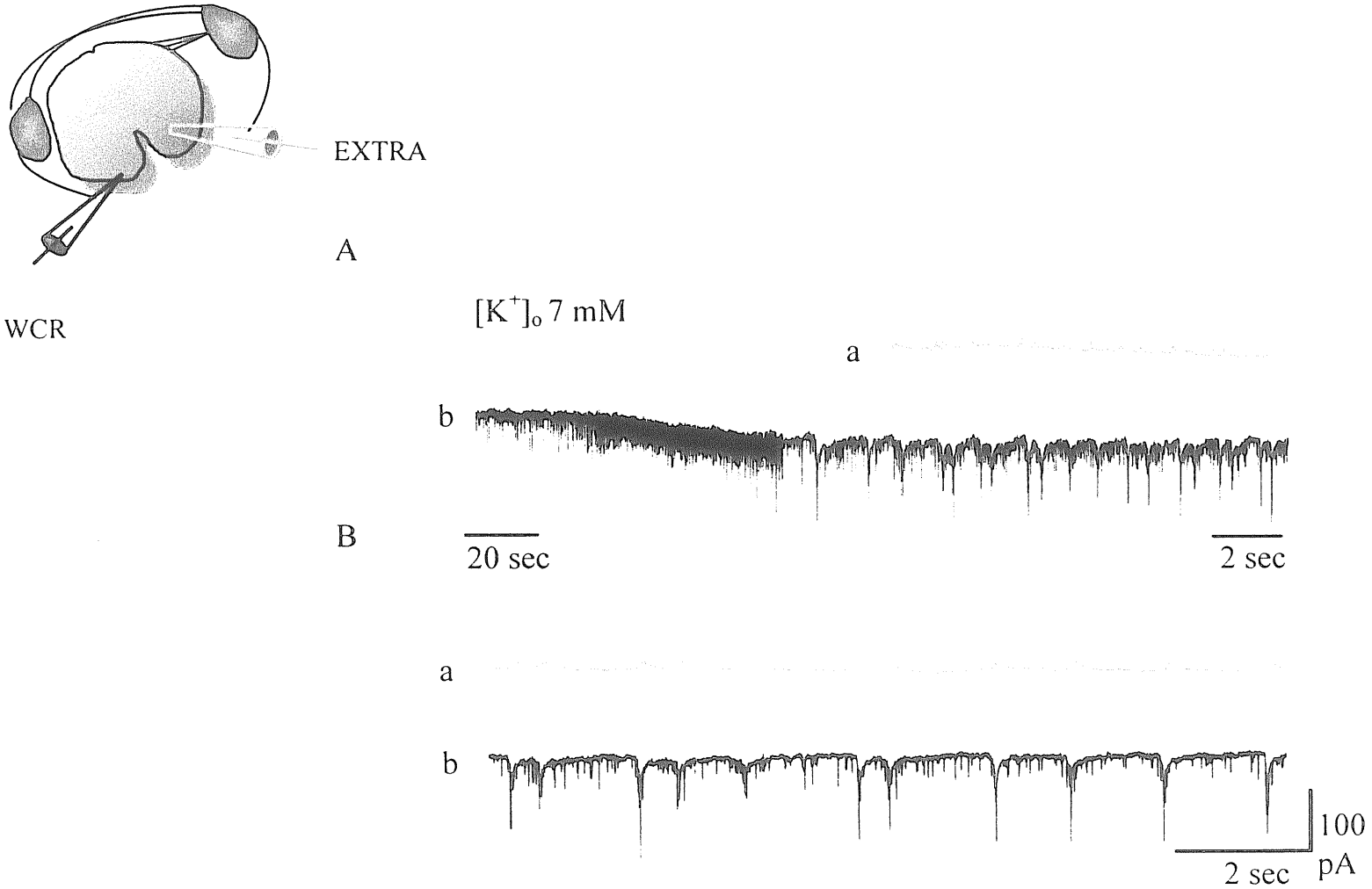

Figure 9. Schematic drawing of the position of the field (EXTRA) and patch (WCR) electrodes within the organotypic slice. A, Simultaneous field (a) and whole cell recordings (b) during perfusion of high K^+. Regular, rhythmic bursts are detected with both electrodes although with opposite polarity. Note the similarity in cycle period and burst duration between the two recordings. B: In the presence of high K^+ spontaneous rhythmic activity stabilizes at 5 min in both ventral horns as shown by the two tracings (field and patch recordings, a and b, respectively). Note that the extracellular recorded events occur with a delay from the patch recorded ones.

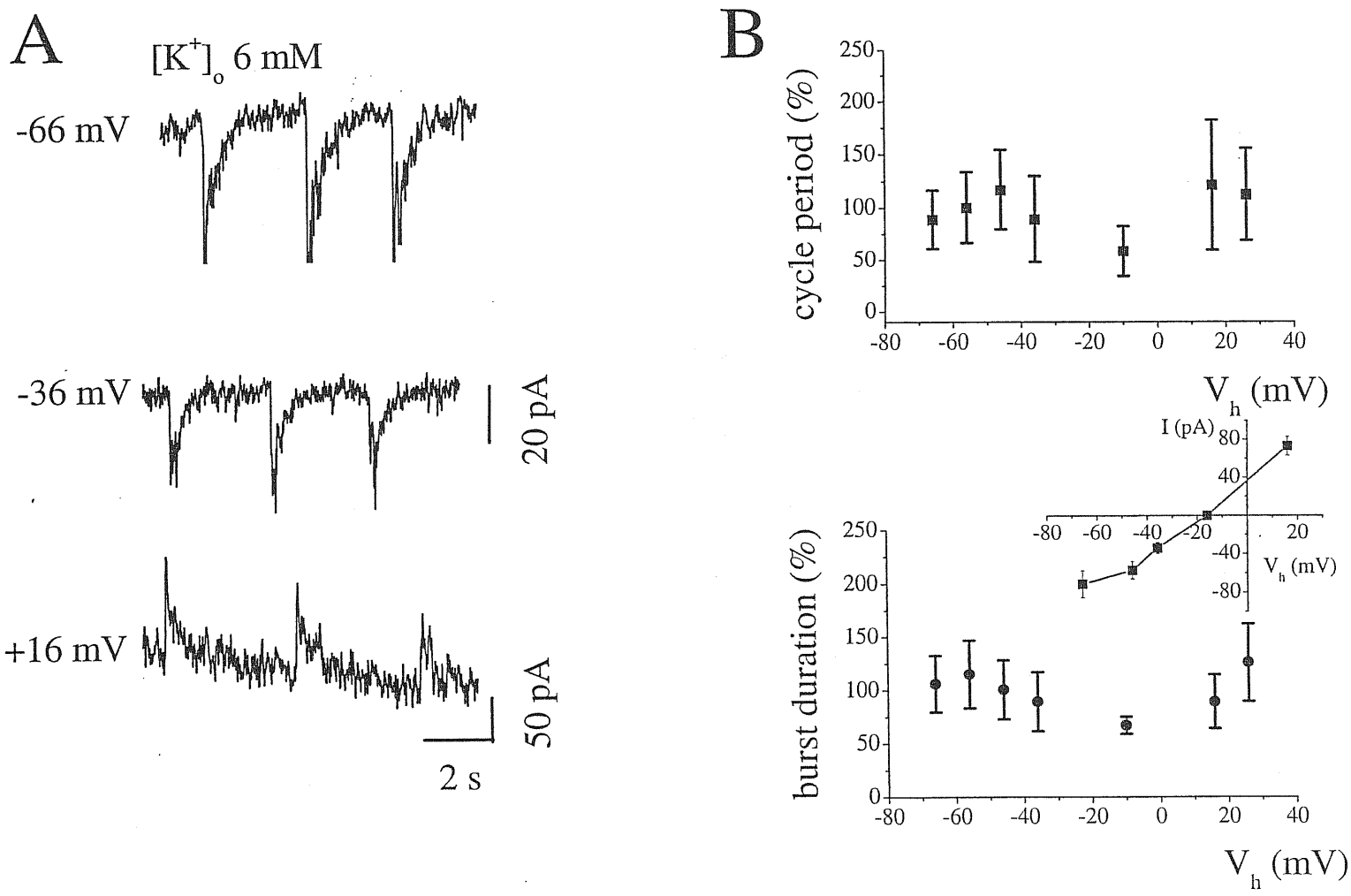

Figure 10. **A**: Bursting currents are inward at V_h of -66 mV (top), decrease in amplitude at -36 mV (middle) and are outward at V_h of +16 mV (bottom). **B**: On a sample of 6 interneurons, cycle period (top) and burst duration (bottom) are plotted against V_h. Values are expressed as % of cycle period and burst duration recorded in each neuron at -56 mV V_h. Note that these values are not affected by changes in V_h. The inset in **B** shows the I/V curve obtained by plotting burst amplitude against V_h (same cell as in **A**). Note the lack of linearity in the range of negative potentials and that the reversal potential is around -18 mV.

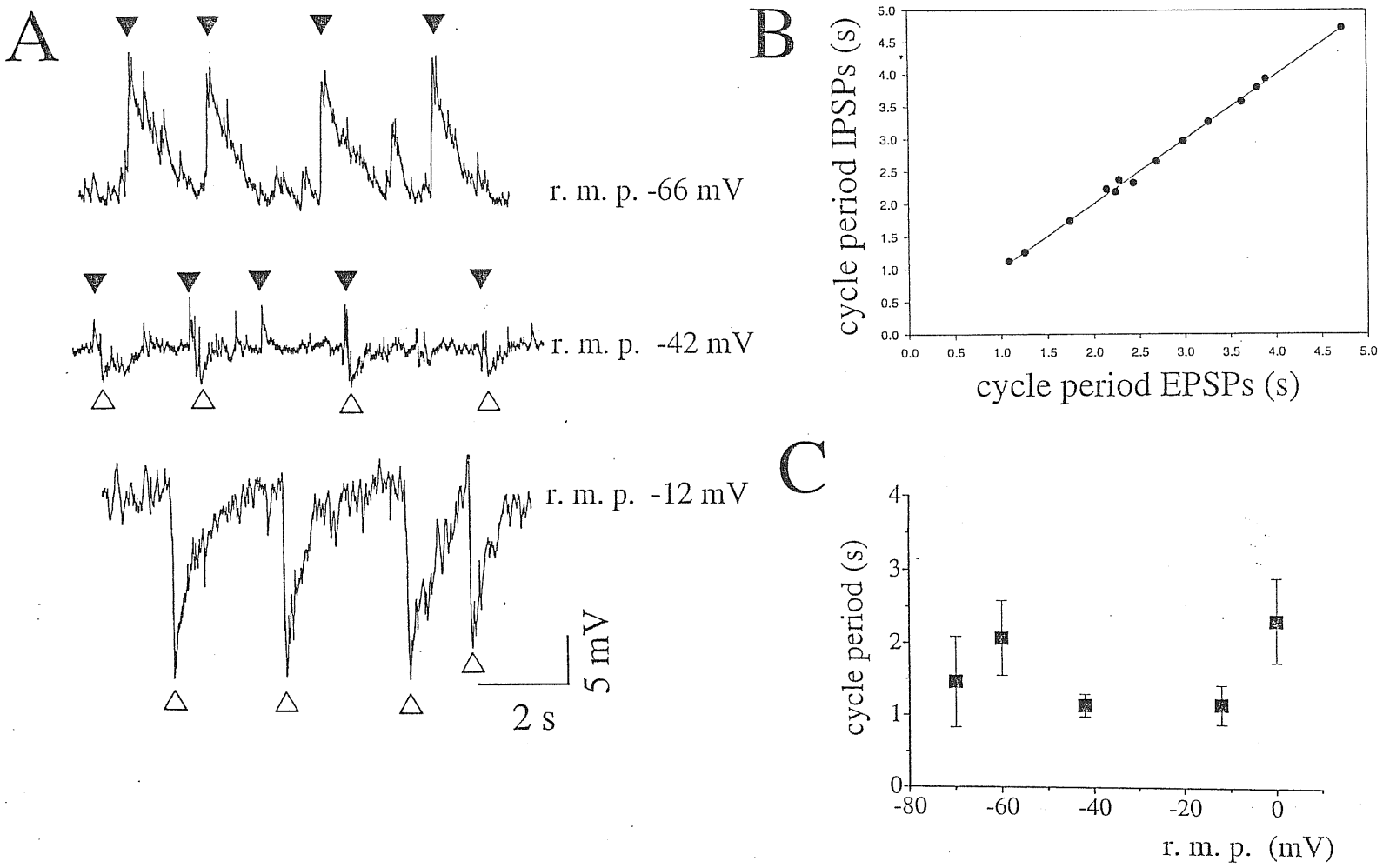

Figure 11. A: current clamp recordings in the presence of 7 mM K^+ are shown at three different levels of resting membrane potential (r.m.p.). At -42 r.m.p. depolarizing potentials (filled triangles) precede hyperpolarizing components marked by open triangles. At -66 mV only large depolarizing events are manifested while at -12 mV events consisted mainly of large hyperpolarizing potentials. **B**: plot of cycle period of EPSPs (abscissa) versus the one of IPSPs (ordinate) during rhythmic bursting evoked by high K^+ at - 42 mV r.m.p. Data are collected from the cell shown in A. **C**: Cycle periods are not significantly affected changing the r. m. p. (same cell as in **A**).

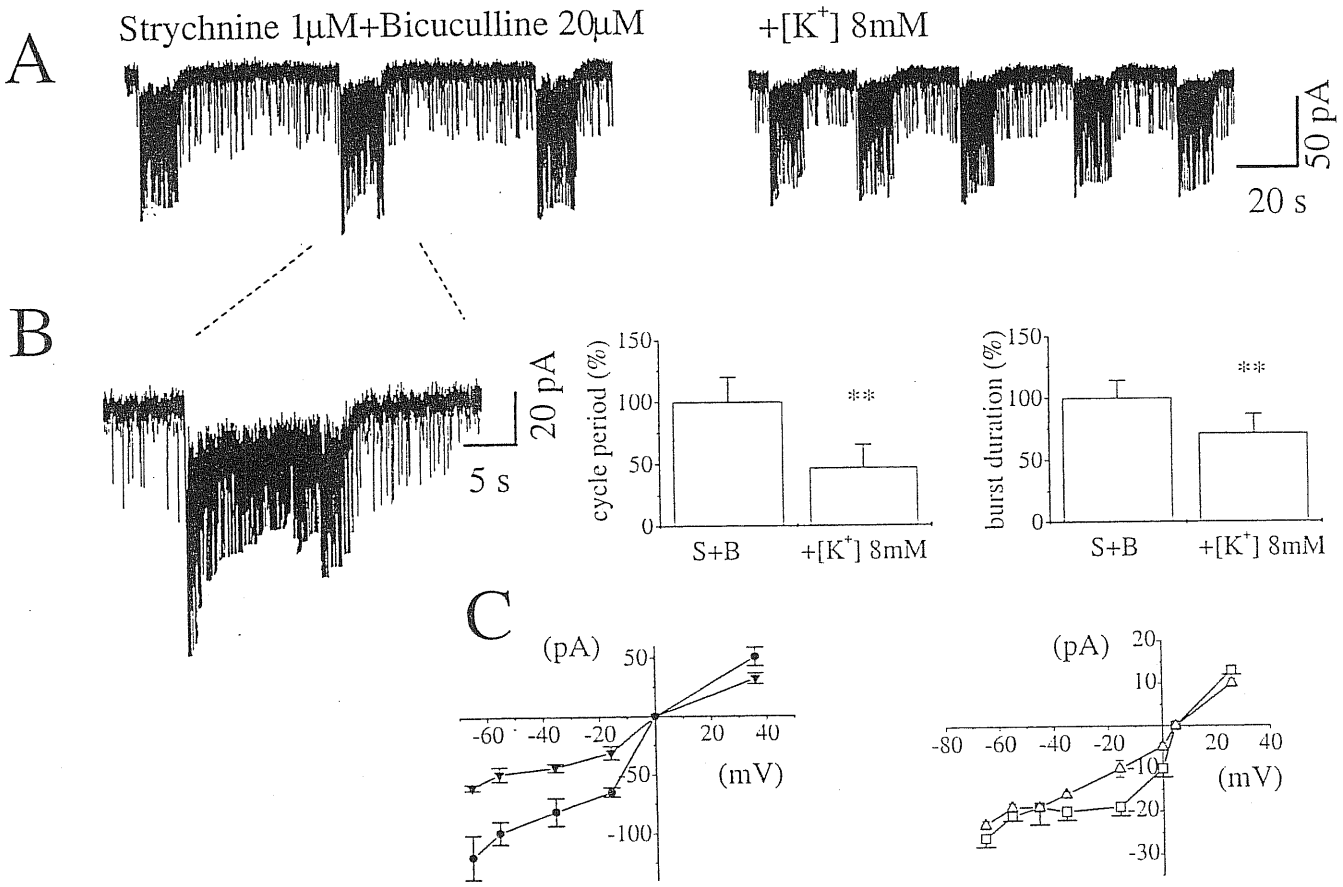

Figure 12. A: Strychnine and bicuculline induce sustained rhythmic bursting activity of ventral horn interneuron (left). Increased K^+ concentration in the presence of strychnine and bicuculline shortens both cycle period and duration of bursting (right). **B**: A single burst elicited by strychnine and bicuculline is shown in an expanded time scale (left, from **A**). In the middle and right are shown plots of cycle period and burst duration in strychnine plus bicuculline solution (S+B) and subsequent raising extracellular K^+ to 8 mM (n=5 cells). Note that 8 mM K^+ significantly (**) reduced cycle period and decreased (**) burst duration. **C**: Burst amplitude in the presence of strychnine and bicuculline is plotted against V_h. Left: I/V relation before (filled circles) and after (filled triangles) high K^+ application (same cell as in A). Note that burst amplitude in the presence of K^+ is reduced and that the two curves display the same reversal potential). Right: I/V relation before (open squares) and after (open triangles) 10 μM CPP superfusion (different cell from A, C). Note that application of CPP linearizes the plot.

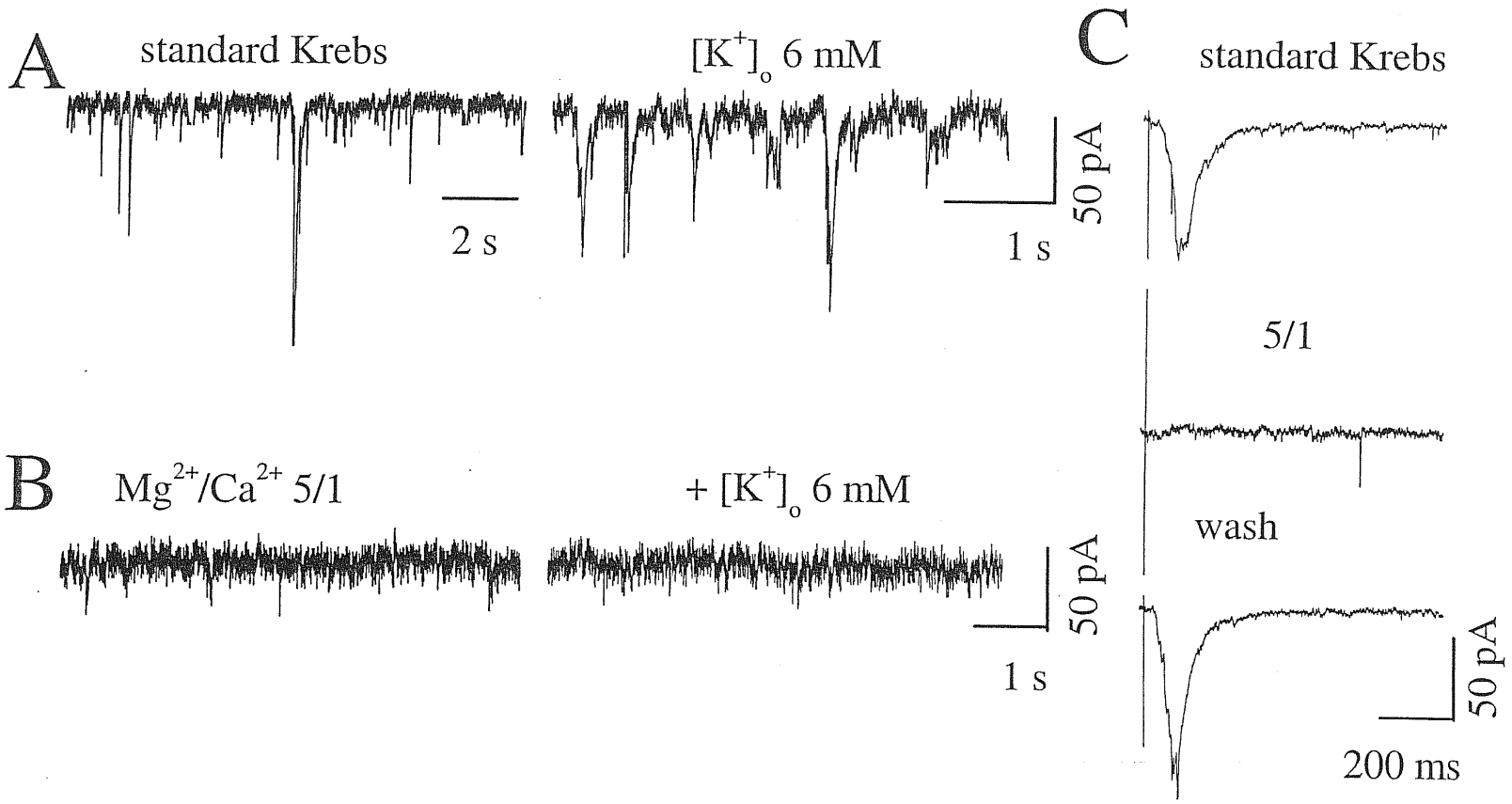

Figure 13. A: spontaneous synaptic activity in control condition (left) turns into a patterned activity in the presence of high K^+ (right). **B**: On the same cell spontaneous synaptic activity is highly reduced in the presence of external solution with a 5/1 ratio of Mg^{2+}/Ca^{2+} (left). In these conditions addition of 6 mM K^+ fails to induce rhythmic bursting (right). **C**: PSCs evoked by DRG stimulation in the same interneuron as in **A** are shown in control solution (top). Evoked PSCs disappear in the presence of the 5/1 external solution (middle) and recover after washout in control solution (bottom). Each panel is an average of 5 consecutive evoked responses.

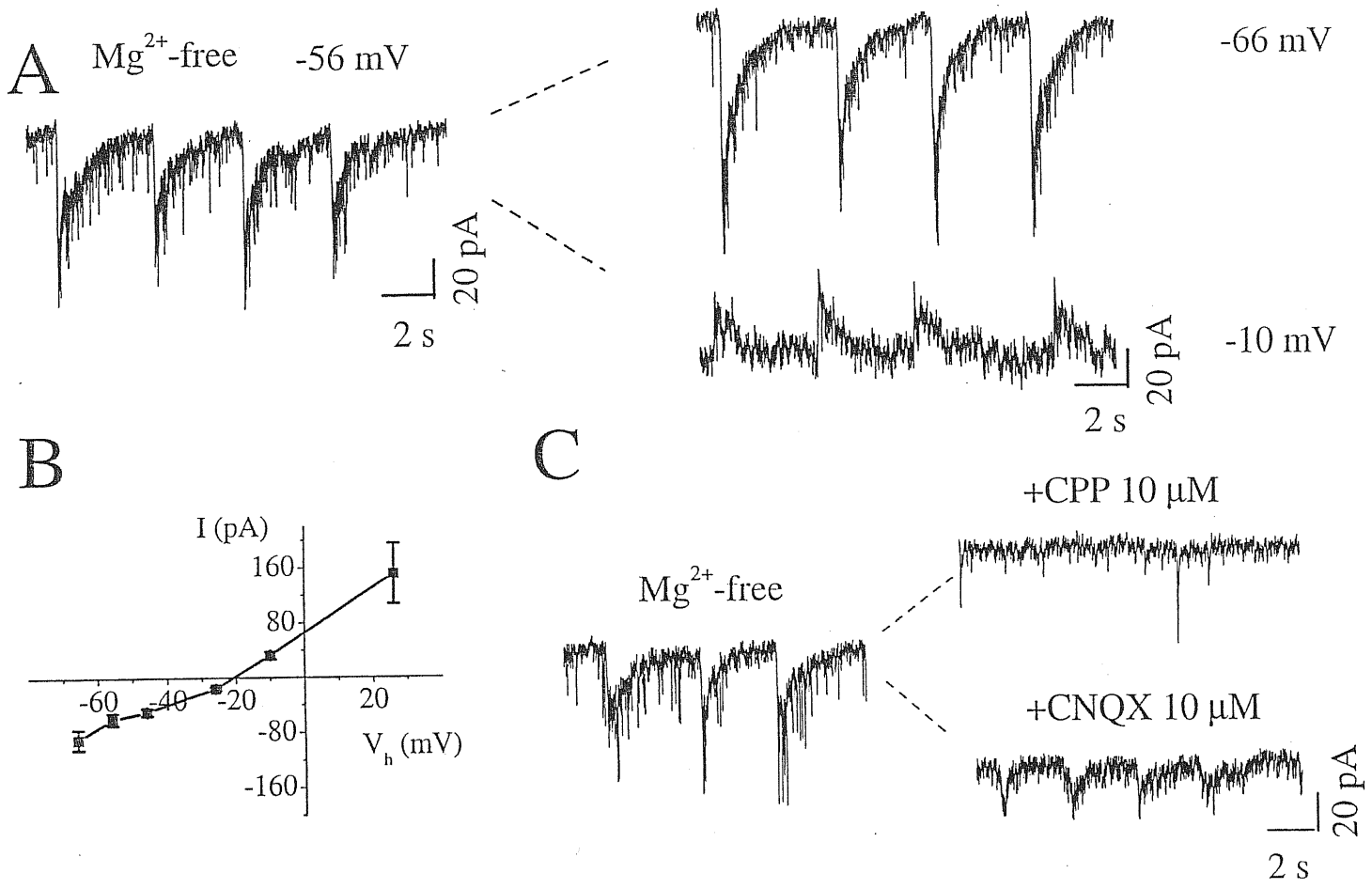

Figure 14. A: In the presence of Mg^{2+} free solution rhythmic bursting spontaneously develops after 5-10 min (left). Bursting currents are inward at V_h -66 mV, and outward at V_h -10 mV (right). **B**: I/V relation of burst amplitude against membrane potential (same cell as in A). Note that the reversal potential is around -20 mV. **C**: Rhythmic bursting induced by Mg^{2+}free solution (left) is fully blocked by CPP application (top right) but it persists in the presence of CNQX (bottom right), although with reduced amplitude and duration. In this cell cycle period is not affected by CNQX.

Control culture

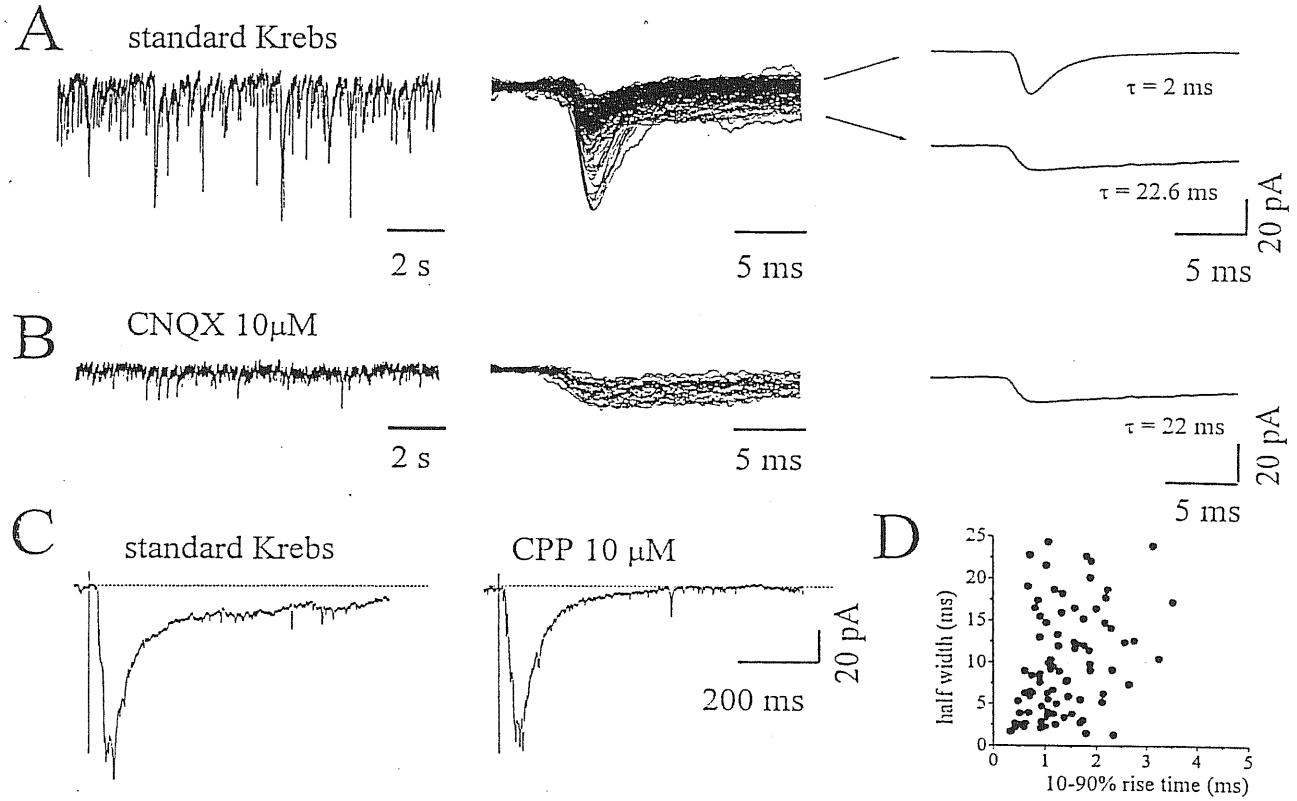

Figure 15. A: Spontaneous synaptic activity from a ventral interneuron is composed by inward currents of variable amplitude (left); single PSCs comprise events with fast or slow decay time (middle, superimposed tracings). Rise time and decay time are measured from the fast PSC average (top right: 0.8 ms, τ = 2 ms, respectively) and the slow PSC average (bottom right: 1.1 ms, τ = 22.6 ms, respectively). **B**: Application of CNQX (left, same cell as in A) completely blocks fast events leaving only slow ones (middle, superimposed traces). Kinetics are measured on the average of slow decay events (right, τ = 22 ms, 1.5 ms rise time). **C**: Synaptic currents evoked in the same interneuron as in **A** and **B** by DRG stimulation are shown in standard solution (left) and in the presence of CPP (right); each panel represents the average of 7 consecutive evoked polysynaptic currents. The application of CPP reduces the area subtended by the evoked PSC by 38%. Dotted lines indicate the baseline. **D**: scatter plot of rise time *versus* half width (same cell as in A); regression analysis reveals no linear relationship between these two parameters (r^2 =0.006, Pearson correlation coefficient = 0.07).

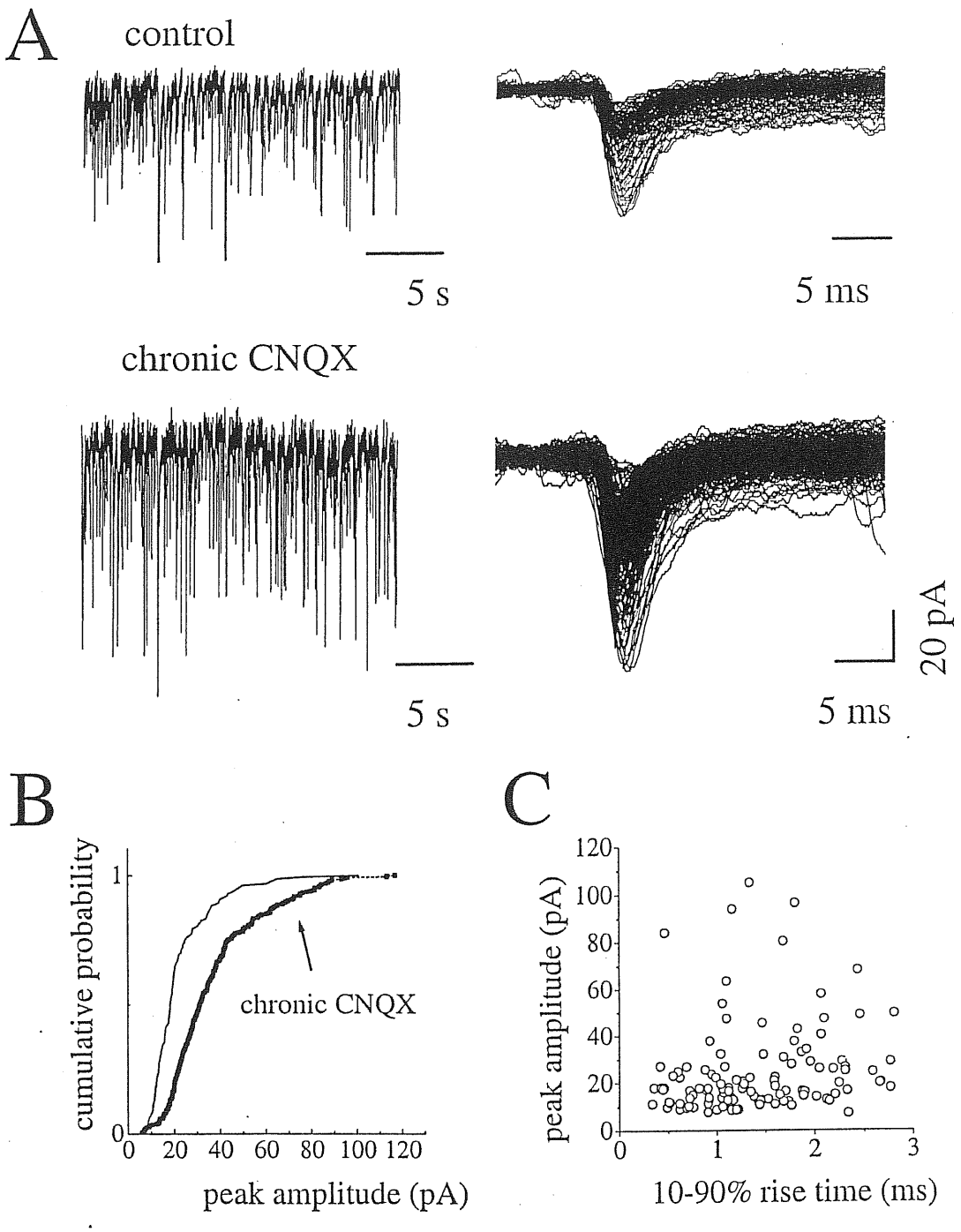

Figure 16. A: Spontaneous synaptic currents in standard Krebs are shown in both control culture (top, left) and chronic CNQX treated sister culture (bottom, left). Single PSCs are shown to the right, note that both fast τ and slow τ events are present in the control interneuron (top right) while in that from the chronic CNQX culture only fast τ PSCs are detected (bottom right). **B**: cumulative amplitude plot for PSCs recorded in control culture and in chronic CNQX sister culture; the entire distribution of PSC amplitudes includes larger values for CNQX treated interneuron (arrow). **C**: scatter plot of rise time against peak amplitude in control culture (same cell as in A) reveals no linear relationship between these parameters ($r^2 = 0.00003$, Pearson correlation coefficient = 0.006).

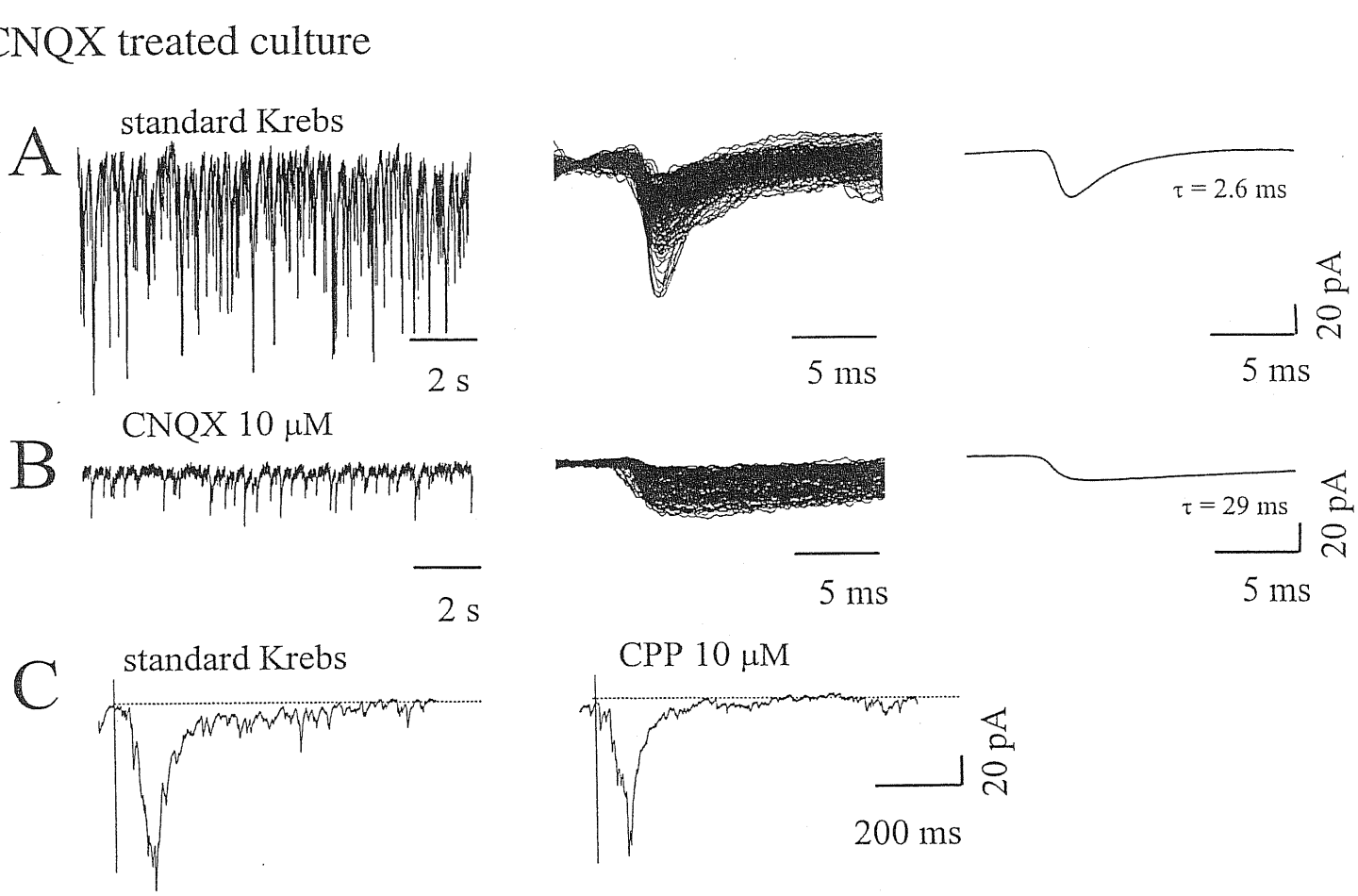

Figure 17. A: Recordings from a ventral interneuron in CNQX treated culture (left) show very intense spontaneous activity; PSCs comprise only fast τ events (superimposed in the middle) with τ of 2.6 ms, 0.8 ms rise time (measured on the average PSC, right). **B**: block of AMPA/kainate receptors by CNQX (left, same cell as in A) fully abolishes fast τ PSCs and unmaskes slow τ events; middle: single events are superimposed and kinetics are measured from the average PSC (right, τ = 29 ms and rise time = 1.6 ms). **C**: DRG stimulations evoke polysynaptic currents in the patched ventral interneuron. Evoked currents in standard Krebs (left) appear reduced (by 41%) in area after the application of CPP (right); each trace represents the average of 5 subsequent evoked PSCs.

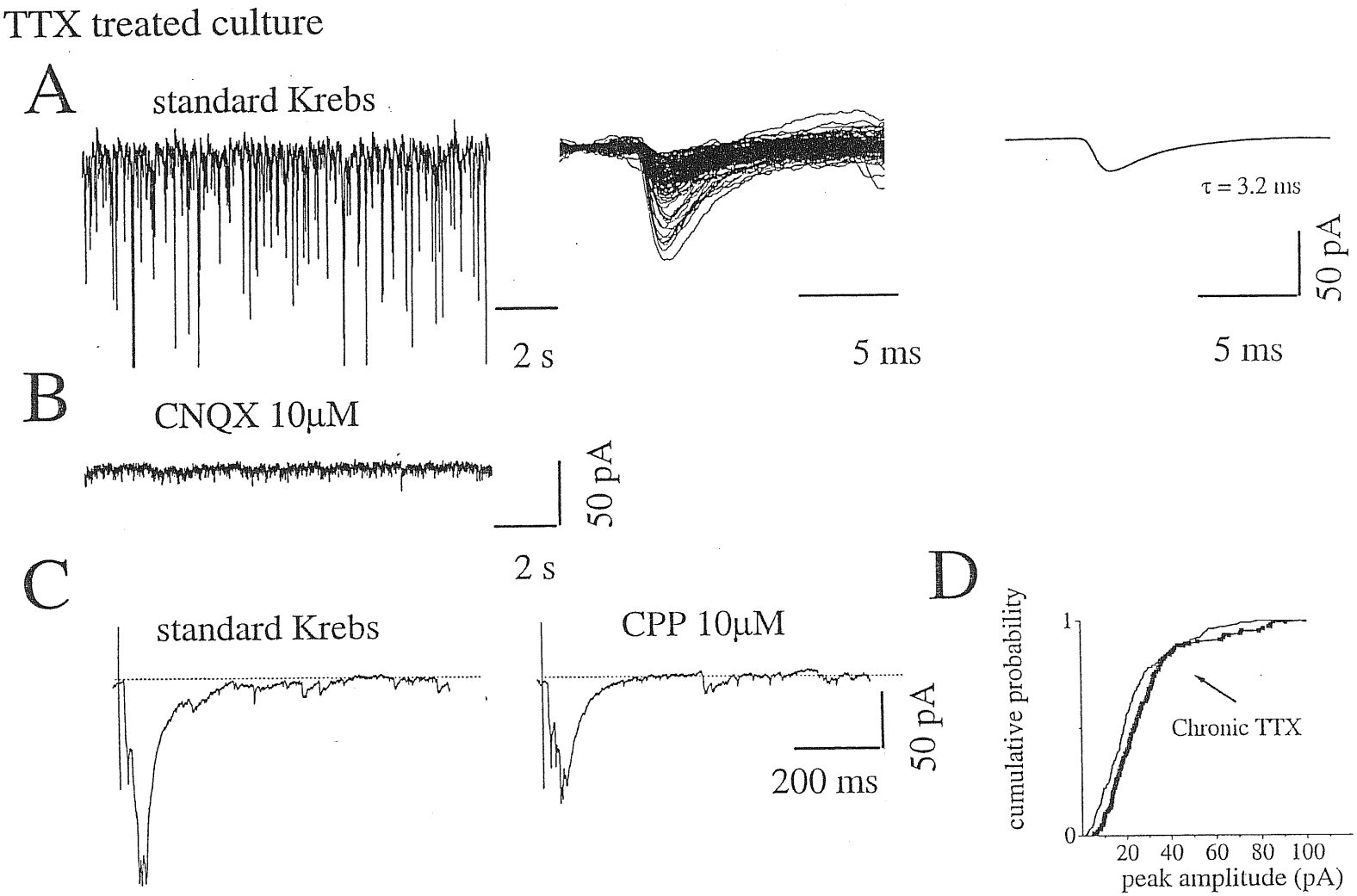

Figure 18. **A**: Spontaneous activity recorded from an interneuron in a chronic TTX culture (left); only fast τ events are detected (superimposed in the middle). From their average (right) rise time (0.9 ms) and τ (3.2 ms) values are measured. **B**: addition of CNQX blocks all fast events leaving no residual activity (same cell as in A). **C**: evoked PSCs elicited by DRG stimulations are shown in standard solution (left) and in the presence of CPP (right); dotted line represents the baseline current. The effect of CPP on the evoked PSC area consisted in 44% reduction. Each panel represents the average of 5 subsequent evoked PSCs. **D**: cumulative amplitude distribution for PSCs obtained after chronic TTX treatment (see arrow) or in control culture shows no statistically significant difference

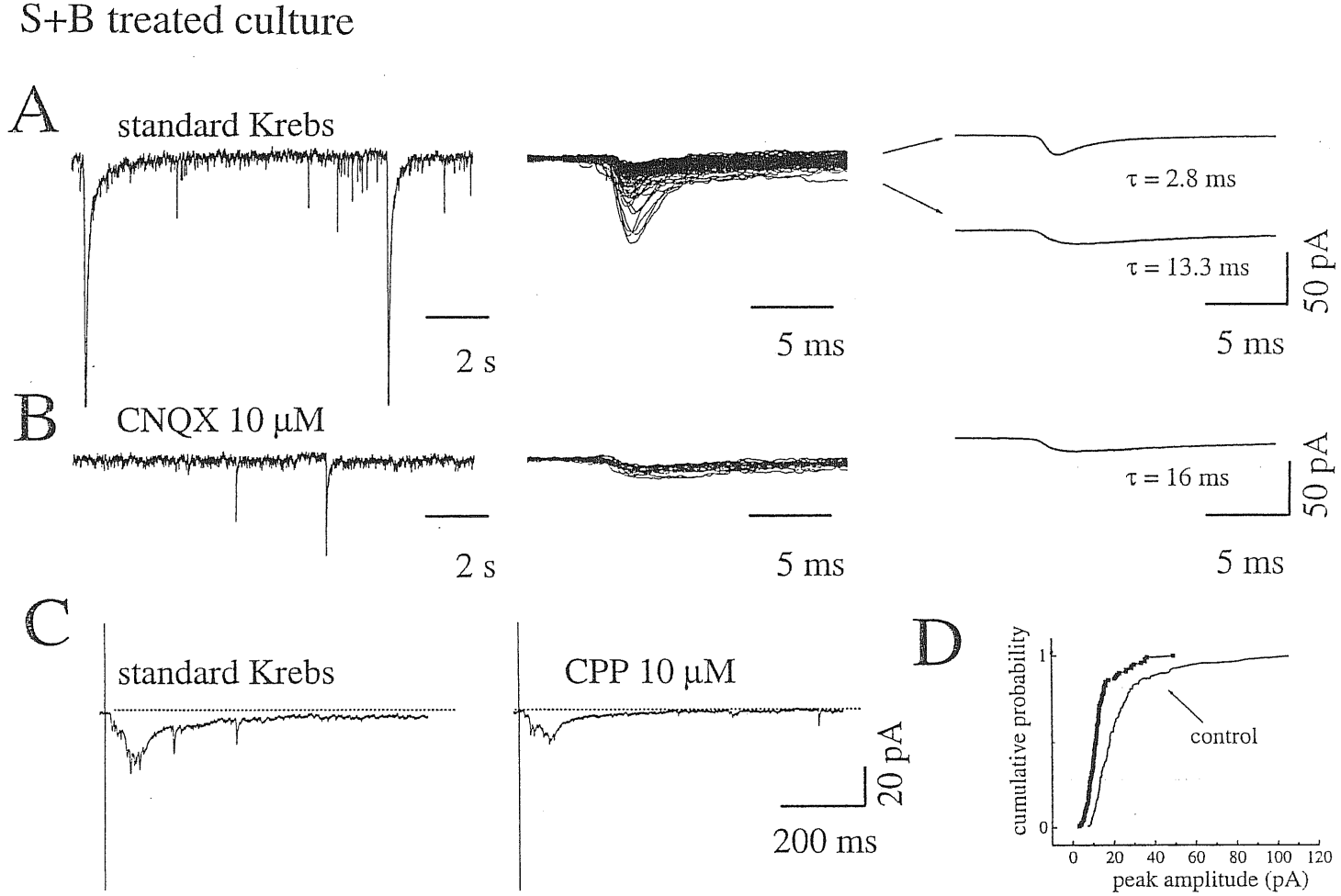

Figure 19. A: Spontaneous synaptic activity from a ventral interneuron appears as bursts of inward currents (left) followed by quiescent periods during which both fast and slow PSCs (middle, superimposed traces) are detected; kinetics are measured from the average of fast PSCs (top right: 0.9 ms rise time and 2.8 ms τ) and of slow ones (bottom right: 1.5 ms rise time and 13.3 ms τ). **B**: application of CNQX (same cell as in A) abolishes spontaneous bursting (left) and blocks fast events; only slow events survive (middle, superimposed traces) with kinetics (right) similar to those normally found in standard Krebs. **C**: Evoked synaptic currents induced by stimulation of DRG (left) appear strongly reduced in area (by 60%) during the application of CPP (right). Each trace (left and right) is the average of 8 subsequent responses. **D**: Cumulative probability plot of PSC amplitudes from a ventral interneuron in control (see arrow) and in chronic strychnine *plus* bicuculline sister culture: the entire amplitude distribution for PSCs deviates toward smaller values for the treated interneuron.

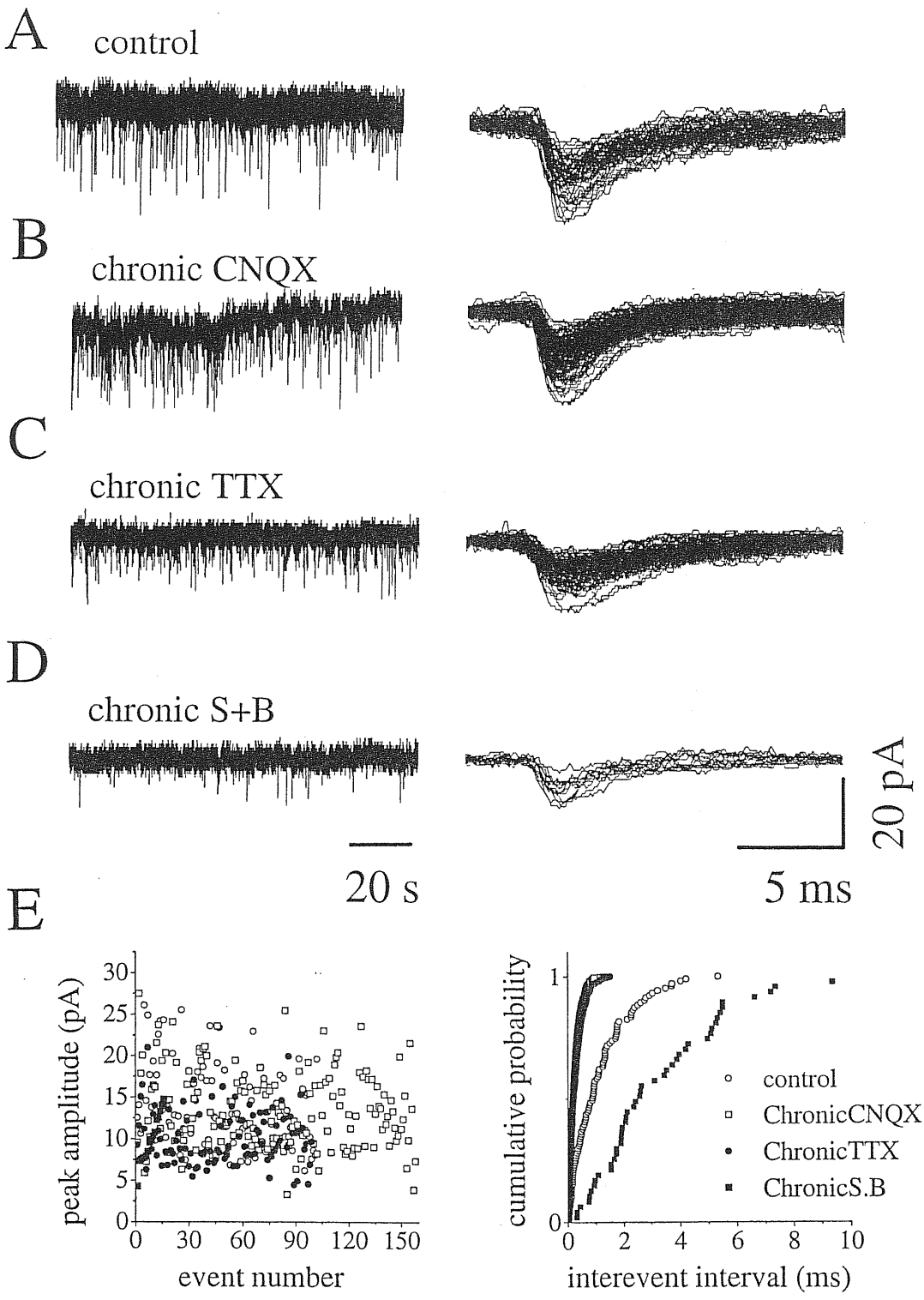

Figure 20. **A**: Recordings from a ventral interneuron in the presence of TTX from a control culture (left): events are superimposed on the right. **B**: miniature currents in interneuron from chronic CNQX culture (left): note the higher frequency of mPSCs (superimposed traces, right) compared to control culture. **C**: spontaneous mPSCs from a chronic TTX culture display higher frequency (superimposed traces, right) compared to control. **D**: miniature currents recorded from an interneuron in a chronic strychnine *plus* bicuculline culture (left) present a low frequency (superimposed traces, right) compared to the other culture conditions (**A**, **B**, **C**). **E**: distribution of mPSC amplitude (left) and mPSC inter-event distribution plot (right) from the cells shown in A-D. In the right hand panel the plot for chronic CNQX, TTX and strychnine plus bicuculline (S.B) are significantly different from control. Note almost complete overlap of CNQX data with TTX ones.

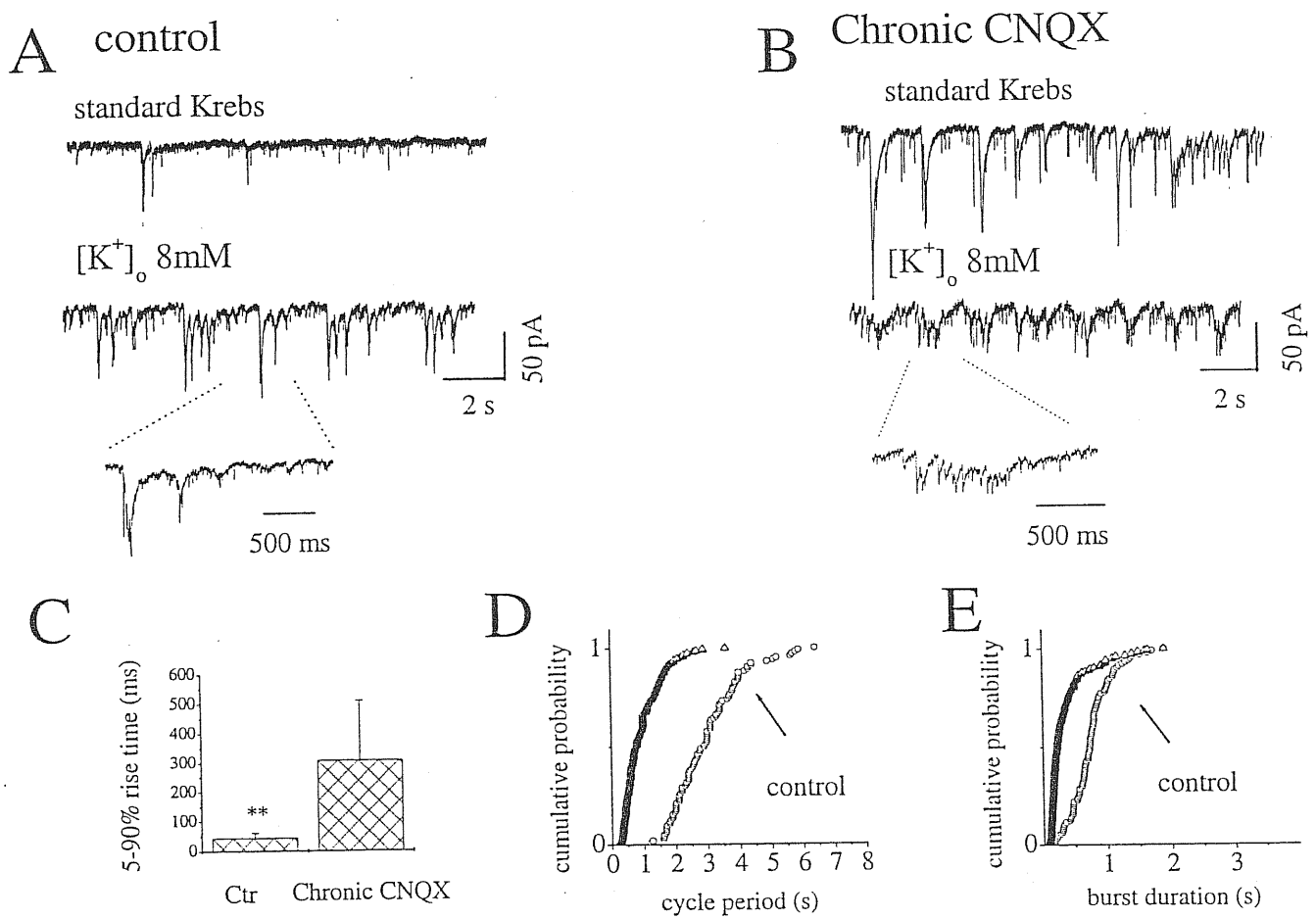

Figure 21. A: Spontaneous synaptic currents in standard Krebs from a control ventral interneuron (top). Increased extracellular K^+ induces regular rhythmic bursts of inward current (middle). A magnified burst trace (bottom) shows the typical shape (rise time 38.6 ± 14.9 ms). **B:** Intense spontaneous synaptic activity as is recorded from a chronically CNQX treated ventral interneuron (top). In the presence of 8 mM extracellular K^+, rhythmic currents appear with shorter cycle period and burst duration than control cultures (middle). The burst shape (bottom, expanded trace) is characterized by a slow rise time (288 ± 220 ms) **C:** Histogram of burst rise times in high K^+ in control and in chronically CNQX treated cultures. Data are collected from a group of interneurons. **D, E:** Cumulative scatter plots for cycle period (**D**) and burst duration (**E**) in high K^+ in control (circles) and chronically CNQX treated cultures (triangles). The overall cumulative distribution for both parameter deviates toward smaller values for treated interneurons.

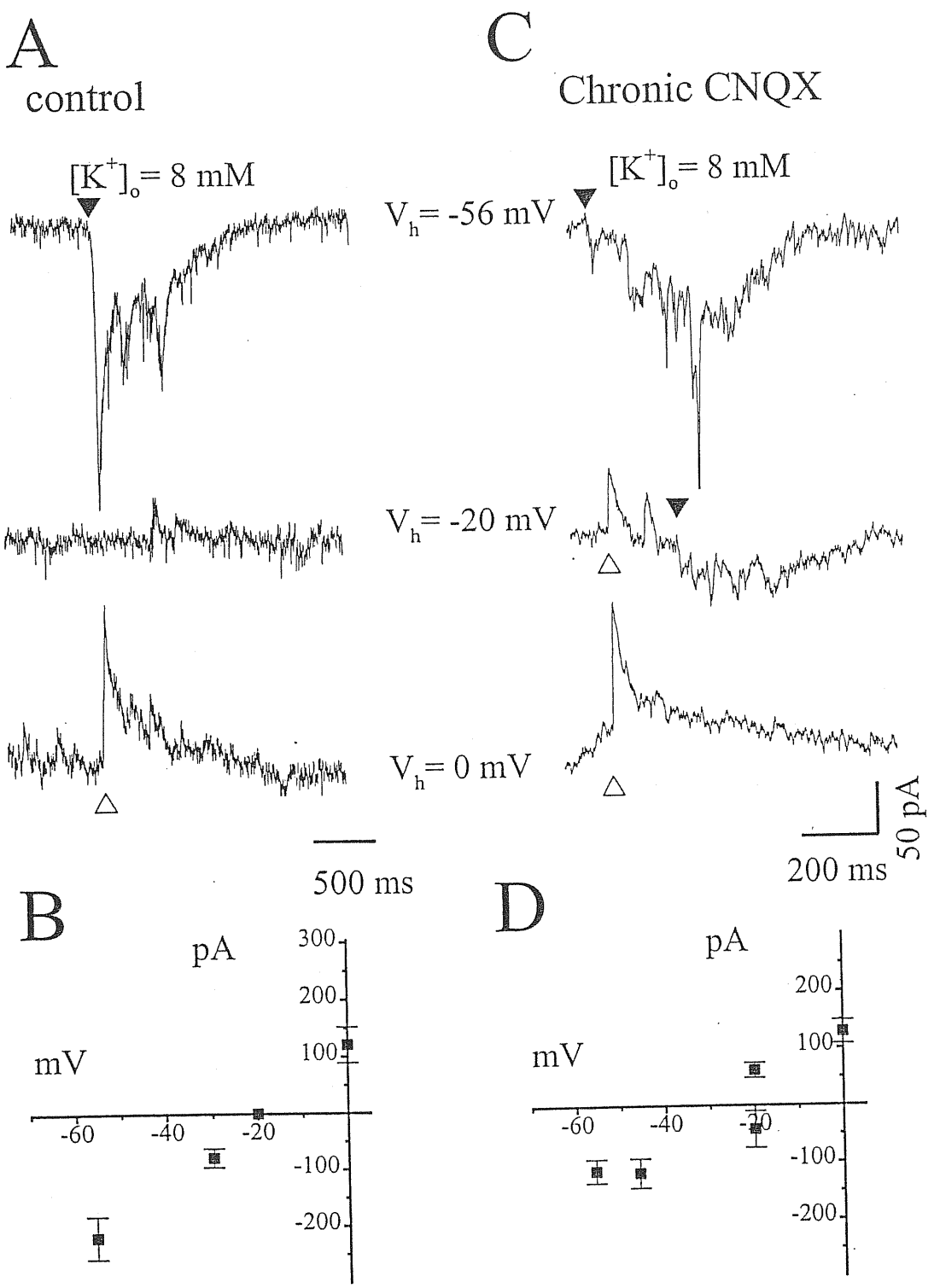

Figure 22. A: Single bursts in the presence of 8 mM $[K^+]_O$ in a control culture. At V_h = -56 mV burst is inward (top, filled triangle). Burst at V_h = - 20 mV is not detectable although there are some inward and outward PSCs (middle) whereas at 0 mV, burst is completely outward (bottom, open triangle). **B:** I/V curve obtained plotting mean burst amplitude against V_h (same cell as in **A**). **C:** Single bursts in the presence of high K^+ in a chronic CNQX culture. At -56 mV the burst is fully inward (top, filled triangle) however when V_h is - 20 mV (middle) the burst is composed of an early outward component (open triangle) followed by an inward one (closed triangle). At 0 mV burst is completely outward (bottom, open triangle). **D:** Mean burst amplitude is plotted against V_h in a chronically CNQX treated interneuron (same cell as in **C**). Note that at V_h = - 20 mV there are two distinct components with opposite polarity.

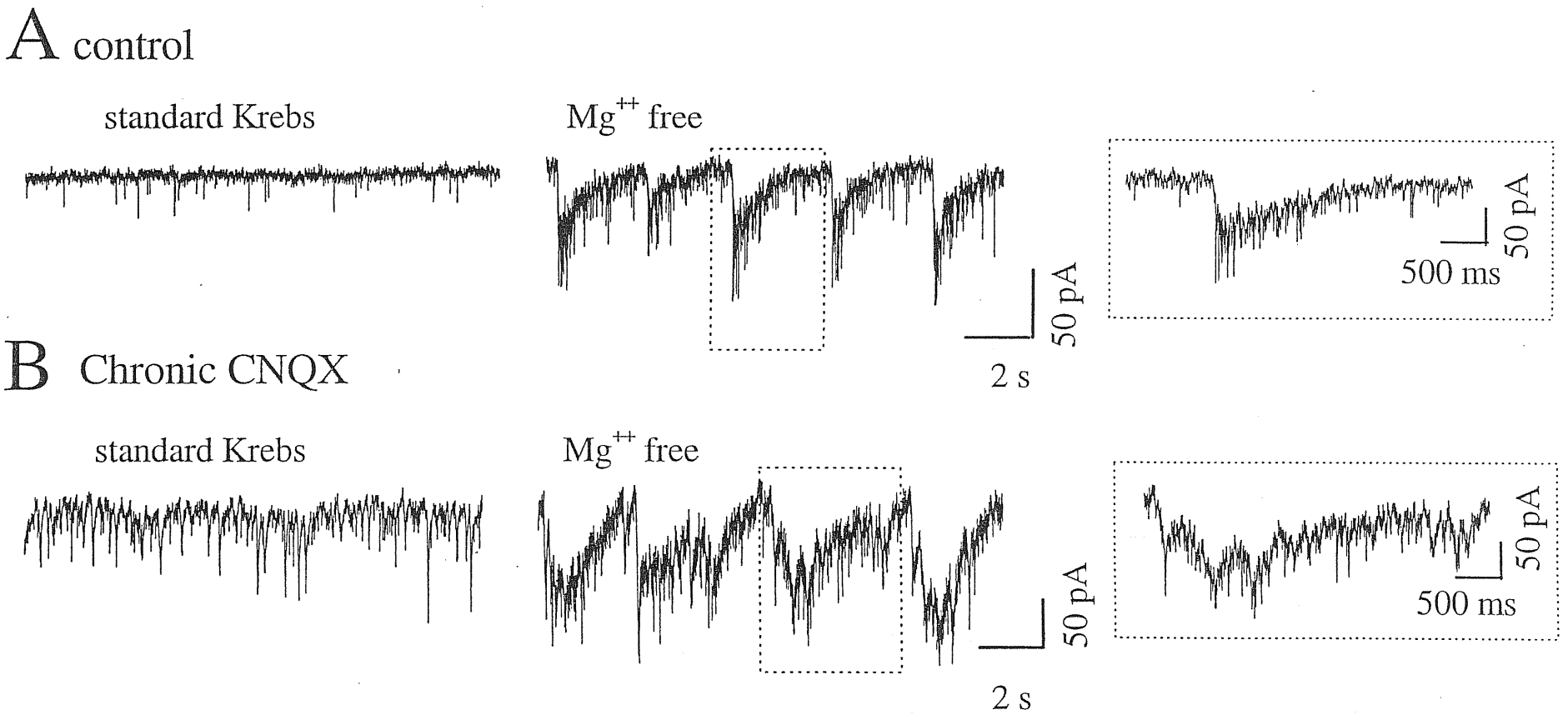

Figure 23. A: Spontaneous random PSCs (left) turn into rhythmic bursts of inward currents (middle) in the presence of Mg^{2+}-free solution. At the right, one of such a burst in an expanded time scale is shown (note the rapid rise time, 54.1 ± 24.6 ms). **B**: Spontaneous currents from a ventral interneuron chronically treated with CNQX in standard solution (left). Mg^{2+}-free solution induces regular rhythmic bursts (middle) with frequency and duration comparable to control cultures but with slower rise time (295.5 ± 190.8 ms, right).

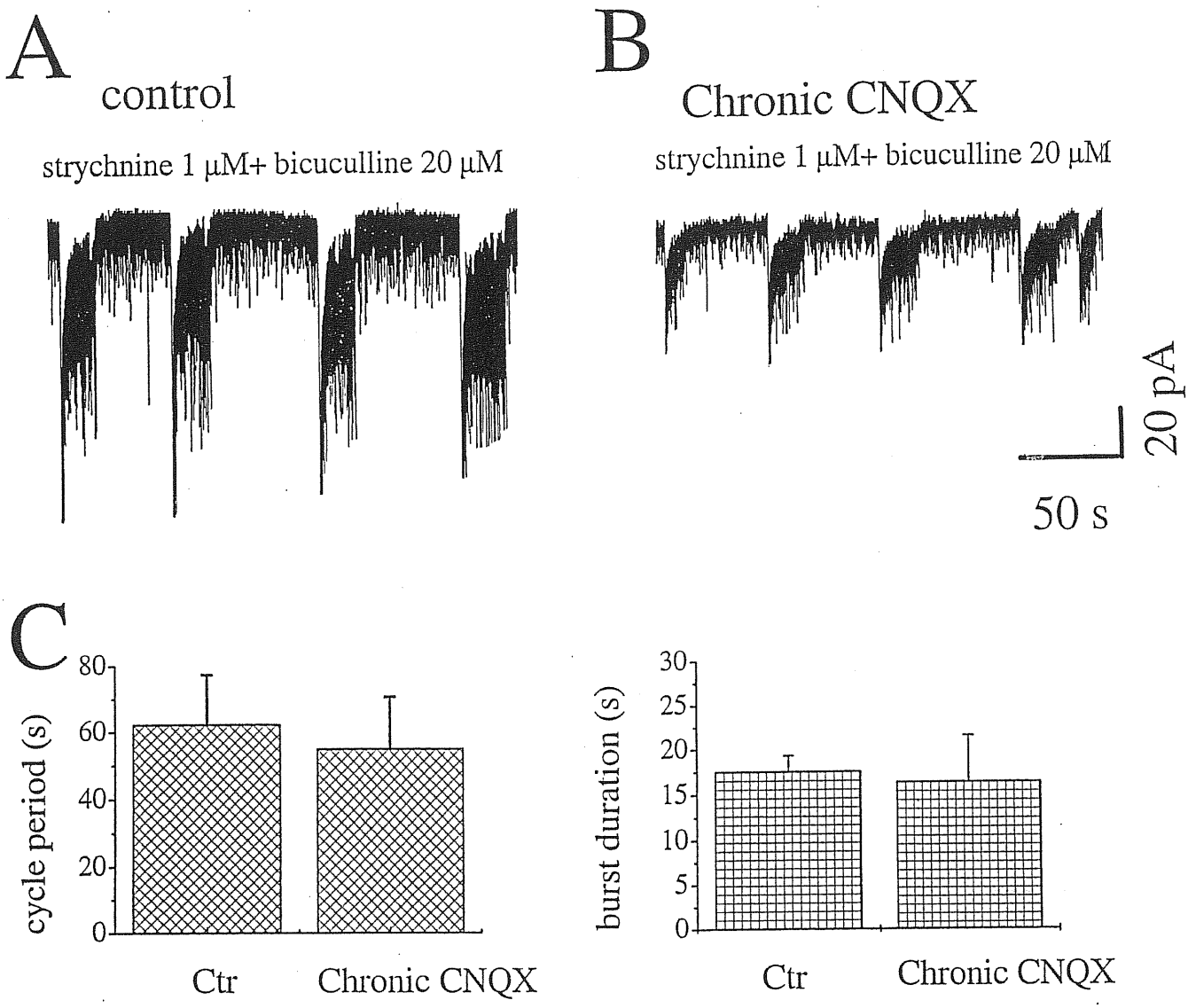

Figure 24. Block of glycine and $GABA_A$ receptor evokes large, regular rhythmic bursts of inward current both in untreated (**A**) and in chronically treated cultures (**B**). The periodicity and the duration of such an activity is comparable as shown by histograms in **C** (n=5). In the presence of the blockers burst rise time was 31.2 ± 15.1 ms and 45.3 ± 17.3 ms in control and treated cultures respectively.